FIU Electronic Theses and Dissertations   University Graduate School

3-30-2009

Elemental Analysis of Glass and Ink by Laser Ablation Inductively Coupled Plasma Mass Spectrometry (LA-ICP-MS) and Laser Induced Breakdown Spectroscopy (LIBS)

Benjamin E. Naes
Florida International University, benjamin.naes@fiu.edu

FLORIDA INTERNATIONAL UNIVERSITY

Miami, Florida

ELEMENTAL ANALYSIS OF GLASS AND INK BY LASER ABLATION

INDUCTIVELY COUPLED PLASMA MASS SPECTROMETRY (LA-ICP-MS) AND

LASER INDUCED BREAKDOWN SPECTROSCOPY (LIBS)

A dissertation submitted in partial fulfillment of the

requirements for the degree of

DOCTOR OF PHILOSOPHY

in

CHEMISTRY

by

Benjamin E Naes

2009

To: Dean Kenneth Furton
    College of Arts and Sciences

This dissertation, written by Benjamin E Naes, and entitled Elemental Analysis of Glass and Ink by Laser Ablation Inductively Coupled Plasma Mass Spectrometry (LA-ICP-MS) and Laser Induced Breakdown Spectroscopy (LIBS), having been approved in respect to style and intellectual content, is referred to you for judgment.

We have read this dissertation and recommend that it be approved.

_____
Yong Cai

_____
Bruce McCord

_____
Andrew Macfarlane

_____
Alexander Mebel

_____
José R. Almirall, Major Professor

Date of Defense: March 30, 2009

The dissertation of Benjamin E Naes is approved.

_____
Dean Kenneth Furton
College of Arts and Sciences

_____
Dean George Walker
University Graduate School

Florida International University, 2009

DEDICATION

To my parents Roger and Toni and for my wife, Jennifer and our late baby daughter Lilly, who provided much of the inspiration behind the body of work presented here. Without my family and their support through the most difficult of times (rest in peace Lillian Emily Naes), I may not have succeeded and likely would have given up. Therefore, I share my success with them, whom I admire and love dearly.

ACKNOWLEDGMENTS

First and foremost I want to acknowledge my wife and my family for their undying support throughout this journey…what a journey it has been. Furthermore, I give praise to God, who has always channeled my life in an amazing and fulfilling fashion.

In addition, I would like to express my gratitude to my graduate committee: Dr. José R. Almirall, Dr. Yong Cai, Dr. Bruce McCord, Dr. Alexander Mebel, and Dr. Andrew Macfarlane for their guidance and support. I especially would like to thank Dr. José Almirall for offering me the opportunity to work in his research group and for supporting my endeavors in and out of FIU; his guidance and wisdom has helped make me into the student I am today.

I would like to acknowledge FIU, the Department of Chemistry and Biochemistry, the International Research Forensic Institute, the Dean's office, and the Graduate Student Association for all the support, funding, etc. over the past 4+ years. Without their support, I would not have been able to expand my knowledge base nor see many of the places that I have while representing FIU at numerous academic conferences. The LIBS study for the forensic analysis of glass was supported by the National Institute of Justice (NIJ), grant 2005-IJ-CX-K069, and thus that is an important acknowledgement.

I have to personally thank those who have collaborated with me on the various projects that I undertook, the extended list includes Dr. Jhanis Gonzalez and Dr. Richard Russo at the Lawrence Berkeley National Laboratory, Dr. Cleon Barnett (former post doc) now at Alabama State University, Scott Ryland at the Florida Department of Law Enforcement, Sayuri Umpierrez (former Almirall group member and part of the Miami Dade Crime Lab), and Robert Romanowski at the United States Secret Service.

ABSTRACT OF THE DISSERTATION

ELEMENTAL ANALYSIS OF GLASS AND INK BY LASER ABLATION

INDUCTIVELY COUPLED PLASMA MASS SPECTROMETRY (LA-ICP-MS) AND

LASER INDUCED BREAKDOWN SPECTROSCOPY (LIBS)

by

Benjamin E Naes

Florida International University, 2009

Miami, Florida

Professor José R. Almirall, Major Professor

The necessity of elemental analysis techniques to solve forensic problems continues to expand as the samples collected from crime scenes grow in complexity. Laser ablation ICP-MS (LA-ICP-MS) has been shown to provide a high degree of discrimination between samples that originate from different sources. In the first part of this research, two laser ablation ICP-MS systems were compared, one using a nanosecond laser and another a femtosecond laser source for the forensic analysis of glass. The results showed that femtosecond LA-ICP-MS did not provide significant improvements in terms of accuracy, precision and discrimination, however femtosecond LA-ICP-MS did provide lower detection limits. In addition, it was determined that even for femtosecond LA-ICP-MS an internal standard should be utilized to obtain accurate analytical results for glass analyses.

In the second part, a method using laser induced breakdown spectroscopy (LIBS) for the forensic analysis of glass was shown to provide excellent discrimination for a

glass set consisting of 41 automotive fragments. The discrimination power was compared to two of the leading elemental analysis techniques, µXRF and LA-ICP-MS, and the results were similar; all methods generated >99% discrimination and the pairs found indistinguishable were similar. An extensive data analysis approach for LIBS glass analyses was developed to minimize Type I and II errors en route to a recommendation of 10 ratios to be used for glass comparisons.

Finally, a LA-ICP-MS method for the qualitative analysis and discrimination of gel ink sources was developed and tested for a set of ink samples. In the first discrimination study, qualitative analysis was used to obtain 95.6% discrimination for a blind study consisting of 45 black gel ink samples provided by the United States Secret Service. A 0.4% false exclusion (Type I) error rate and a 3.9% false inclusion (Type II) error rate was obtained for this discrimination study. In the second discrimination study, 99% discrimination power was achieved for a black gel ink pen set consisting of 24 self collected samples. The two pairs found to be indistinguishable came from the same source of origin (the same manufacturer and type of pen purchased in different locations). It was also found that gel ink from the same pen, regardless of the age, was indistinguishable as were gel ink pens (four pens) originating from the same pack.

TABLE OF CONTENTS

LIST OF TABLES

LIST OF FIGURES

LIST OF ABBREVIATIONS AND ACRONYMS

ICP-MS	Inductively Coupled Plasma Mass Spectrometry
LA-ICP-MS	Laser Ablation Inductively Coupled Plasma Mass Spectrometry
fs	Femtosecond
ns	Nanosecond
LIBS	Laser Induced Breakdown Spectroscopy
μXRF	Micro X-ray Fluorescence
SEM-EDS	Scanning Electron Microscopy–Energy Dispersive Spectrometry
AAS	Atomic Absorption Spectroscopy
NAA	Neutron Activation Analysis
ASTM	American Society for Testing and Materials
NIST	National Institute of Standards and Technology
SRM	Standard Reference Material
FGS	Float Glass Standard
LBNL	Lawrence Berkeley National Laboratory
FIU	Florida International University
Nd:YAG	Neodymium: Yttrium Aluminum Garnet
DRC	Dynamic Reaction Cell
HR-ICP-MS	High Resolution Inductively Coupled Plasma Mass Spectrometry
IS	Internal Standard
ppm	Parts Per Million
UV	Ultraviolet

IR	Infrared
cps	Counts Per Second
SD	Standard Deviation
RSD	Relative Standard Deviation
MDL	Method Detection Limits
FTIR	Fourier Transform Infrared Spectroscopy
USSS	United States Secret Service

1   INTRODUCTION

In the modern era of forensic science, the role of the forensic examiner is constantly evolving as new and often improved analytical techniques and methodologies are developed to counteract present and future scientific challenges. The rise in interest of forensic science in mainstream media has contributed to its popularity and sparked interest in the scientific community, which has produced benefits and drawbacks alike. The benefits, such as increased forensic related research, new methodologies, advancement in education, etc. has certainly outweighed the drawbacks. The major repercussion that has surfaced is related to an inaccurate public perception (or understanding) on how forensic science really works, the challenges of sample analysis and the complexity of such challenges, and the strength of the analytical results en route to either convicting or exonerating a suspect in a court of law. Thus, it is up to the forensic science community to combat or address these issues by supplementing the lack of knowledge (throughout the general public) with fundamental science that speaks for itself.

Trace analysis is one area of forensic science that has evolved considerably in the last decade or so, where the ultimate conclusion from a forensic point of view is whether or not two samples are a "match" (indistinguishable) or if they are not (distinguishable) and what that actually means. The idea of match criteria has brought about important questions and was recently highlighted in a recent report by the National Research Council released by the National Academy of Sciences [1]. With respect to the current status of forensic science, the report called for an "overhaul" of a "badly fragmented"

system [1] which in the realm of trace evidence analysis (and comparisons) included recommendations on development of universal methodologies (from sample collection to analysis to data interpretation) and the research to validate the accuracy and reliability of such methods. The report also called for laboratory accreditation (and the enactment of quality control measures) and the creation of a code of ethics by which all forensic scientists should adhere to [1]. With respect to trace evidence comparisons, reducing or eliminating both Type I (false exclusions) and Type II (false inclusions) errors is crucial to any forensic case.

Furthermore, simply stating that a glass fragment collected at a crime scene is a match to a known source is not sufficient, especially if the conclusion is based on refractive index measurements that have limited discrimination power. The lack of discrimination has led to the development of analytical techniques, such as laser ablation inductively coupled plasma mass spectrometry (LA-ICP-MS), which have been shown to provide increased discrimination power and has reduced the error rate associated with sample comparisons. With regard to concluding that samples are a match, a statement should be made that reinforces that conclusion, such as "the glass fragment at the crime scene and the known sample was indistinguishable at the 95% confidence interval, meaning that these glass sources were likely produced in the same manufacturing plant at about the same time". The statement preceding this sentence is supported by glass population studies [2-6], and future population studies will continue to further validate current analytical methodologies for forensic glass comparisons. The concept of match criteria, and the attributing population studies used to validate such determinations, can be extended to other matrices of forensic interest. In my dissertation, population studies

and the associated conclusions for forensic glass and gel ink analyses will be presented along with the methods used to generate those determinations.

The original hypothesis regarding femtosecond LA-ICP-MS was that it would provide improved figures of merit and thus be less matrix-matched dependent. With respect to the LIBS part, it was hypothesized that a competitive method could be developed for the forensic analysis and discrimination of glass. For the ink project, the hypothesis was that LA-ICP-MS can be used for the characterization and discrimination of gel ink pens.

1.1   Significance of the Study

Two new methods will be presented for the analysis of forensic glass and gel inks, in addition to a study which assessed and compared the figures of merit of an existing technique, glass analysis by LA-ICP-MS, using two different laser systems. With forensic glass studies, it is important to establish first and foremost the necessity of elemental analysis for the characterization and discrimination of float glass. It has been established in previous studies that refractive index measurements do not often provide the discrimination power necessary for accurate forensic glass comparisons, namely that there is an increased risk of committing Type I and Type II errors [2-3,7-10]. Since glass manufacturers target similar refractive indices and therefore only a small degree of variation may exist between glass sources, the lack of discrimination power can ultimately lead to Type II errors (false inclusion), meaning that a pair was found indistinguishable when the fragments originated from different sources. Elemental analysis helps to minimize the potential to commit these errors and in turn increases

discrimination, which is significant to forensic cases.

In chapter 3, the advantages of femtosecond LA-ICP-MS detailed in the literature will be assessed for the forensic analysis of glass. The figures of merit for glass analysis by femtosecond LA-ICP-MS will be compared to the less complex and less expensive approach of nanosecond LA-ICP-MS. Studies using different quantification approaches in addition to the use (or non-use) of an internal standard will be presented. The latter concept is particularly important to the scientific community because if femtosecond LA-ICP-MS can provide accurate and precise results without the need of an internal standard, then analyses on other matrices where a good internal standard is not available could then be readily performed (i.e. forensic analysis of paint).

Secondly, a method (including an extensive data analysis study) using laser induced breakdown spectroscopy (LIBS) will be presented and the glass discrimination results are compared to two of the leading techniques in elemental analysis of materials, micro X-ray fluorescence (µXRF) and LA-ICP-MS. The significance concluded from this study was that LIBS provided a viable alternative to the aforementioned approaches with respect to discrimination power (all techniques generated 99% discrimination potential). Besides providing similar discrimination power, the advantages of LIBS include faster analysis times (or higher sample throughput), reduced complexity of use and the instrumentation can be purchased at a fraction of the cost compared to µXRF and LA-ICP-MS. These advantages are particularly significant to forensic labs where high there are limited resources to acquire or substantiate the purchase of expensive instruments.

Finally, an analytical method was developed for the analysis of black gel inks (on paper) by LA-ICP-MS. A study of this type is of particular interest to the forensic

community because currently there is no method in existence for the discrimination of this class of ink. More specifically, the components of gel inks cannot be separated by the chromatographic techniques (i.e. thin layer chromatography) typically employed in forensic document examination or questioned document laboratories [11]. Once a method was established, it was then tested by conducting two population/discrimination studies in conjunction with a single pen (within pen) variation study and a within (pen) pack variation study.

2 ANALYTICAL COMPARISON OF NANOSECOND AND FEMTOSECOND LA-ICP-MS FOR THE ELEMENTAL ANALYSIS OF GLASS

2.1 Glass Matrix

By definition, glass is referred to any amorphous transparent or translucent material that is comprised of a mixture of silicates and was inherently produced by fusion and eventual solidification from the molten state (of these silicates) in the absence of crystallization [12]. The main constituent in glass is silicate (or from an elemental viewpoint, silicon) and for commercial glass manufacturing the source most utilized to acquire the silicate backbone is sand (SiO_2).

Typically, other oxides are added during the manufacturing of glass such as lime (CaO), soda ash (Na_2O), and potash (K_2O) which assist with reducing key (and economical) factors like the melting point of SiO_2 and viscosity [12]. Other raw materials (including recycled materials) are added for various reasons depending on the desired finished product, such as lead oxide (PbO) to increase refractivity, boron oxide (B_2O_3) to lower thermal expansion and create borosilicate glass, and aluminum oxide (Al_2O_3) to

increase durability, as well as numerous coloring (or decolorizing) agents as well as oxidizing (or reducing) agents [12].

In glass matrices, there can be any number of possible trace elemental combinations, which are attributed to the raw materials or to the manufacturing process itself. As a result, there is a high degree of variation among the elemental profiles for glasses circulating in the population of which characterization and forensic analysis is possible. For discrimination purposes, the elements of interest in glass are not the major components but rather the trace elements (or unintended) components which inherently make glass sources distinguishable.

Many types of glass exist in the general population, but one of (if not) the most common type encountered in forensic casework is float glass which encompasses many subtypes of glass, including automotive windshields, side and rear windows and architectural glass. The term float comes from the processes by which these flat glasses are produced, the molten fused glass "floats" on a bed of liquid tin en route to cooling hence the name float glass. This process is favorable to manufacturers because the finished product has uniform thickness and typically does not require additional finishing steps or procedures [12].

All of the presented research in my dissertation involves the characterization and discrimination of float glass sources by elemental analysis. The short list of crimes where forensic glass evidence is often encountered includes burglaries, vandalism, and hit-and-run accidents, among others.

2.2   Elemental Analysis of Glass

Several analytical methods exist for determining the elemental composition of glass, including inductively coupled plasma mass spectrometry (ICP-MS), micro X-ray fluorescence (µXRF), scanning electron microscopy with energy dispersive X-ray spectroscopy (SEM-EDS) and laser ablation-inductively coupled plasma mass spectrometry (LA-ICP-MS), each of which has its advantages and disadvantages [8]. The comparison of the given techniques and others, such as atomic absorption spectroscopy (AAS), neutron activation analysis (NAA) and inductively coupled plasma atomic emission spectroscopy (ICP-AES), has been reviewed extensively in the literature [9-10]. Two of those techniques (µXRF and LA-ICP-MS) will be compared to the analysis of glass by laser induced breakdown spectroscopy (LIBS) in the following chapter; additional details including background information for those techniques are presented there.

Of these techniques, LA-ICP-MS offers increased sensitivity, the capability to perform quantitative analysis over a wide range of elements and isotopes, and excellent precision, all of which translate into improved discrimination potential. Despite these advantages, the major disadvantage of this technique is the associated cost of the instrumentation, which has prevented many forensic laboratories from acquiring a LA-ICP-MS.

Previous research that helped with the advancement of forensic analyses of glass using elemental analysis includes the work by Hickman in 1986 [2], where ICP-AES was used to determine the concentrations of Mg, Ba, Mn, Fe, Al and Sr for a glass sample set/database consisting of 1350 samples [2]. With these elemental concentrations,

combined with refractive index measurements and multi-variate statistics (squared mean Euclidian distances), Hickman was able to classify casework glass samples into two separate groups, sheet and non-sheet glasses; and when tested, a high degree of accurate classification over a six year period was obtained [2]. In 1986, Ryland targeted classification of glass samples into the two most common types of forensic glass evidence, container glass and sheet glass [2]. The approach was to first compare Mg concentrations by scanning electron microscope/X-ray fluorescence microprobe (SEM-microprobe) analysis with the approach that sheet glass samples typically contain greater than 2% Mg while container glass samples have Mg concentrations less than 1% [3]; by this method, 81% of container glasses were correctly classified. Element ratios were then used to attempt further classification and it was found that 93% proper classification was achieved by this method (for instance, Ca/Fe proved to be a good discriminating ratio) [3]. Koons et al. reported the use of ICP-AES in 1988 to determine the element composition of 184 glass samples (concentrations of Al, Ba, Mg, Fe, Sr, Mn, Ca, Na, and Ti) to discriminate sheet glass from container glass [4]. Koons et al. used principal component analysis (PCA) and cluster analysis to correctly classify 180 of the 184 samples [4]. Additionally, complete discrimination by manufacturing plant was obtained via cluster analysis [4] meaning that the elemental composition of glass samples can potentially be traced back to the glass manufacturer. Becker et al. concluded in 2001 that the discrimination of float glass samples, using several elemental analysis techniques, including SEM-EDX, µ-XRF, and ICP-MS, was possible where refractive index measurements found such samples indistinguishable [5], The research also pointed out that despite discriminating the sample set, the former two techniques (SEM-EDX and µ-

XRF) were less discriminating than ICP-MS. The improved sensitivity of and quantification of additional discriminating elements led to higher discrimination power [5].

Furthermore, a protocol was developed and later published by the American Society of Testing and Materials (ASTM) for the forensic analysis of glass by dissolution ICP-MS (ASTM E-2330-2004) [13]. The digestion and dissolution ICP-MS protocol, initially drafted in our research group, provided the details on how to digest and compare glass fragments for forensic purposes. The digestion method consists of the combined use of HNO_3, HF, and HCl and heat to completely dissolve the glass in preparation for dissolution ICP-MS [13]. The next step in the evolution of glass analysis was to compare a relatively new technique at the time, LA-ICP-MS to digestion ICP-MS. It was concluded that LA-ICP-MS provided similar figures of merit (accuracy, precision, and discrimination) for the analysis of glass samples of similar and differing sources of origin [6]. This was an important step for reasons specified in the laser ablation description section. Now a technique for glass analysis could be used in place of the difficult and dangerous digestion methods. Given the fractionation issues encountered with nanosecond LA-ICP-MS analyses, fractionation (where the elemental composition of the ablated mass is different from the composition of the bulk sample) in glass was studied [14]. From this research it was demonstrated that fractionation was not a factor in the accurate quantitative analysis of glass by LA-ICP-MS [14]. Furthermore, sampling strategies for the forensic analysis of glass by LA-ICP-MS detailed the significance of representative sampling for container and headlamp glass; it was also concluded that float glass is homogeneous even at the mass range sampled by laser ablation, typically less

than a microgram of material removed [15]. In addition, it was shown that accurate and comparable results (for standard reference materials NIST 612 and NIST 610) can be obtained for various sized fragments down to 0.1 mm in size using LA-ICP-MS [16]. Latkoczy et al., as part of a collaborative and inter-laboratory effort reported good agreement in the same glass sample results performed in different laboratories. In addition, a new set of glass reference materials, FGS01 and FGS02, were introduced for the quantification of glass as an alternative to NIST 612 and 610. These standards were more similar in composition (or better matrix-matched) to actual float glass samples and analyses showed that the use of these glasses for quantification provided an improvement in accuracy [17].

The next step involving the forensic analysis of glass by our group and collaborators included the application of laser induced breakdown spectroscopy (LIBS), which will be discussed in the next chapter, and the research presented in the present chapter, and whether or not the performance advantages of femtosecond laser ablation ICP-MS (fs-LA-ICP-MS) over nanosecond laser ablation ICP-MS (ns-LA-ICP-MS) reported in the literature equated into improved figures of merit (accuracy, precision, limits of detection, and discrimination) for the analysis of float glass. The ultimate question asked was whether the additional cost of a femtosecond laser could be justified for the continued advancement of glass analysis and other applications of forensic interest.

2.3   Methodology

2.3.1   Instrumentation

2.3.1.1   Introduction

Some of the presented data was generated at FIU (the nanosecond LA-ICP-MS data) while the femtosecond LA-ICP-MS data was generated by the collaborator in this project, Dr. Jhanis Gonzalez, who works under the direction of Professor Richard Russo at the Lawrence Berkeley National Laboratory (LBNL) in Berkeley, CA. The aforementioned group was a key contributor to the project because they possess and maintain a femtosecond laser ablation ICP-MS system which allowed for the comparison to our nanosecond laser ablation ICP-MS system. The Russo group was one of only a handful of groups that had such instrumentation at the time the project was begun. All of the respective data analyses for both the nanosecond and femtosecond LA-ICP-MS were performed at FIU.

2.3.1.2   Laser Ablation Principles and Considerations

Laser ablation is a solid sampling technique used to remove finite amounts of matter from a solid matrix via use of a laser. The ablation of the material from the surface occurs by combination of complex processes including melting, fusion, sublimation, vaporization and finally explosion (of the material from the matrix) [18]. The ablation process and the degree of mass removal is dependent on the sample's (or material's) ability to absorb energy from the delivered laser pulse. Upon laser to sample interaction, if the energy of the laser pulse exceeds the binding energy of the atomic infrastructure of

the material, an atom is ejected. With laser ablation, the amount of material removed (or ablated) from the material is inversely proportional to the pulse duration (or pulse width). Nanosecond laser sources require laser intensities of 10^8-10^9 W/cm^2 [19-20].

The ablation process is characterized by either thermal or non-thermal mechanisms, or sometimes both, which is dependent on the wavelength and the pulse width of the laser utilized [18, 21-23]. With thermal mechanisms, sample melting and vaporization occur as a result of absorption of the laser light by the electrons in the sample lattice, this absorbed energy is then transferred into the sample lattice. As a result, fractionation could result via thermal mechanisms which are inherent on the differing phase transitions of the elements [24-25]. On the contrary, non-thermal mechanisms are characterized by the elimination of the discussed heating affects (encountered with the thermal processes). Moreover, when the energy of the photon exceeds the binding energy of the atoms, the laser radiation can rupture the sample (atomic) lattice without heat dissipation into the sample, which results in an explosive ejection of atoms and ions which directly represent the sample composition (elemental fractionation issues are eliminated) [21-23].

During the ablation process, four thresholds occur at different time intervals, as presented in Figure 1 [18]. On the femtosecond time scale, the absorption of the laser pulse (or energy) causes electronic excitation and electrons are subsequently emitted from the sample surface on the picosecond time scale [18]. When additional laser energy is pulsed onto a sample surface or into the sample lattice, vaporization and ionization occur via collisions with the surrounding gas, which causes a laser induced plasma (or plume) to be generated on the nanosecond time scale [18]. The laser induced plasma (or

emission of light) is the basis for the LIBS experiment, which will be discussed in the next chapter. During this stage of the ablation process, plasma shielding can occur because the laser beam interacts with the growing plasma and can subsequently be absorbed or reflected by the generated laser induced plasma [18]. Plasma shielding can be avoided by using shorter laser wavelengths; for shorter wavelength (UV) lasers, the beam more efficiently penetrates into the plasma ultimately causing more efficient bond breaking and less fractionation [18]. Finally, on the microsecond time scale, the particles are ejected from the surface by means of normal evaporation and explosive boiling [18]. These ablated particles are then carried into the inductively coupled plasma, via a constant flow of gas, which atomizes and ionizes the ablated mass en route to detection via mass spectrometry (MS) or emission spectroscopy (AES) [26-27].
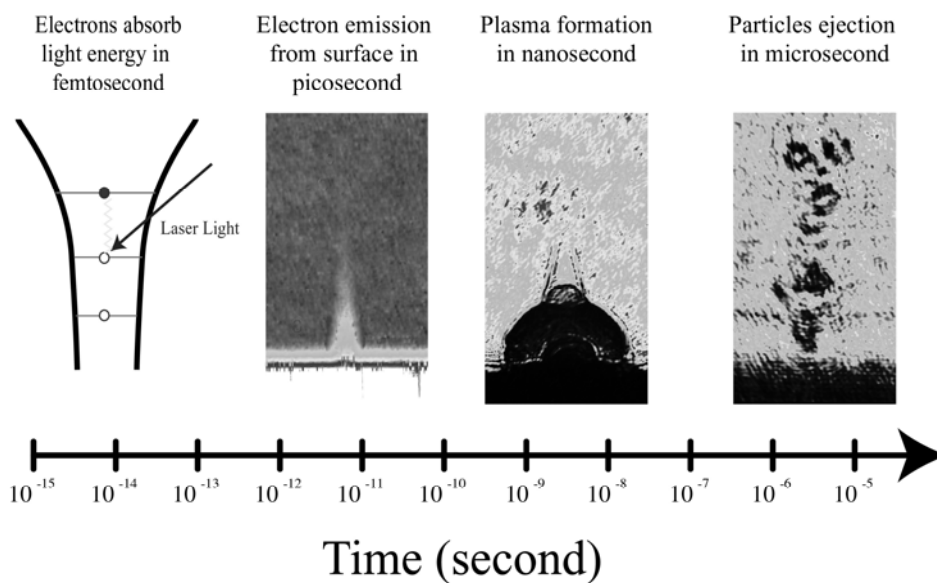
Figure 1. Time scale and events associated with laser ablation. Figure was extracted from Russo RE, Mao X, Mao SS (2002) Anal Chem 74:70A-77A [18].

A typical laser system contains a laser source (typically, a nanosecond Nd:YAG source operating at 1064nm or one of its harmonic wavelengths, 532nm, 266nm, 213nm, etc.), fairly simple optics (a series of mirrors and lens needed for focusing the laser beam), a camera (for viewing the sample surface), a pressurized ablation cell (which has a carrier gas line running into and out of the cell), and a computer to control the collective system (where ablation parameters are controlled and changed) [26-27].

2.3.1.2.1   Advantages of Laser Ablation

In comparison to traditional dissolution techniques, LA offers many advantages without compromising selectivity and sensitivity. Dissolution methods involve sampling a portion of the solid material under investigation, placing the sample aliquot (usually milligrams) into a digestion vessel, adding concentrated acid(s) and finally digesting the material with use of a controlled heating device over a specified period of time (usually several hours or more). The sample digests are then diluted into a specified volume and ultimately analyzed. Such methodology is prone to contamination issues, including contributions from the sample container, from the added solvents (acids and water), and from the atmosphere, especially in the case of open vessel digestions. Digestion methods are also prone to sample loss or even analyte loss (volatile components) and depending on the method, there can be serious exposure-related hazards that must be considered when heating concentrated acid solutions [26-27].

Laser ablation, however, requires virtually no sample preparation, which eliminates many of the problems associated with dissolution methods and increases sample throughput [26]. Another major advantage for laser ablation offers over its

dissolution counterpart is related to sample size requirements, which are generally in the sub-microgram range for most ablation methods versus milligrams of material (or more) needed for dissolution methods [26]. Reduced sample sizes are especially beneficial to certain applications where there is often a limited amount of sample, such as in forensics. As a result of the small amount of sample consumed, laser ablation is considered a nondestructive technique (or virtually nondestructive) [26].

2.3.1.2.2 Disadvantages of Laser Ablation

As with any analytical technique or instrument, there are several disadvantages that are important to consider. Since laser ablation is a direct sampling technique some issues or disadvantages are unavoidable. First of all, since the sample consumption significantly reduced with laser ablation in comparison to dissolution methodologies, the sample is (or can be) less representative of the bulk, which is why laser ablation is considered a microchemical approach, whereas dissolution/digestion procedures are considered bulk analyses. Nonetheless, multiple sampling locations can increase sample representation and thus enhance characterization. In addition, since a smaller amount of mass enters the ICP-MS, laser ablation typically has higher detection limits than dissolution ICP-MS. In terms of quantitative analysis, quantification of the ablated mass is often difficult because matrix matched standard reference materials may not be available. The reason matrix-matched standards are important is because accurate quantification by laser ablation (ICP-MS) is directly correlated to the ablation rate (the amount of mass ablated per laser pulse), which is inherent to the respective sample matrix [26]. If the sample set under investigation is of different composition than the standard

being used for quantitative analysis, the laser to sample interaction (and ultimately sampling) is different, which makes associations inaccurate. In other words, even with similar compositions, some assumptions must be made when performing quantitative analysis by LA-ICP-MS. However, despite the lack of matrix-matched standards, some applications have utilized the NIST series glass standards for quantification and successful results (in terms of accuracy) have been obtained. Nevertheless using a non matrix-matched standard is not recommended because the ablation rate between the standard and the samples under investigation will be different which significantly decreases the accuracy of the measurement [26]. Another disadvantage and probably the most studied variable related to laser ablation is elemental fractionation, which occurs (or is defined as when) the ablated mass is different in composition from the bulk sample [26]. Fractionation can be intrinsic (matrix related) and/or it can occur as a function of the ablation process (dependency on laser irradiance, wavelength, pulse width, and pulse duration); fractionation can even be a product of ablation transport (in relation to carrier gas and the ablation chamber/tubing) and/or it can occur within the inductively coupled plasma itself [26]. Research has shown that utilizing higher laser irradiances and shorter pulse durations significantly reduces fractionation [26]. In particular, with shorter pulse durations and higher laser irradiances, smaller particle size distributions are generated and are more readily transported and efficiently atomized/ionized in the inductively coupled plasma [26].

2.3.1.2.3 Femtosecond Laser Ablation Principles

All of the work referenced previously involved the use of nanosecond laser ablation systems. It has been reported extensively in the literature [18, 26-30] that nanosecond laser ablation is associated with elemental fractionation, which as alluded to earlier can occur at any stage of the ablation process, including upon laser to sample (laser to matter) interaction, during sample transport into the inductively coupled plasma (ICP), which is partially dependent on particle size distributions, and during particle vaporization inside the ICP itself, which is characterized by plasma conditions and particle size distributions [18, 26-30]. The degree of fractionation in each of these stages not only is dependent on the laser pulse duration (or pulse length) but on other parameters related to the laser utilized (i.e. wavelength, energy, repetition rate, etc.) as well as the physical-chemical properties related to the sample matrix itself (i.e. absorption, thermal diffusion, composition, etc) [18, 26-30]. Nonetheless, laser wavelength and pulse duration are believed to be two primary parameters influencing laser ablation and fractionation effects. In the case of glass samples, the ablation efficiency (ablated mass per pulse), particle size, and particle size distributions are dependent on wavelength [18, 26-30].

Nevertheless, the influence and effects of laser wavelength is more evident when low photon energy wavelengths (IR) are compared to high photon energy wavelengths (UV) and such effects are negligible when a UV laser is compared to another UV laser if the laser energies are similar (i.e. 213nm versus 266nm) [28-30]. Several studies have shown that improved ablation efficiency, smaller particle size, and narrower particle distributions were obtained when shifting from IR to UV wavelength lasers [28-30]. The

other factor that must be considered which can improve the ablation characteristics (efficiency, particle size distributions) is laser pulse duration, often called pulse length. It has been well documented that when laser energy is delivered on the nanosecond time scale (pulse length), the transfer time is sufficient to thermally dissipate the photon energy (from the applied laser) into the sample lattice as heat which in turn causes sample melting and elemental fractionation [26, 31-32]. However, with femtosecond laser ablation, because of its shorter pulse duration most of the photon energy from the laser pulse is converted into kinetic energy and thereby use of femtosecond laser sources minimizes the thermal affects and fractionation associated with nanosecond laser ablation [26, 31-32]. The thermal related (and sample melting) phenomenon can be visually seen in Figure 2, which shows interferometry images (analysis performed by Jhanis Gonzalez as part of this study) for both femtosecond and nanosecond laser ablation operated at the same parameters (line scan, the same spot size and the same fluence). As can be seen in Figure 2, there is a clear difference in the heating effects of nanosecond laser pulses (thermal dissipation of the laser energy into the sample matrix) which ultimately causes the melting issue (observed on the sides of the ablated line) mentioned previously.

(a) fs-LA-ICP-MS, NIST 612   (b) ns-LA-ICP-MS, NIST 612
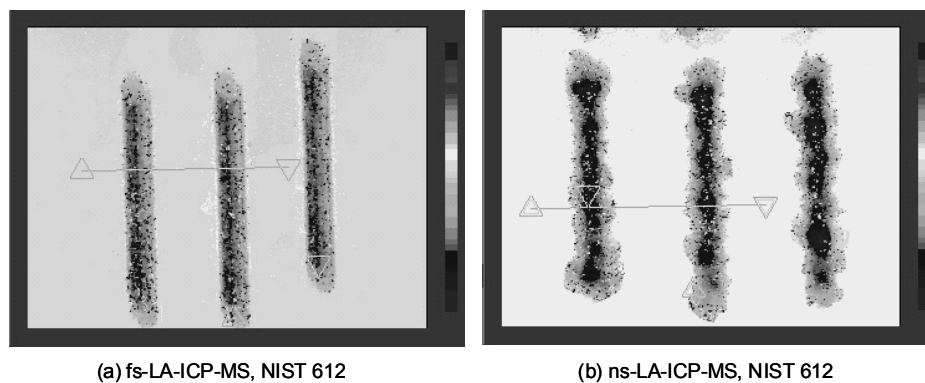
Figure 2. Interferometry images depicting thermal dissipation effects (and subsequent melting) of NIST 612 using nanosecond laser ablation, (a) represents femtosecond laser ablation and (b) represents nanosecond laser ablation, respectively. Images are courtesy of Jhanis Gonzalez at the Lawrence Berkeley National Laboratory (LBNL).

Russo et al. concluded that femtosecond LA-ICP-MS was superior to nanosecond LA-ICP-MS with respect to accuracy and precision for the analysis of brass and NIST silicate glasses [31]. Poitrasson et al. found similar results with their comparison of the two laser systems, namely for the analysis of monzanite, zircon and NIST glasses [33]. Gonzalez et al. found that femtosecond laser ablation improved the internal (the precision within a single ablation spot) and external repeatability (the precision between ablation spots) of the ICP-MS measurements of NIST 610 and NIST 612 glasses [32]. In a separate study, Gonzalez et al. concluded that the use of femtosecond laser ablation improved the accuracy and precision over nanosecond laser ablation for the analysis of lead in zinc-based alloy standard reference materials without use of an internal standard [34]. In addition, Poitrasson et al. concluded that femtosecond LA-ICP-MS was less matrix dependent in comparison to nanosecond LA-ICP-MS [33], which is consequently the overall consensus within the laser ablation community.

The question asked in this study was whether or not the performance advantages of femtosecond laser ablation ICP-MS (fs-LA-ICP-MS) over nanosecond laser ablation ICP-MS (ns-LA-ICP-MS) reported in the literature equates into improved figures of merit (accuracy, precision, limits of detection, and discrimination) for the analysis of float glass standards and actual casework samples. And, ultimately, if the additional cost of a femtosecond laser could be justified for continued advancement of glass analysis and other applications of forensic interest.

2.3.1.3 Laser Ablation Systems Description

2.3.1.3.1 Nanosecond Laser Ablation

The first of two laser ablation systems utilized in this study is a New Wave Research UP213 system (Fremont, CA) based at FIU. The laser system is equipped with a Nd:YAG, Q-switched laser operating at 213nm and a pulse width of 4ns. Besides the laser, the laser ablation system has a number of key components that make the ablation and the eventual mass transfer into the ICP-MS possible. For instance, the optics are important for accurately directing the laser pulses on the targeted area of a sample and causing the desired laser to sample interactions. Samples are housed in an ablation cell that has a constant gas flow of helium going into and out of the cell (and into the inductively coupled plasma), which allow for efficient mass transport. The provided software allows for ablation parameters to be altered according to the sample matrix, including energy, spot size, repetition rate, ablation mode, etc. The exact parameters for this particular system are reported in Table 1 which can be found in the following section.

2.3.1.3.2   Femtosecond Laser Ablation

The second laser ablation system utilized in this study is located in the Lawrence Berkeley National Laboratory in Berkeley, CA. The laser, as listed in Table 1, is a Spectra Physics Hybrid (Waltham, MA) system operating at 266nm and a pulse width of 150fs. The delivery and sample viewing optics were the same as with the nanosecond laser ablation system described previously. In their case, the laser has been stripped from a New Wave Research UP213 system, at any rate the remaining functions of this device (ablation cell, gas flows, delivery optics, etc.) are exactly the same as with the nanosecond system at FIU. The laser is directed from an optics table by a series of mirrors and lenses and into the stationary laser ablation system where sample selection and analysis is performed.

Table 1. Femtosecond and nanosecond LA-ICP-MS instrumentation and parameters.

	Femtosecond LA-ICP-MS (LBNL)	Nanosecond LA-ICP-MS (FIU)
Laser Ablation	**Spectra Physics Hybrid (150 fs)**	**New Wave Research Nd:YAG (4 ns)**
Wavelength	266 nm	213 nm
Energy	0.2 mJ	0.6 mJ
Repetition Rate	10 Hz	10 Hz
Spot Size	45 μm	55 μm
Fluence	13 J/cm^2	25 J/cm^2
ICP-MS	**VG-Elemental PQ3**	**Perkin Elmer Elan DRC II**
RF Power	1400 W	1500 W
Plasma Gas Flow (Ar)	14.2 L/min	16.0 L/min
Auxillary Gas Flow (Ar)	1.0 L/min	1.0 L/min
Carrier Gas Flow (He)	0.9 L/min	0.9 L/min
Make-up Gas Flow (Ar)	0.9 L/min	0.9 L/min
Detector	Standard Mode	Standard Mode
Dwell Time	8.0 ms	8.3 ms

2.3.1.4 ICP-MS Principles and Considerations

Inductively coupled plasma techniques, namely ICP-AES and ICP-MS, have revolutionized elemental and isotopic composition determinations for a variety of matrices, including solid, liquid, and gases; furthermore, the advantage of such techniques is that they offer rapid, simultaneous, multi-element determinations for elements at major, minor, and trace concentrations [35].

The basic construction of a typical ICP-MS instrument can be broken down into five distinct parts: (1) a sample introduction system, (2) the inductively coupled plasma, (3) an interface between the plasma and the spectrometer regions, (4) a set of ion focusing lenses, and (5) the mass spectrometer, all of which serve separate and important functions but work collectively to achieve the desired analytical result. Traditionally, samples are introduced into the inductively coupled plasma (ICP) as an aerosol, which is produced from an aqueous sample and use of a pneumatic nebulizer (equipped with a spray chamber). Nevertheless, other states of matter can also be introduced into the ICP, one of which is covered and utilized extensively in the work presented in this dissertation, laser ablation, which as discussed is a solid sampling technique that introduces sub-micrograms of solid material into the inductively coupled plasma (ICP).

The small particles of matter (solid, liquid, or gaseous) generated by the sample introduction system are introduced into the argon inductively coupled plasma by a steady stream of argon (or in the case of the laser ablation experiments presented here use a mixture of argon and helium). The inductively coupled plasma is generated and sustained under atmospheric conditions with a combination of several mechanisms. The plasma itself is initially generated via a spark from a Tesla coil, which introduces seed (or free)

electrons into the torch characterized as an argon-rich atmosphere (provided by a constant flow of argon) [35]. The steady flow of argon contained within a quartz tube (or torch) is located in the center of a copper induction (or load) coil through which a high frequency electric current is continuously passed (the applied current is produced by a radio frequency generator). An intense magnetic field is generated by a combination of the applied electric current and continual collisions between neutral argon atoms and free electrons. The abundance of ionic species and electrons result and thus sustain (or maintain) the inductively coupled plasma even during sample introduction [35]. Hence, the argon plasma offers great stability and robustness in a chemically inert environment. On a technical level, the self-sustaining argon ICP generates high gas temperatures (~4500-8000K), high electron temperatures (~8000-10000K) and high electron densities (~10^{15} cm^{-3}) [35]. With such plasma characteristics and a high ionization potential (15.75 eV), the inductively coupled plasma is capable of vaporizing, atomizing, exciting, and ionizing most elements on the periodic table [35].

The newly formed ions generated by the ICP are then extracted by a series of interface cones (sample and skimmer cones) which take the ions from the atmospheric conditions needed by the plasma and into the high vacuum conditions necessary for mass spectrometry. Before the ions reach the mass spectrometer, they pass through a set of ion lenses which help direct or focus the ions into the mass analyzer [35]. Although several types of analyzers exist, the most common type of mass analyzer found in ICP-MS systems is the quadrupole, which is consequently the type of analyzer used to generate the research presented in this dissertation. The quadrupole uses a combination of direct (+) and a radio frequency alternating currents (-) to separate the ions based on their

respective mass to charge ratios. By applying different voltages to the four cylindrical rods of the quadrupole system, specific masses are selectively removed while others are allowed to pass through and ultimately reach the detector [35]. The typical resolving power for most commercial quadrupole instruments is 300, which is equivalent to one mass unit [35]. The detector converts the generated signal into a mass spectrum where the magnitude of a given peak is proportional to concentration of that species in the measured sample. A schematic of a typical ICP-MS system can be found in Figure 3.
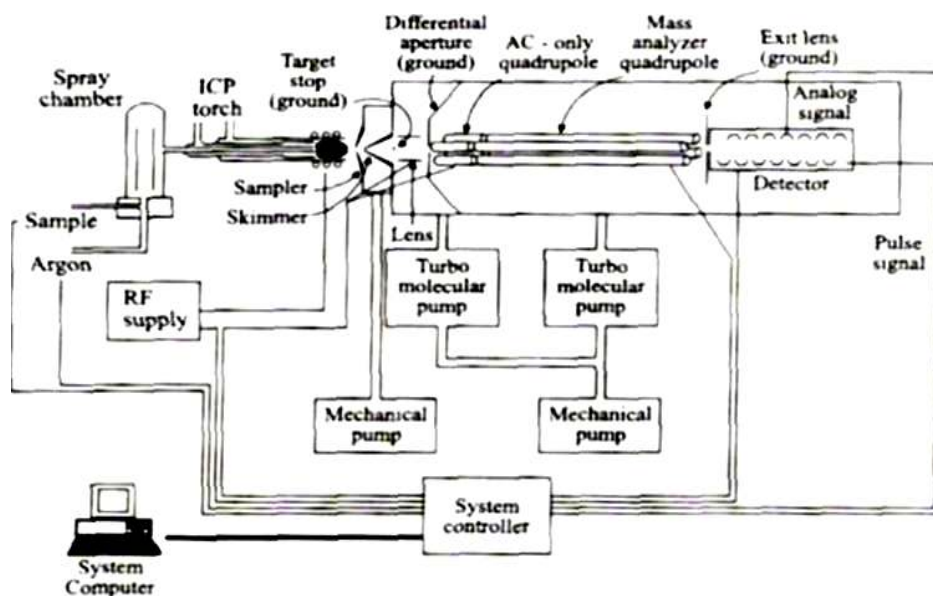
Figure 3. Schematic of a typical ICP-MS system. The figure was extracted from Skoog DA, Holler FJ, Nieman TA (1998) Principles of Instrumental Analysis, 5th Edition, Harcourt Brace, PA [36].

2.3.1.4.1 ICP-MS Interferences

The main sources of spectral interferences encountered in ICP-MS are: (1) isobaric interferences, where there is direct overlap of an isotope of one element that has the same nominal mass as an isotope of another, (2) doubly-charge species, which are the

result of an atom losing two electrons in the inductively coupled plasma, and (3) polyatomic ions, which are the combination of two or more atomic species [35]. Polyatomic interferences are the main source of interfering species encountered in inductively coupled plasma mass spectrometry [35]. Polyatomic species typically arise (and thus show up on a mass spectrum) from the sample preparation steps, the atmosphere, or from the sample matrix itself. Oxygen, nitrogen, hydrogen to name a few, and high concentration of sodium and calcium, when recombined with other atomic species cause spectra overlap for certain isotopes, which often cannot be separated using a typical quadrupole mass analyzer [35]. Instead use of quadrupole instruments equipped dynamic reaction cells or magnetic sector detectors are needed for correct detection of certain isotopes, such as $^{56}Fe^+$ which is not resolved from $^{40}Ar^{16}O^+$ by quadrupole ICP-MS. The two options listed here are very different mechanisms by which say ^{56}Fe can be correctly identified and quantified. With the utilization of a dynamic reaction cell (DRC), a reactant gas is added, such as methane, into a cell inserted prior to the quadrupole mass analyzer and the reactant gas reacts with the interfering species to form a new polyatomic ion and thus leaving the parent ion to be detected [37-40]. With magnetic sector instruments (or high resolution, HR-ICP-MS) the resolving power can be up to R=10000 in high resolution mode, which in turn allows for the separation of species that are 0.01 mass units apart, like $^{56}Fe^+$ from $^{40}Ar^{16}O^+$, as versus one mass unit separation for quadrupole detectors. In brief, for magnetic sector detectors, the ion beam is doubly focused. The ions are first accelerated through the ion lenses and into a magnetic field, which is dispersive with respect to the mass to charge ratio, then the ions reach the electrostatic analyzer which separates ions with respect to energy [41]. Although both of

these instruments (DRC and HR-ICP-MS) were available for use at FIU, they were not used for the projects summarized in this work for a few reasons. The quadrupole system is the most popular and most utilized ICP-MS, in forensic and other analytical labs because of its affordability and reduced complexity in comparison to DRC and HR-ICP-MS, and it was important to develop and/or test methods using a quadrupole system for that reason. In addition, the sample analysis time is increased with DRC and HR-ICP-MS and some elements must be excluded from the element menu and/or separate analyses must be performed. Therefore, although greater resolution and detection can be achieved using DRC and HR-ICP-MS, the number of elements that can be analyzed is limited and sample throughput is significantly decreased (as is sample consumption).

2.3.1.5 ICP-MS Systems Description

The two ICP-MS systems used for this study were both quadrupole-based systems, which consequently are the most common types of ICP-MS utilized in forensic laboratories. The ICP-MS used at FIU was a Perkin Elmer 6100 DRC II instrument (Waltham, MA) while the LBNL instrument was a VG-Elemental PQ3 ICP-MS (Waltham, MA), both of which were run and maintained under optimized conditions following the criteria stated in the next paragraph/section.

2.3.1.6 LA-ICP-MS Optimization

Collectively the two systems (laser ablation plus ICP-MS) described above were optimized using NIST 612 (National Institute of Standards, Boulder, CO) as the reference standard, which has elemental concentrations for various elements at ~40ppm. The optimization protocol involved ablating the said reference glass at 100% energy, a spot

size of 55μm, and use of the line (or rastering) ablation mode (10μm/sec scan rate); the gas flows into and out of the ablation cell, as well as the make-up gas going into the ICP, were adjusted to achieve the desired ICP-MS values per element described below. The optimization criteria followed for both instrumental setups consisted of the following isotopes and their respective targeted values (in parentheses): ^{7}Li (>1500cps), ^{49}Ti (>1000cps), ^{57}Fe (>800cps), ^{59}Co (>8000cps), ^{139}La (>10000cps), ^{140}Ce (>14000cps), ^{232}Th (>3000cps), ^{238}U (>3000cps), background signal at 220 mass units (<2cps), fractionation (Th/U=1±0.2), percent doubly charged species (Ca^{++}<3%), and percent oxides (ThO<3%). The latter three criteria are important to reduce the degree of sample fractionation as well as to reduce polyatomic interferences, which is especially important for glass matrices where a large percentage of oxides are present. The observed values were recorded on a daily basis for quality control purposes and for preventive (or regular) maintenance-related issues.

2.3.2 Sample Descriptions and Preparation

2.3.2.1 Glass Source Descriptions

2.3.2.1.1 Glass Standards

One glass standard reference material, NIST 612, and two reference glasses, FGS01 and FGS02 (BKA, Germany), were utilized as the external calibration source(s) for all data presented in this section of the dissertation. The first of which is a certified standard reference material that has concentrations at ~40ppm for each element in the matrix while the latter two calibration sources (FGS01 and FGS02) are matrix matched

glasses produced to resemble typical elemental compositions found in actual float glass samples meaning that the concentrations vary by element as versus a consistent concentration across all elements found with NIST 612 [17]. The availability of these reference glasses and NIST 612 were used to quantify float glass standard reference material NIST 1831, as well as a float glass sample set of forensic interest which will be described in the next section. The concentrations per element utilized for quantification purposes (or reference purposes in the case of NIST 1831) in this study can be found in Table 2. In Table 2, the stated concentrations stem from previous work, the superscript "a" represents values reported by NIST [13], the superscript "b" from Latkoczy's paper [17], and "c" from Trahey's work [42].

Table 2. Reference concentrations for the single point calibration standards (NIST 612, FGS01 and FGS02) utilized for quantification and evaluation purposes. Values are in units of parts per million (ppm).

element	NIST 612[a]	FGS01[b]	FGS02[b]	NIST 1831[c]
Mg	77.44	23900	23400	21166
Al	11164.6	1500	7400	6381
Ti	48.11	69	326	114
Rb	31.63	8.6	35	6.11
Sr	76.15	57	253	89.11
Zr	35.99	49	223	43.35
Ba	37.74	40	199	31.51
La	35.77	4.3	18	2.12
Ce	38.35	5.2	23	4.53
Nd	35.24	5.1	25	1.69
Hf	34.77	3.2	15	1.09

2.3.2.1.2   Casework Glass Sample Set

The glass set used in this study includes 11 forensic casework float glass samples provided by Scott Ryland at the Florida Department of Law Enforcement (FDLE, Orlando, FL). The sample set includes both architectural and automotive glass fragments, which were found to be indistinguishable by refractive index measurements (each of the associated samples had a refractive index of 1.5186). Nonetheless, the sample set under investigation here demonstrates the importance of why elemental analysis is often necessary to compliment refractive index measurements and thus ensure accurate discrimination of glass samples collected at crime scenes. If refractive index measurements were the sole discrimination technique used, there would be 0% discrimination and a high degree of Type II errors (false inclusions). The sample descriptions for the FDLE casework glass set can be found in Table 3.

Table 3. Glass source descriptions for the casework sample set provided by FDLE. Thickness measurements are reported with a deviation of ±0.1mm.

source ID	thickness (mm)	glass type	source description
W103	4.81	float	vehicle side window
W107	4.93	float	vehicle side window
W129	4.87	non-float	sliding glass door
W132	5.61	float	display case
W152	5.82	float	bathroom window (outer pane)
W153	4.75	non-float	bathroom window patterned (inner pane)
W165	4.73	float	store window
W174	4.89	float	vehicle side window
W206	5.69	float	store window
W232	5.63	float	business window

2.3.2.2   Sample Preparation

Each of the standards and samples mentioned above were treated as independent samples and therefore the same general format of sample preparation was followed for each. Although bulk sample preparation steps are not necessary for LA-ICP-MS analyses because of its solid sampling approach, each sample fragment in this study was initially rinsed with 5% HNO_3 prior to analysis to remove surface contaminants. Sample analysis was performed on the non-float side.

2.3.3   Experimental

2.3.3.1   Element Menu

The element/isotope menu for this study represented 11 elements, with the majority representing minor and trace elements/isotopes that are typically utilized for forensic glass comparisons [2-7]. More specifically, the isotopes analyzed in this study included: ^{25}Mg, ^{27}Al, ^{49}Ti, ^{85}Rb, ^{88}Sr, ^{90}Zr, ^{137}Ba, ^{139}La, ^{140}Ce, ^{146}Nd and ^{178}Hf. The internal standard used in this study is ^{29}Si because silicon the most abundant element found in float glass and due to its large concentration (>70%) and the associated signal, the concentration difference between glass samples is considered to be negligible.

2.3.3.2   Sample Analysis

Three different quantification strategies were employed and each standard (NIST 612, FGS01 and FGS02) was thus treated as a single source calibrator and run at the beginning and end of the respective analytical sequences. A minimum of three replicates of each calibration standard were run and the average intensity of the standard replicates

was then used to quantify the float glass standard (NIST 1831) and actual casework glass samples. Nine replicates of NIST 1831 were analyzed for each LA-ICP-MS system; three replicates of NIST 1831 were run at the beginning of the analytical sequence, three were run in the middle, and three replicates were run at the end to provide a comprehensive assessment across the entire analytical sequence and to study the variation across the entire run. Between the sample replicates/analyses of NIST 1831, three replicates of each casework glass sample (W103, W107, etc.) were analyzed.

2.3.4   Data Analysis

2.3.4.1   Data Integration and Quantification

Integration of each time-resolved spectra, associated to a given sample replicate and generated by the ICP-MS, was conducted using Glitter software (Macquarie, Australia), where the count rate (or intensity) per isotope was determined via the difference between the raw analytical signal (ablation) and the gas blank signal (pre-ablation). Once the respective count rate per isotope was found, additional data analysis was carried out utilizing Microsoft Excel (Redmond, WA) and the quantification equation found below [43] along with the stated reference values for each standard listed in Table 2. In Equation 1, "S" represents normalized sensitivity, "R_{AN}" represents the count rate for the sample ("SAM"), "R_{IS}" is the count rate for the internal standard, and finally "C_{AN}" represents concentration of the sample and calibration standard respectively [33].

$$C_{AN_{SAM}} = \frac{R_{AN_{SAM}}}{S} \qquad where \qquad S = \left(\frac{R_{AN_{CAL}}}{C_{AN_{CAL}}} \right) \left(\frac{R_{IS_{SAM}}}{R_{IS_{CAL}}} \right) \left(\frac{C_{IS_{CAL}}}{C_{IS_{SAM}}} \right) \qquad \text{Equation (1)}$$

31

The quantification approach described by Longerich et al. [43] was utilized to quantify (see the previous equation) float glass standard reference material NIST 1831 and the casework glass samples. It should be noted that for quantification purposes, and in relation to the provided equation, the concentration of silicon (used as the internal standard) was assumed to be the same for all glass samples analyzed; therefore, the right hand side of the equation (C_{IS}/C_{IS}) would equal 1 which simplifies the equation. Each (single point) quantification approach (NIST 612, FGS01, and FGS02, respectively) was applied to each sample replicate utilizing the same analytical signal, with and without the use of the internal standard ^{29}Si. In addition, the exact same glass fragments and standards were analyzed in each lab utilizing the associated setups outlined in Table 1.

2.3.4.2 Accuracy and Precision

Comparisons of accuracy (in terms of % bias) and precision (% RSD) were evaluated for the analysis of NIST 1831 as was the precision across the casework sample set. For the current study, accuracy was expressed in terms of percent bias, which is the percent error of each individual mean when compared to the respective reference value. Negative percent bias values indicate concentration values that were below the stated reference values and positive percent bias values indicate values that were found to be greater than the said reference values.

2.3.4.3 Method Detection Limits

Method detection limits were determined by using Equation 2, which uses Poisson counting statistics instead of the typical detection limit equation (MDL = blank$_{signal}$ + 3$\sigma_{blank\ signal}$). These calculations were performed using the Glitter data

integration/reduction software mentioned previously. The reason why this approach was used for calculating the detection limits is due to the lower counts associated with laser ablation data (and the associated instability of the time-resolved spectra) in comparison to dissolution ICP-MS, where a more constant sample flow is introduced and more signal stability is obtained. In the given equation, *B* represents the total number of counts in the background interval (data integration of the blank segment of each time-resolved spectra just prior to the onset of ablation). The detection limit per element provided in Table 8 (found in the results and discussion section) are actually the calculated average method detection limit for all the respective samples in the sequence.

$$MDL = 2.3\sqrt{2B}$$
                                                                Equation (2)

2.3.4.4   Discrimination

Discrimination analysis for the 11 casework glass sample set was performed using Systat 11 (Chicago, IL) wherein the concentrations, found via the quantification strategies discussed above, in the respective glass samples were compared utilizing analysis of variance (ANOVA) function with Tukey's honestly significance test (HSD) at the 95% confidence interval. Using the N(N-1)/2 rule, for 11 samples the total number of possible (pairwise) comparisons was 55. For the pairs found indistinguishable by ANOVA, a t-test at the 95% confidence interval was used to further discriminate the associated samples. With the utilization of the 95% confidence interval, there is a 5% probability of committing a Type I error (false exclusion). When the confidence interval is increased to 99%, that leaves only a 1% chance (or less) of committing a Type I error, however at the same time the probability of committing a Type II error (false inclusion)

increases. With respect to forensic casework, Type II errors (saying that two samples originated from the same source when they did not) should be reduced or eliminated, if possible. In other words, although both types of errors pose problems for the forensic examiner, arguably from a forensic point of view data that presents a higher percentage of Type I errors and a lower percentage of Type II errors is preferred over the contrary. After application of the t-test, if the two statistical approaches did not discriminate the samples, then the samples were hence statistically indistinguishable meaning that they share very similar (or statistically the same) elemental profile and were likely from the same source of origin. More specifically, these glass samples probably originated from the same manufacturing plant and were produced at about the same time.

2.4   Results and Discussion

2.4.1   Accuracy and Precision

2.4.1.1   Nanosecond LA-ICP-MS

For nanosecond (ns) LA-ICP-MS, shown in Table 4, considering all of the elements collectively, the accuracy of NIST 1831 was improved (decreased bias) with use of the calibration standard FGS02. The use of NIST 612 as a calibration standard produced the least accuracy, as predicted and shown in a previous study [17]. The associated bias using FGS02 as the calibration standard was found to be less than 5% for most elements. In the case of Sr and Zr, though more different than the reference value (especially in the case of Zr with a bias of 21.2%), the values are in good agreement with the cumulative (mean) values for NIST 1831 obtained in this laboratory over a four year

time period (~100 replicates), namely 76.3ppm and 31.2ppm, respectively. Excellent precision for the nine replicates was obtained (<5%) for the majority of the elements, as shown in Figure 4. The only exceptions are Nd and Hf, where the concentrations are approaching the limits of detection which thus explains why higher %RSDs were obtained. Since the same analytical signal (via integration of the time-resolved spectra) was utilized for each quantification approach, therefore the precision was the same regardless of the quantification approach used.

Table 4. Quantification results for NIST 1831 using different calibration standards, nanosecond LA-ICP-MS, with use of an internal standard. Mean values and standard deviations are in units of parts per million (ppm).

	NIST 612			FGS01			FGS02		
element	mean	std.dev.	% bias	mean	std.dev.	% bias	mean	std.dev.	% bias
Mg	26248.41	293.22	24.0	20657	231	-2.4	21277	238	0.5
Al	6512.83	111.95	2.1	5979	103	-6.3	6368	109	-0.2
Ti	134.57	5.67	18.3	107	5	-6.0	111	5	-2.9
Rb	6.03	0.25	-1.3	7.0	0.3	14.0	5.8	0.2	-5.1
Sr	78.58	2.44	-11.8	80	2	-10.4	79	2	-11.6
Zr	32.01	1.30	-26.2	34	1	-21.2	34	1	-21.2
Ba	30.38	1.65	-3.6	30	2	-5.3	32	2	0.2
La	2.24	0.11	5.5	2.3	0.1	7.2	2.2	0.1	5.4
Ce	4.53	0.26	0.1	4.7	0.3	4.7	4.5	0.3	-0.8
Nd	1.84	0.24	8.9	1.7	0.2	2.9	1.8	0.2	4.8
Hf	0.84	0.11	-22.6	0.9	0.1	-13.6	1.0	0.1	-12.3

Comparing Table 4 (quantification with use of an internal standard) and Table 5 (quantification without an internal standard), particularly looking at the quantification with FGS02 (the best calibration approach for nanosecond LA-ICP-MS), better results were obtained when an internal standard was used. Additionally, a systematic difference between the two data sets (~10%) is also observed, which then improves the accuracy for given elements, such as Sr and Zr.

Table 5. Quantification results for NIST 1831 using different calibration standards, nanosecond LA-ICP-MS, without use of an internal standard. Mean values and standard deviations are in units of parts per million (ppm).

	NIST 612			FGS01			FGS02		
element	mean	std.dev.	% bias	mean	std.dev.	% bias	mean	std.dev.	% bias
Mg	26317.11	3429.53	24.3	25182	3282	19.0	23838	3106	12.6
Al	6521.09	769.24	2.2	7278	859	14.1	7124	840	11.6
Ti	134.66	15.66	18.3	130	15	14.4	124	14	8.6
Rb	6.03	0.70	-1.3	8.5	1.0	38.8	6.5	0.8	6.1
Sr	78.79	10.69	-11.6	97	13	9.3	88	12	-0.9
Zr	32.05	4.06	-26.1	42	5	-4.1	38	5	-11.8
Ba	30.52	4.99	-3.2	37	6	15.9	36	6	12.7
La	2.24	0.32	5.8	2.8	0.4	30.8	2.5	0.4	18.2
Ce	4.54	0.63	0.3	5.8	0.8	27.5	5.0	0.7	11.2
Nd	1.85	0.42	9.7	2.1	0.5	26.5	2.0	0.5	18.1
Hf	0.85	0.19	-22.0	1.2	0.3	5.6	1.1	0.2	-1.1

This improvement in accuracy is not only correlated with the observed systematic difference but is also correlated to an increase in imprecision; the precision is 2 - 4 times better when the internal standard is used for quantification (as noted in Figure 4). Since precision is more critical than bias when comparing/discriminating glass samples analyzed at the same time, quantification with an internal standard is recommended.
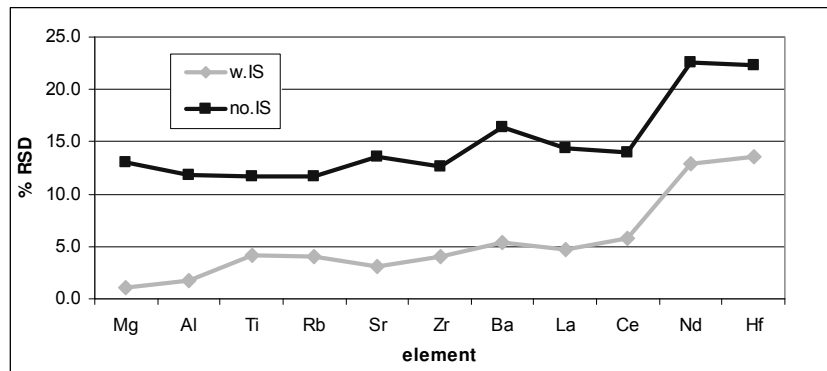
Figure 4. Precision results for NIST 1831 sample replicates, nanosecond LA-ICP-MS, with vs. without use of an internal standard.

2.4.1.2   Femtosecond LA-ICP-MS

With femtosecond (fs) LA-ICP-MS (see Tables 6 and 7) the accuracy of NIST 1831 was also improved by approximately 2-4% when utilizing an internal standard (FGS01). The tables also suggest a ~ 2X improvement in the precision for quantification with an internal standard over the given analytical sequence, which ultimately affects discrimination potential.

Table 6. Quantification results for NIST 1831 using different calibration standards, femtosecond LA-ICP-MS, with use of an internal standard. Mean values and standard deviations are in units of parts per million (ppm).

element	NIST 612			FGS01			FGS02		
	mean	std.dev.	% bias	mean	std.dev.	% bias	mean	std.dev.	% bias
Mg	22647.30	357.18	7.0	19777	312	-6.6	19577	309	-7.5
Al	5209.76	40.32	-18.4	5164	40	-19.1	5452	42	-14.6
Ti	126.07	5.19	10.8	110	5	-3.0	107	4	-6.4
Rb	6.51	0.38	6.6	7.8	0.5	26.9	5.9	0.3	-3.4
Sr	83.05	4.39	-6.8	88	5	-1.0	84	4	-6.1
Zr	30.68	1.67	-29.2	35	2	-19.9	32	2	-25.8
Ba	29.55	1.73	-6.2	31	2	-2.3	30	2	-4.9
La	2.02	0.11	-4.8	2.2	0.1	4.3	2.0	0.1	-7.7
Ce	4.57	0.27	0.9	5.0	0.3	9.3	4.3	0.2	-5.9
Nd	1.65	0.10	-2.2	1.7	0.1	3.3	1.6	0.1	-2.8
Hf	0.83	0.09	-23.8	1.0	0.1	-9.2	0.9	0.1	-14.2

As observed, there is no significant difference in accuracy between the two instrumental setups (compare Table 4 and Table 6); actually, for many elements nanosecond LA-ICP-MS provided better accuracy (less bias) over femtosecond LA-ICP-MS. For quantification with NIST 612, better accuracy was obtained for 3 out of the 11 elements (Al, Rb, and Ba) with nanosecond LA-ICP-MS while Mg, Ti, Sr, and Nd faired better for femtosecond LA-ICP-MS. Nonetheless, this is likely just a product of the ICP-MS (utilized), in which certain elements may perform better on one instrument versus another. For the other two quantification approaches, FGS01 provided greater overall

accuracy for femtosecond LA-ICP-MS and FGS02 provided greater accuracy for nanosecond LA-ICP-MS. Statistically, nanosecond LA-ICP-MS with quantification by FGS02 and use of an internal standard provided the best overall accuracy. The observed improvement in accuracy for nanosecond LA-ICP-MS using FGS02 for quantification is possibly the result of the reference glass values being 4-5 times higher in concentration than the expected concentration for NIST 1831, meaning that this difference in concentration may account for the increased negative bias associated with using another standard at a concentration closer to the expected value, such as with FGS01. The best results for femtosecond LA-ICP-MS in terms of accuracy were obtained when a more similar and matrix-matched standard, like FGS01, was utilized for the quantification of NIST 1831, thus supporting the conclusion of matrix-matched standard and internal standard dependence for accurate femtosecond LA-ICP-MS analyses of glass.

Table 7. Quantification results for NIST 1831 using different calibration standards, femtosecond LA-ICP-MS, without use of an internal standard. Mean values and standard deviations are in units of parts per million (ppm).

	NIST 612			FGS01			FGS02		
element	mean	std.dev.	% bias	mean	std.dev.	% bias	mean	std.dev.	% bias
Mg	21188.21	3036.74	0.1	24016	3442	13.5	18858	2703	-10.9
Al	4873.29	683.73	-23.6	6270	880	-1.7	5251	737	-17.7
Ti	117.78	16.29	3.5	134	19	17.7	103	14	-9.9
Rb	6.07	0.78	-0.6	9.4	1.2	53.6	5.7	0.7	-7.2
Sr	77.45	9.90	-13.1	107	14	19.9	80	10	-9.8
Zr	28.60	3.51	-34.0	42	5	-3.1	31	4	-28.8
Ba	27.53	3.42	-12.6	37	5	18.2	29	4	-8.7
La	1.88	0.25	-11.2	2.7	0.4	26.3	1.9	0.2	-11.4
Ce	4.26	0.51	-6.0	6.0	0.7	32.2	4.1	0.5	-9.7
Nd	1.54	0.15	-9.1	2.1	0.2	24.6	1.6	0.2	-6.9
Hf	0.77	0.07	-29.4	1.2	0.1	9.2	0.9	0.1	-18.2

When comparing nanosecond and femtosecond LA-ICP-MS results in terms of precision, the precision was comparable for the elements under investigation (see Figure 5) with the majority of the values less than 5% RSD for both nanosecond and femtosecond LA-ICP-MS. The observed differences by element are attributed to the instrumental performance for each ICP-MS, where given elements/isotopes may perform better on one or the other optimized LA-ICP-MS system, such as with Nd and Hf for femtosecond LA-ICP-MS where lower detection limits (see the next section) allow for improved quantification and therefore improved precision.
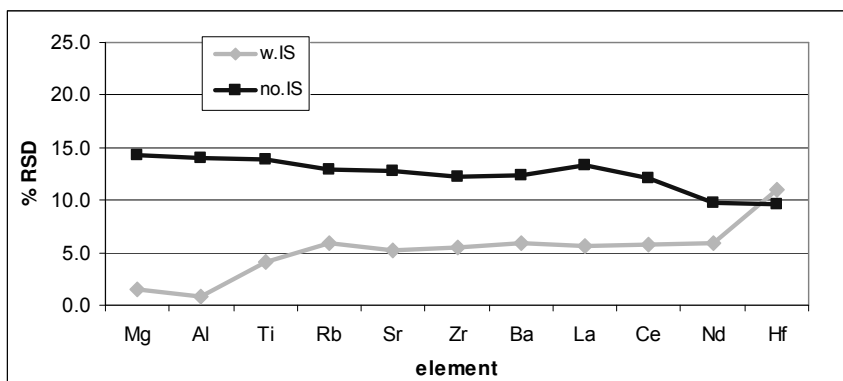
Figure 5. Precision results for NIST 1831 sample replicates, femtosecond LA-ICP-MS, with and without use of an internal standard.

2.4.2   Method Detection Limits

When comparing limits of detection, it is evident that femtosecond LA-ICP-MS provided lower limits of detection, or greater sensitivity on the order of 2-7 times greater, per element than nanosecond LA-ICP-MS. A summary of the respective limits of detection can be found in Table 8. These lower limits of detection are attributed to the higher ablation efficiency (rate) for femtosecond laser ablation as well as ICP-MS

performance, which is also correlated to smaller particle sizes; these advantages have been well documented in the literature [26, 31-34, 44-45]. Despite achieving higher limits of detection for nanosecond LA-ICP-MS, the stated limits of detection are still well below the concentrations found in typical float glass samples, as shown in Table 8 (see "analyte range"). Although lower detection limits are not needed for glass analyses, it should be noted that if lower detection limits are necessary, possibly for other matrices of forensic interest, then femtosecond laser ablation can assist in detecting and quantifying elements close to or lower than the limits of detection demonstrated by nanosecond LA-ICP-MS.

Table 8. Method detection limits for nanosecond (ns) and femtosecond (fs) LA-ICP-MS, respectively. All represented values are in units of parts per million (ppm).

element	ns-LA-ICP-MS	fs-LA-ICP-MS	analyte range
Mg	2.88	1.13	23785.50 - 28717.68
Al	1.34	0.71	433.34 - 3937.77
Ti	3.03	0.54	49.95 - 428.52
Rb	0.14	0.04	0.48 - 4.46
Sr	0.05	0.01	20.77 - 89.02
Zr	0.13	0.02	20.62 - 222.75
Ba	0.32	0.05	5.57 - 38.71
La	0.05	0.01	1.17 - 2.48
Ce	0.05	0.01	1.94 - 4.65
Nd	0.21	0.04	0.69 - 2.24
Hf	0.14	0.05	0.44 - 5.74

2.4.3 Discrimination

In terms of discrimination power, both nanosecond and femtosecond LA-ICP-MS with use of an internal standard provided comparable discrimination (at the 95% confidence interval) for the glass casework sample set used in this study. More specifically, it was determined that all of the possible pairs (55) could be distinguished from each other when using the discrimination capabilities of all the selected elements

combined. A summary of the discrimination results, in terms of the number of indistinguishable pairs and percent discrimination, by element can be found in Table 9. For illustrative and comparative purposes, all elements are shown despite the fact that only three elements (Ti, Sr, and Zr) were necessary to discriminate the glass set by both nanosecond LA-ICP-MS and femtosecond LA-ICP-MS, respectively.

Table 9. Discrimination results, nanosecond (ns) and femtosecond (fs) LA-ICP-MS, with and without use of an internal standard, 55 possible pairwise comparisons.

element	ns-LA-ICP-MS (with IS)		ns-LA-ICP-MS (no IS)		fs-LA-ICP-MS (with IS)		fs-LA-ICP-MS (no IS)	
	No. pairs indistin.	percent discrim.	No. pairs indistin.	percent discrim.	No. pairs indistin.	percent discrim.	No. pairs indistin.	percent discrim.
Mg	54	1.8	53	3.6	23	58.2	12	78.2
Al	24	56.4	34	38.2	6	89.1	20	63.6
Ti	15	72.7	21	61.8	12	78.2	11	80.0
Rb	32	41.8	37	32.7	22	60.0	27	50.9
Sr	7	87.3	23	58.2	10	81.8	10	81.8
Zr	6	89.1	17	69.1	2	96.4	7	87.3
Ba	16	70.9	19	65.5	6	89.1	9	83.6
La	26	52.7	34	38.2	17	69.1	16	70.9
Ce	22	60.0	27	50.9	15	72.7	14	74.5
Nd	36	34.5	32	41.8	16	70.9	17	69.1
Hf	12	78.2	22	60.0	5	90.9	9	83.6
combined	0	100.0	3	94.5	0	100.0	0	100.0

Although the same conclusion was reached (100% discrimination) for both systems when using an internal standard, the discrimination power per element was improved for femtosecond LA-ICP-MS, with the exception of Sr where nanosecond provided 6.5% better discrimination power. The improved discrimination is especially noticeable for some of the more trace (or less concentrated) elements in the element menu for femtosecond LA-ICP-MS, such as Rb, La, Ba and Nd. This observed increase in discrimination can be attributed to the lower detection and therefore greater precision observed across the sample set for femtosecond LA-ICP-MS for some elements, which in turn improved discrimination potential.

The samples were also compared without use of an internal standard. Because of the lack of precision (higher %RSDs) observed for nanosecond LA-ICP-MS, the discrimination power per element was on the order of approximately 2-3 times less. In addition, discrimination analysis combining all elements by nanosecond LA-ICP-MS (without internal standard) yielded 3 indistinguishable pairs. The samples found indistinguishable were not from the same source and did not originate from the same manufacturing plant at about the same time period, therefore not utilizing an internal standard resulted in a Type II error (false inclusion). From a forensic standpoint, committing this type of error should be avoided, which stresses again the importance of using an internal standard for nanosecond LA-ICP-MS glass analyses. For femtosecond LA-ICP-MS without use of an internal standard still provided 100% discrimination, which is remarkable considering the slightly higher degree of imprecision associated without use of an internal standard. As stated, besides having a high degree of variation (or at least detectable variation) with respect to the elemental profiles of the samples being compared, the other major contributing factor for sample discrimination studies will always be sample precision. The precision was superior across the sample replicates for femtosecond LA-ICP-MS even for quantification without use of an internal standard (in most cases values < 5% RSD were obtained).

The precision across the sample set for both nanosecond and femtosecond LA-ICP-MS (for elements Ti, Zr, and Sr) is illustrated in Figures 6 and 7, these figures demonstrate how similar the precision obtained for both systems was when an internal standard was utilized during quantification.
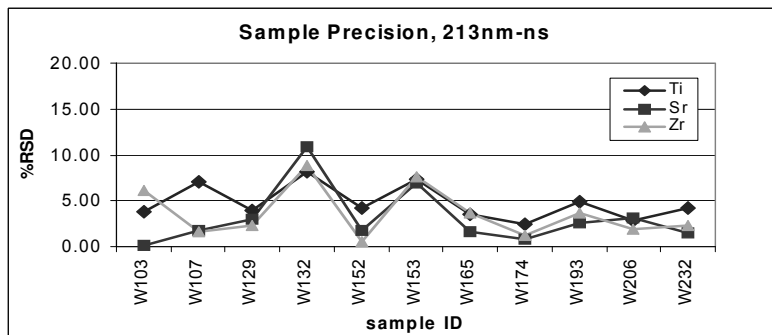
Figure 6. Sample precision for Ti, Sr and Zr across the FDLE casework glass set used for discrimination, nanosecond LA-ICP-MS.
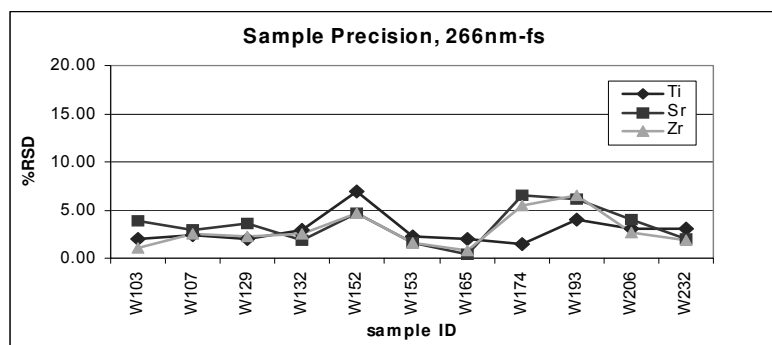
Figure 7. Sample precision for Ti, Sr and Zr across the FDLE casework glass set used for discrimination, femtosecond LA-ICP-MS.

The observed precision for the sample set is different when compared to the precision observed for the 9 replicates analyzed for NIST 1831, where precision values for femtosecond LA-ICP-MS without use of an internal standard were between 10–15% RSD. One explanation for this difference can be found by looking to the analysis sequence itself. Breaking down the 9 replicates into groups of three (three replicates of NIST 1831 were analyzed at the beginning, mid, and end of the sequence), the precision of each group is comparable to that observed for the sample precision by femtosecond LA-ICP-MS without use of an internal standard. Therefore, when sample replicates are

43

run concurrently, as was the case for the discrimination study, it is apparent that good precision can be obtained when an internal standard is not utilized for femtosecond LA-ICP-MS thus leading to a higher degree of discrimination potential. However, the accuracy of the respective measurements is less (note the analysis of NIST 1831) wherein the comparison values are then subject only to the analytical signal (not normalized to an internal standard), which can fluctuate over time. Thus, comparisons of samples over different days or even over the course of a single day would be inaccurate and thus lead to a potential increase in Type I and Type II errors. Therefore, it is recommended that use of an internal standard when quantifying and comparing glass samples even for femtosecond LA-ICP-MS.

As an illustration to demonstrate the similarities in the data used to discriminate the casework samples by nanosecond and femtosecond LA-ICP-MS, the percent composition per sample are shown in Figures 8 and 9. It can clearly be seen that almost identical elemental profiles were observed for each of the 11 casework samples for nanosecond and femtosecond LA-ICP-MS, respectively when using an internal standard for quantification purposes. Although illustratively plotted here in % (with 100% equivalent to the three elemental percentages combined), the actual composition of these elements is in the low to mid parts per million (ppm) range. Hence, overall from precision to accuracy to discrimination potential, similar results were obtained for femtosecond and nanosecond LA-ICP-MS when using an internal standard and an appropriate quantification standard.
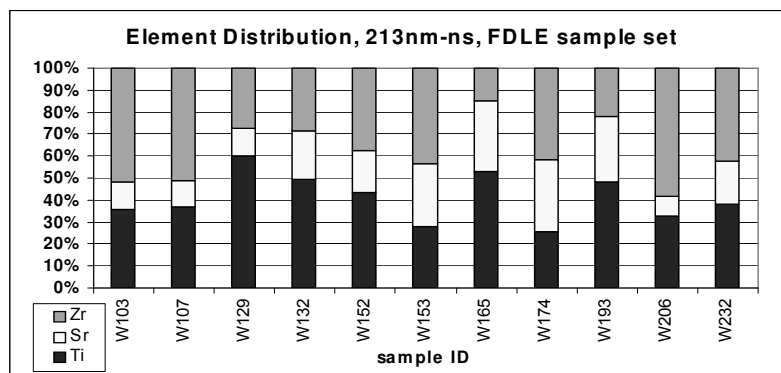
Figure 8. Elemental distribution across the FDLE casework glass set for three elements (Zr, Sr and Ti), nanosecond LA-ICP-MS.
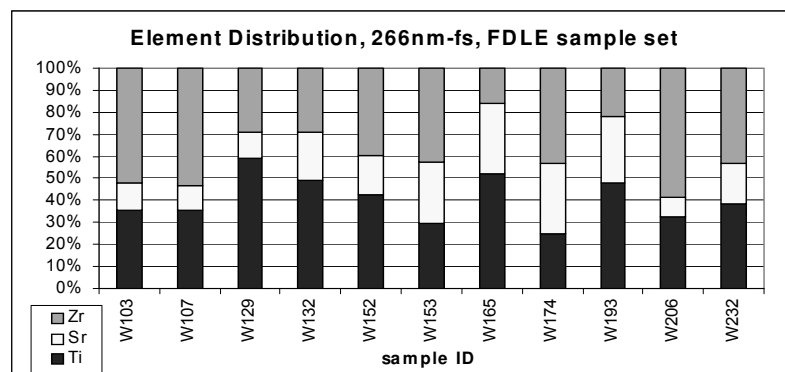
Figure 9. Elemental distribution across the FDLE casework glass set for three elements (Zr, Sr and Ti), femtosecond LA-ICP-MS.

2.5   Conclusions

Two different LA-ICP-MS systems, a nanosecond (ns) LA-ICP-MS and a femtosecond (fs) LA-ICP-MS, were utilized for quantitative analysis of float glass standard reference material (NIST 1831). Three quantification approaches were compared (SRM NIST 612 and reference glasses FGS01 and FGS02 as calibrators) with and without the use of an internal standard (^{29}Si). Nanosecond and femtosecond LA-ICP-

MS were compared in terms of the figures of merit important to any analytical method, accuracy, precision, and limits of detection, and for forensic cases, discrimination power. The results demonstrate that the use of an internal standard is necessary for most of the elements analyzed. In terms of accuracy and precision, nanosecond LA-ICP-MS and femtosecond LA-ICP-MS provided comparable results for the quantification of NIST 1831. The greatest accuracy when quantifying NIST 1831 was obtained when reference glasses FGS02 for nanosecond LA-ICP-MS and FGS01 for femtosecond LA-ICP-MS, respectively, were used. These particular quantification standards are more matrix-matched to NIST 1831 (and to float glass samples collected from crime scenes) than NIST 612, ultimately meaning that accuracy for both nanosecond and femtosecond LA-ICP-MS is dependent on the quantification approach used.

Nanosecond LA-ICP-MS had higher detection limits (lower sensitivity) than femtosecond LA-ICP-MS where limits of detection were on the order of 3-10 times lower. Nevertheless, detection limits for nanosecond LA-ICP-MS were well below the typical concentrations found in glass samples collected from most crime scenes. Thus, lower detection limits achieved by femtosecond LA-ICP-MS did not provide any additional advantage over nanosecond LA-ICP-MS in this case. Femtosecond LA-ICP-MS also yielded slightly better discrimination power per element (~ 2-3% more discrimination per element when compared to nanosecond LA-ICP-MS). However when all the casework samples were compared using a combination of all 11 elements in the detailed method (and representing major, minor, and trace elements), both nanosecond and femtosecond LA-ICP-MS were able to discriminate all of the 55 possible pairs (or 100% discrimination power). As a result of the reduced precision associated with the

quantified glass sample replicates when an internal standard was not used, three pairs were found indistinguishable by ANOVA for nanosecond LA-ICP-MS that should have been discriminated (evidence of Type II errors); these pairs were discriminated by application of a t-test. Femtosecond LA-ICP-MS without the use of an internal standard and combining all elements for discrimination also provided 100% discrimination power. However, it is more likely that Type I and Type II errors would be increased when comparisons are made without use of an internal standard, particularly when samples are analyzed in different sequences or on different days. Thus, it is suggested that a quantification approach that employs an internal standard be utilized even for femtosecond LA-ICP-MS when analyzing glass samples.

Overall, nanosecond LA-ICP-MS and femtosecond LA-ICP-MS provided similar figures of merit in terms of accuracy, precision and discrimination power, the exception was that lower method detection limits were achieved for femtosecond LA-ICP-MS. Therefore despite this advantage, which is considered to be negligible since the detection limits for nanosecond LA-ICP-MS were well below the concentrations found in typical float glass samples, the additional cost of a femtosecond laser would be very difficult to justify for glass sample analyses and comparisons in typical forensic laboratories.

3   LIBS FOR THE ELEMENTAL ANALYSIS AND DISCRIMINATION OF GLASS, A COMPARISON TO MICRO-XRF AND LA-ICP-MS

3.1   Glass Matrix

Since this chapter also discusses the analysis of glass, the matrix related discussions that have preceded this chapter are also relevant here. Therefore, for more information regarding the elemental composition of glass, please refer to chapter two.

3.2   Elemental Analysis of Glass by LIBS

Laser induced breakdown spectroscopy (LIBS) is a relatively new application for the forensic analysis of glass. However, within the last few years, three studies were published regarding the utility of this technique for forensic glass comparisons and each had a different approach (especially in terms data analysis). The short list includes some of the work presented in this dissertation, which also appears in a publication regarding the discrimination potential of LIBS [46]. Research presented by Rodriguez-Celis et al. demonstrated the use of linear and rank correlations to compare glass samples (comparing entire LIBS spectra and/or by masking parts of the associated spectra) and it was concluded that 100% identification of glass samples in the collected set was achieved [47]. In the other publication, by Bridge et al., LIBS was used to achieve 83% discrimination of glass samples using pairwise comparison analysis and use of element ratios [48], however, there was no mention of how Type I or Type II errors were tested for and reduced or eliminated. In addition, Bridge et al. used different detector gate delays, between 2.0μs to 6.5μs depending on the sample being analyzed [48]. The large variations in the gate delays ultimately affects the spectra generated and the result is that

different emission lines are present or absent, which is dependent on plasma evolution characteristics. As a result, if samples are being compared for discrimination purposes, as they were in the referenced paper [48], it is absolutely necessary that all parameters remain constant in order to achieve the most accurate comparisons possible.

3.3   Methodology

3.3.1   Introduction

Herein, I describe the analysis and discrimination of a float glass sample set of forensic interest by LIBS and its subsequent comparison to the discrimination results obtained for two other elemental analysis techniques, µXRF and LA-ICP-MS. The data presented in this chapter was a product of a collaborative effort amongst different research groups, including µXRF data acquisition and analysis by Scott Ryland at FDLE, sample collection (of the 41 glass sample set used for the comparison) and LA-ICP-MS data acquisition by Sayuri Umpierrez (a former master's student under Dr. Almirall), and LIBS data acquisition and analysis, assisted by Dr. Cleon Barnett (a former post doctoral associate in the Almirall laboratory).

In addition to the comparative study already mentioned, some early LIBS results (and the methodology behind those results) have been included mainly because the results show some advantages of using dual pulse LIBS in comparison to single pulse LIBS that may be of use to those who may follow up on this work. At any rate, after obtaining what were thought to be optimum parameters (obtained with a commercial LIBS system), the same 41 glass sample set (under investigation in the comparison study) was analyzed and the results were far less than stellar when compared to say LA-ICP-

MS. Therefore, the methodologies and results from this early work were added simply as an illustration of the initial failures encountered and, more importantly, the great progress that was made with respect to handling of LIBS data for forensic glass comparisons. The early work has been characterized (and subsequently marked) as LIBS (Early Crossfire Studies) while the most recent LIBS methods and results are simply called just LIBS; hopefully this will help reduce any potential confusion.

3.3.2   Instrumentation

3.3.2.1   LIBS Principles and Considerations

Although laser induced breakdown spectroscopy (LIBS) has been around for many years, the technique as an analytical chemistry tool is relatively new. In terms of analytical chemistry, LIBS falls under the broad category of atomic emission spectroscopy, and therefore the same fundamentals with respect to sample (or element) absorption and excitation apply to LIBS as well.

In brief, during a LIBS experiment, a laser to sample interaction causes an emission of light from the sample surface, the emission produced by this interaction is characteristic of the composition of the sample. The emitted light can then be collected via a basic optical spectrometer, which translates the captured light into an emission spectrum, which ultimately can be used for characterization purposes. More specifically, in typical LIBS experiments, a high powered laser is focused onto a sample surface, within picoseconds free and loosely bound electrons in the sample matrix interact with the laser pulse [18, 49-50]. The pulse width for LIBS is typically in the ~3-5ns range for reasons that will become evident as the processes are described. The electron interaction

with the laser pulse occurs through inverse bremsstrahlung processes as additional electrons (from the sample) are ejected via energetic collision [18, 49-50]. The process (or ionization cascade) repeats and repeats, with the free electrons absorbing energy from the laser pulse, which then cause additional collisions and in turn cause additional electrons to be emitted from the sample matrix, until a thermally hot laser induced plasma evolves from the sample surface [18, 49-50]. Plasma evolution into the microsecond time scale results in electronic and ionic recombination, which causes the plasma to cool and eventually extinguish as the molecules and atoms relax from the excited state down to the ground state. The relaxation step is characterized by a wealth of atomic, ionic and even molecular emission lines, which in turn can help determine sample composition and thus makes analytical chemistry possible [18, 49-50].

3.3.2.1.1 Advantages of LIBS

A LIBS setup is fairly simple, less complex and rather inexpensive compared to laser ablation. The major components of a LIBS system includes a laser source (or multiple laser sources for dual pulse setups), a spectrometer equipped with a fiber optic cable, a set of optics to deliver the laser pulse and capture the emitted light, and a device (computer or delay generator) to control and synchronize the triggering of the laser and spectrometer, respectively. Multiple emission events in conjunction with the generated laser induced plasma at each laser pulse interval can be captured spectrally and stored in a relatively short period of time. Therefore, sample throughput is high; actually it takes more time to qualitatively analyze a given spectrograph than it does to collect it.

3.3.2.1.2 Disadvantages of LIBS

The drawbacks related to LIBS includes higher degrees of imprecision (% RSDs typically > 10%), higher limits of detection (in the ppm range) [49], and those issues that are just grouped together because of the "infancy" of the technique, such how to handle the data (data analysis) as well as the analytical approach itself. In addition, a flat sample surface for LIBS analyses is often necessary to ensure optimum laser to sample interaction and optimal detection, this is especially important when making sample comparisons. Nonetheless, the flat surface requirement can be countered simply by the utilization of a pliable mounting media, such as clay, as long as the mounting media does not contaminate the sample. And, in relation to that, slightly larger sample sizes due to sample destruction may be necessary in comparison to laser ablation, especially in the case where a laser operating at 1064nm (~100mJ) is utilized, which results in a considerable amount of surface damage in comparison to a UV laser (at maximum energy).

3.3.2.2 Figures of merit for LIBS, µXRF and LA-ICP-MS

Despite the disadvantages mentioned in the last section, the instrumentation is comparatively inexpensive in relation to the more mature analytical techniques of µXRF and LA-ICP-MS. In addition, LIBS is less complex to operate, it has the capability for portability, and the analyst can generate large quantities of data over a short period of time (a rapid approach to elemental analysis). A general comparison of these three techniques (LIBS, µXRF and LA-ICP-MS can be found in Table 10.

Table 10. Figures of merit comparison for LIBS, µXRF and LA-ICP-MS. Some details were adapted from Almirall JR, Trejos T (2007) Forensic Sci Rev 18:73-96 [7].

Parameter	µXRF	LA-ICP-MS	LIBS
Operating Principle	Highly energetic X-rays knock out an inner shell electron. Relaxation of an outer shell electron into the vacant position causes emission of characteristic X-rays	Laser photons remove material from sample. Submicron-sized particles are transported into the ICP which atomizes and ionizes the ablated material; ions are detected by MS	Laser photons induce matrix breakdown at sample surface. Characteristic emission lines are produced in the UV, VIS, and near IR range
Accuracy	Semi-quantitative	Quantitative	Semi-quantitative
Precision	Fair – good (5-10% RSD)	Excellent (< 5% RSD)	Fair – good (5-20% RSD)
Sensitivity	100 ppm	< 1 ppm	10 - 50 ppm
Discrimination	Very good - excellent	Excellent	Good – very good
Complexity	Easy to use	Difficult to use	Very easy to use
Sample Consumption	Nondestructive	Almost nondestructive	Almost nondestructive
Throughput	~30 min / analysis	~3 min / analysis	~30 sec / analysis
Cost	~ $120,000	~ $210,000	$50,000 - $150,000

3.3.2.3 LIBS Systems Description

3.3.2.3.1 LIBS (Early Crossfire Studies)

The very first ("version 001") Photon Machines Crossfire LIBS system (San Diego, CA), which has since been commercialized, was used for the initial LIBS experiments involving glass analysis and comparisons. The particular device, which has since been replaced by the second generation Crossfire system, was developed with the intension to conduct LIBS measurements in a less complex and more user-friendly environment. With this approach, the analyst would not need a wealth of knowledge or experience regarding the technique, which makes it marketable to analytical laboratories.

The Crossfire system had a camera to view the sample and a software program that allowed the operator to control everything from detector and laser pulse delays to laser energy, etc. Nevertheless, the intensions of user friendliness vanished nearly after arrival and setup. The instrument, and use thereof, became complicated and oftentimes it took manipulation of the optics and creation of man-made devices to position parts, like the fiber optic cable to make spectroscopic measurements to achieve the desired analytical signal. As a result, the initial goals of the device were reversed.

Nonetheless, the initial Crossfire had the capability of doing single, dual and even triple pulse LIBS experiments. Data regarding both single and dual pulse experiments can be found in the results and discussion section. The parameters by which spectral analysis was conducted with the Crossfire can be found here. The Crossfire system was equipped with two Q-switched Nd:YAG lasers: a New Wave Research Tempest laser (Fremont, CA) operating at 266nm (with a pulse width of 3-5ns, ~25mJ energy per pulse) and a New Wave Research Solo PIV laser (Fremont, CA) operating at 1064nm (3-5ns pulse width, ~100mJ) situated orthogonal to the UV laser. The PIV laser had a dual laser head and thus could be used to deliver laser pulses simultaneously from the same source. An Andor Mechelle 5000 Spectrometer equipped with an ICCD, with a spectral range of 200-950nm and a resolution of R=5000, was utilized for spectroscopic measurements. More details concerning the equipment above can be found in the next section.

For the single pulse experiment, the 266nm laser was utilized at full energy (~25mJ) and the laser was fired at a 1Hz repetition rate, the gate delay on the spectrometer was 1μs with a gate pulse width of 10μs, and a total of 10 spectra were accumulated (which coincided with 100 laser shots). The fiber optic cable was manually

positioned at a 45° angle (to the sample surface) and argon gas was blown onto the sample surface. The use of argon had previously been determined to provide signal enhancement. For the dual pulse experiment, the same parameters were utilized with the exception of the gate delay, which had to correlate to the second pulse (IR, 1064nm) fired orthogonal to the first pulse (UV, 266nm) at a 0.5μs delay; thus, the detector delay was set at 1.5μs to capture the plasma reheating and hence signal enhancement.

3.3.2.3.2 LIBS

Experiments were conducted using a custom LIBS system constructed at FIU by a former post doc in our lab, Dr. Cleon Barnett. The LIBS system was equipped with a New Wave Research Q-switched Nd:YAG Tempest laser (Fremont, CA) operating at 266nm and a pulse width of 3-5ns (full width half maximum), which was chosen for this analysis due to an observed improved laser-to-sample interaction with glass and thus improved precision (as versus the laser typically used for LIBS analyses, 1064nm). A 3X beam expander was utilized to enlarge the beam diameter to approximately 11mm. The laser beam was then focused perpendicular to the sample surface using a plan-convex lens with a focal length (f) of 150mm. Laser energies of ~25mJ per laser pulse and a spot size of approximately 190μm remained constant throughout the analytical sequence and all LIBS analyses were conducted under atmospheric pressure in air. Light (emission) from the laser induced plasma was imaged from the side (parallel to the sample surface or 90° in relation to the laser beam being fired) by a pair of plano-convex lenses (f=75mm) which focused and transmitted the laser induced plasma emission into an optical fiber that had a diameter of 50μm. The fiber optic cable was coupled to the entrance slit of an

Andor Mechelle 5000 spectrometer (South Windsor, CT) equipped with an Andor iStar Intensified Charge Coupled Device (ICCD), which converted the image of the light being emitted at laser to sample interaction into a spectrograph. The spectral range collected for each sample ranged from 200-950nm with a resolution of ~5000. The repetition rate for the spectrometer was set at 0.67Hz, at this repetition rate the spectrometer could capture a complete set of data (full spectrum) for each laser shot. Both the laser flashlamp and the Q-switch were externally controlled using a Berkeley Nucleonics' Model 565 Delay Generator (San Rafael, CA), which allowed for all signals being sent by each of the respective devices to be in sync in conjunction with the optimized program. The emission lines generated by the laser induced plasma were accumulated at a 1.2µs delay upon plasma ignition with an integration width of 3.5µs. The term accumulated in the previous sentence means that all the acquired spectra were added together to arrive at one cumulative spectrum, although software did permit the analyst to look at each of the spectra in that accumulated signal if warranted. A schematic of the LIBS setup utilized for this part of the study can be found in Figure 10.
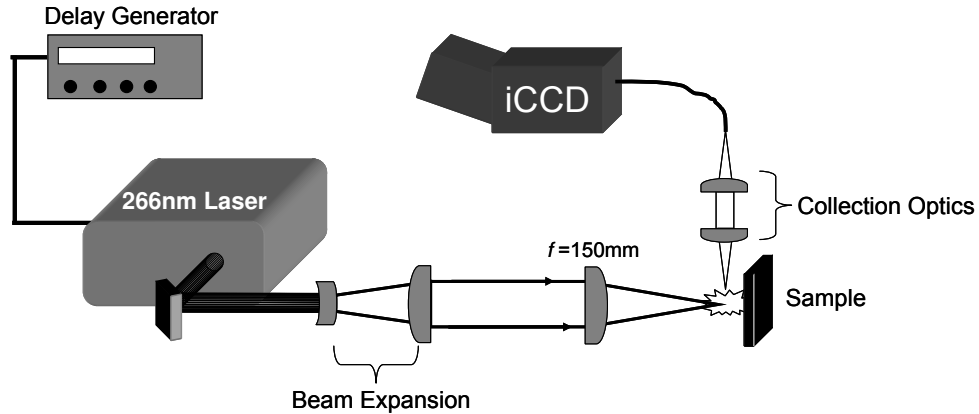
Figure 10. Experimental setup for LIBS measurements. iCCD stands for intensified charge-coupled device and f is the focal length.

3.3.2.4 µXRF Principles and Considerations

Since the current chapter deals primarily with the forensic analysis of glass by LIBS and its comparison to the two leading techniques used in forensic labs for elemental analysis, LA-ICP-MS and what this section encompasses micro X-ray fluorescence (µXRF), only a few statements will be made regarding the theory behind µXRF. With XRF sample excitation is brought about by focusing a X-ray beam onto the surface, absorption of the primary beam causes relaxation and elements will emit their own characteristic X-rays which are typically captured by an energy dispersive detector where simultaneous detection of multiple element is possible [36]. Most applications involve the utility of µXRF for qualitative purposes, although semi-quantitative and quantitative analyses are possible when matrix-matched standards are available. The main disadvantages include larger sample size requirements (than LA-ICP-MS and possibly LIBS depending on the laser utilized) and the necessity of having a flat surface for proper µXRF analyses. Despite some disadvantages, the main advantage and its attractiveness

to forensic labs is that µXRF is a nondestructive technique, which can be used for many types of analyses, such as forensic paint examinations [7].

3.3.2.5 µXRF System Description

An EDAX Eagle Micro X-Ray Fluorescence Spectrometer (Mahwah, NJ) equipped with a rhodium X-ray tube was utilized for the µXRF part of the study. The instrument was operated with a 40kV excitation potential, a 17µs time constant, and 40-45% dead time. Other instrumental parameters for the stated device included a 300µm diameter focusing capillary and 1200s of live count time. The sample chamber was operated under low vacuum conditions.

3.3.2.6 LA-ICP-MS Principles and Considerations

The background information stating the principles behind and utility of LA-ICP-MS for forensic glass analyses was covered in chapter two.

3.3.2.7 LA-ICP-MS System Description

A New Wave Research UP213 Laser Ablation system (Fremont, CA) coupled to a Perkin Elmer ELAN 6100 DRC II ICP-MS (Waltham, MA) was used for the LA-ICP-MS part. The parameters, including the ICP-MS conditions, can be found in Table 1. For ease of reference, however, the laser equipped in the ablation system was a Nd:YAG (4 ns) Q-switched laser operating at 213nm and 100% energy (27.2 J/cm^2 fluence). Single spot ablation mode was used with a spot size of 55µm and a repetition rate of 10Hz, the time length for sampling was 60sec. Helium with a flow rate of 0.9 L/min was the carrier gas into and from the ablation chamber, the carrier gas then coupled to argon (1 L/min) prior

58

to entering the ICP. The ICP-MS parameters included an RF power of 1500W, a plasma gas (argon) flow rate of 16 L/min, an auxiliary (argon) flow rate of 1 L/min, and a dwell time of 8.3 ms.

3.3.3 Sample Descriptions

3.3.3.1 Glass Standards

Standard reference materials NIST 612 and NIST 1831 were utilized for optimization of each of the aforementioned instrumental setups (LIBS, μXRF and LA-ICP-MS). These two standard reference materials were used either for direct optimization, quantification, or for quality control purposes. More specifically, the standards were used for optimization and quality control measures for LIBS and XRF. For LA-ICP-MS analyses, NIST 612 was used as an external calibration source ultimately for quantitative analysis of the glass sample set while NIST 1831 was used as a calibration verification sample (second source check standard) to ensure optimum accuracy and precision across the given sample sequence.

3.3.3.2 Automotive Glass Sample Set

The sample set of interest in this study was comprised of 41 different automotive glass fragments extracted directly from 14 different vehicles located in junkyards in and around Miami, FL. The respective glass sample set included seven side window fragments, 6 rear window fragments, and 28 laminate windshield fragments (which comprised 14 inside and 14 outside samples/fragments). All of the associated glass samples came from automotive vehicles produced between the years of 1995 and 2005.

For each of the three analytical techniques (LIBS, µXRF and LA-ICP-MS), the non-float side of the glass samples was used for analysis.

3.3.4 Data Analysis

3.3.4.1 LIBS (Early Crossfire Studies)

Sample replicates were analyzed by accumulating 10 LIBS spectra into one spectrum (a feature of the spectrometer), with three replicates per sample. Further data reduction was performed using Origin software (OriginLab Corporation, Southampton, MA) wherein peak selection occurred and the associated intensities were transferred into an Excel spreadsheet where means, standard deviations, and %RSDs were tabulated.

Peak selection included the following emission lines: 285.5nm (Mg), 317.9nm (Ti), 407.7nm (Sr), 445.5nm (Ca) and 646.3nm (Fe). These peaks were chosen on the basis of their presence in the samples and associated peak presence when NIST 1831 was analyzed (for peak verification purposes). Other factors that influenced the selection of these particular lines included peak shape and what appeared to be variation in intensities across the sample set. These peak intensities (correlated to an element) were then ratioed to each other, which increased the precision of the sample replicates. Thus, all ten possible ratios were used for discrimination purposes, the list included: Ti/Fe, Mg/Fe, Ti/Ca, Ca/Sr, Fe/Sr, Ti/Sr, Ca/Mg, Ti/Mg, Ca/Fe and Mg/Sr. The same discrimination protocol mentioned in chapter two was followed here, which consisted of ANOVA with Tukey's honestly significance test, using the 95% confidence interval.

3.3.4.2 LIBS

Each sample replicate LIBS spectrum was collected as a result of accumulating spectra for 50 laser shots. After each spectrum was acquired, the sample was rotated to a new spot for a total of 5 spots or replicate analyses per sample. Twenty-two (22) peaks/emission lines were initially chosen for data analysis based on their presence across all 41 glass samples; the selected peaks included 9 different elements, Al, Ca, Fe, K, Mg, Na, Si, Sr and Ti. Both peak intensities (peak heights) and peak areas (via integration) were evaluated statistically with respect to the sample replicates; it was observed that peak areas provided greater precision when compared to just using peak heights or intensities. Since precision is an important factor in discriminating samples, peak areas were utilized for further data reduction purposes. From the 22 peak areas detailed above, every possible ratio was performed and compared with respect to discrimination potential; this resulted in 231 possible ratios [N(N-1)/2 where N is the number of peaks].

Since extensive work was conducted with respect to determining the optimum data analysis approach for glass data generated with the LIBS setup, the steps taken and the reasoning behind the final discrimination approach will be discussed in part here and then finished in the Results and Discussion section. In brief (and somewhat of a prelude of things to come), discrimination for each individual ratio was conducted on the 41 glass set using a student t-test at the 95% confidence interval to coincide with the confidence intervals utilized for LA-ICP-MS and µXRF and thus make the comparison between techniques more valid. A program was created by my colleague Dr. Cleon Barnett using Mathematica (Wolfram Research, Champaign, IL), which assisted greatly with many of the necessary determinations made with respect to how to efficiently and effectively

analyze LIBS data (including peak selection, integration and precision assessments, etc.), with the ultimate goal to optimize glass discrimination by LIBS.

One of the most important steps in determining what protocol for LIBS data analysis for glass comparisons should be followed was the utility of a 42nd sample fragment as a quality control measure. The 42nd sample was the same sample analyzed twice during the analytical sequence, once towards the middle of the run and again at the end, and thus the elemental composition was exactly the same as a previous sample. The sample duplicate was treated as an individual sample throughout the entire analytical approach and was then used to eliminate ratios that provided a false exclusion (or Type I error), meaning that the same sample was discriminated when it came from the same source of origin. Based on this factor, 146 ratios (out of 231) gave a false exclusion whereas 85 ratios made the accurate conclusion, namely that the same sample was found indistinguishable.

Of these 85 ratios, 10 were selected based on their respective degrees of discrimination; note that associated ratios were not repeated, such as 394.4nm/460.7nm (Al/Sr) and 460.7nm/394.4nm (Sr/Al), despite having equivalent and/or greater discrimination power than a non-associated ratio. These 10 ratios and their individual discrimination results are reported in Table 11. The final step in this approach was to limit the number of ratios utilized for discrimination to only 6 ratios (of the 10) in combination in order to remain consistent with the number of ratios used to discriminate the sample set by μXRF, which was also 6.

Table 11. The ten element ratios used for discrimination of the glass sample set by LIBS.

#	peak ratio	description	# indist.pairs	% discrimination
1	394.4nm / 330.0nm	Al/Na	70	91.5
2	766.5nm / 643.9nm	K/Ca	84	89.8
3	394.4nm / 371.9nm	Al/Fe	86	89.5
4	438.4nm / 766.5nm	Fe/K	90	89.0
5	534.9nm / 766.5nm	Ca/K	91	88.9
6	371.9nm / 396.2nm	Fe/Al	91	88.9
7	766.5nm / 645.0nm	K/Ca	93	88.7
8	394.4nm / 460.7nm	Al/Sr	104	87.3
9	460.7nm / 766.5nm	Sr/K	104	87.3
10	818.3nm / 766.5nm	Na/K	141	82.8

3.3.4.3 µXRF

Five replicate analyses were performed on each glass fragment in the 41 glass sample set with a sampling target area defined by the 300µm diameter X-ray spot. The element menu consisted of six elements (K, Ca, Ti, Fe, Sr, and Zr) and respective peak intensities were acquired per element for each sample. Taking these sample peak intensities, further data reduction was conducted where the element intensities were subdivided into six element ratios (Ca/Fe, Sr/Zr, Ca/K, Fe/Zr, Fe/Sr and Fe/Ti) to be used for sample comparison/discrimination purposes. The intensities of the K alpha peaks corresponding to each of the respective elements were determined following background subtraction utilizing peak de-convolution and generation software. These particular element ratios are routinely used for glass casework examinations at FDLE and are the product of many years of experience and discrimination studies conducted by Scott Ryland at FDLE. In addition, the match criteria used routinely at FDLE is a three sigma criterion, which was followed for all sample (pairwise) comparisons by µXRF. More specifically, the three sigma rule characterizes a sample (via the ratios mentioned earlier)

based on the mean value (of all the sample replicates) ± three times the standard deviation. If a collective sample ratio overlapped with another sample ratio, then the two pairs were declared to be indistinguishable by the three sigma criterion. If there was no statistical overlap between two sample signals (or ratios in this case) then the samples were discriminated. At any rate, the pairs found indistinguishable were subjected to a t-test at the 95% confidence interval and some pairs within the sample set were further discriminated (thus reducing the amount of indistinguishable pairs and increasing the percent discrimination for that approach).

3.3.4.4 LA-ICP-MS

Three replicates (pertaining to different sampling or ablated spots) for each sample were analyzed by LA-ICP-MS. The element menu for this technique included five isotopes chosen due to their excellent discrimination power: ^{49}Ti, ^{85}Rb, ^{88}Sr, ^{90}Zr, and ^{137}Ba with ^{29}Si used as the internal standard. The quantification of each elemental concentration was calculated using Glitter software (Macquarie Ltd, Australia), where a single point calibration source (NIST 612) and the internal standard (^{29}Si) were used to convert intensity (counts per second) via integration of time-resolved spectra into concentration (in ppm). The resulting elemental concentrations were then used to characterize the given samples and ultimately to associate two glass fragments (meaning indistinguishable or what forensic examiner's would call a match or "likely to have originated from the same source) or to discriminate a given glass fragment from another fragment (meaning they are significantly different with respect to elemental composition).

The data analysis utilized for the LA-ICP-MS results included a combination of pairwise comparison analysis using ANOVA in Systat 11 (San Jose, CA) with Tukey's honestly significant difference test (HSD). The pairs found indistinguishable by pairwise comparison analysis were subjected to a t-test at the 95% confidence interval (via Microsoft Excel, Redmond, WA). Thus, a given pair found indistinguishable using the combination of the two data analysis strategies was ultimately determined indistinguishable, meaning the fragments have very similar (almost exact) elemental profiles and likely were produced in the same manufacturing plant at approximately the same time.

3.4 Results and Discussion

3.4.1 LIBS (Early Crossfire Studies)

Upon acquisition of Photon Machine's multi-pulse capability device, work in the area of method development had to be performed prior to any actual sample analysis. The parameters addressed included the number of shots and acquisitions, the gate pulse width, the detector gate delay, argon pressure (or non-use), etc. Once a method was established for both single (UV, 266nm) and double pulse LIBS (UV, 266nm → IR, 1064nm), the glass sample set consisting of 41 automotive glasses was analyzed.
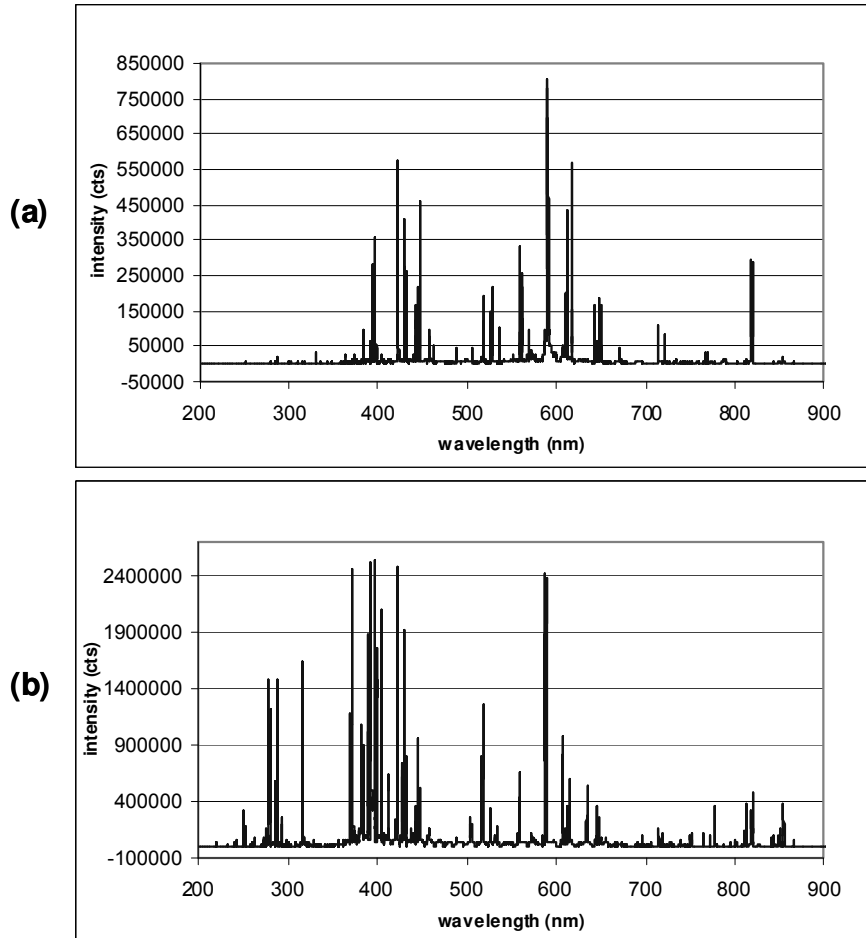
Figure 11. (a) Single pulse LIBS and (b) dual pulse LIBS spectra for a float glass sample.

Figure 11 shows the effects of dual pulse LIBS full spectrum, as compared to single pulse LIBS for sample 1 in the 41 glass sample set. Notice that in the dual pulse experiment [Figure 11(b)], the signal is enhanced by a factor of about 30, depending on the peak and the spectra is more "rich" (or abundant) in spectral lines. It is important to point out that the scaling on the y-axis (intensity) between Figure 11(a) and 11(b) is different so it may appear that some single pulse peaks are larger than the dual pulse experiment when they really are not. Dual pulse LIBS provided greater sensitivity, but as discussed it also generated additional spectral lines that may (or may not) be helpful with

sample characterization and ultimately discrimination. By expanding the baseline and overlaying the respective spectra (dual pulse spectra plus single pulse spectra) as in Figure 12, these differences and enhancement effects can be further visualized. More specifically, for the first spectra, see Figure 12(a) which depicts the region between 275nm and 300nm, with single pulse (UV, 266nm laser) there are very few peaks, most of which would be hard to discern from the background signal. However, when the dual pulse experiment was performed on the same sample, eight additional peaks in this specified region were present. Figure 12(b) demonstrates   signal enhancement by utilizing dual pulsed LIBS in comparison to the same peaks found for single pulse LIBS. Signal enhancement by dual pulse LIBS has been reported in the literature [49].
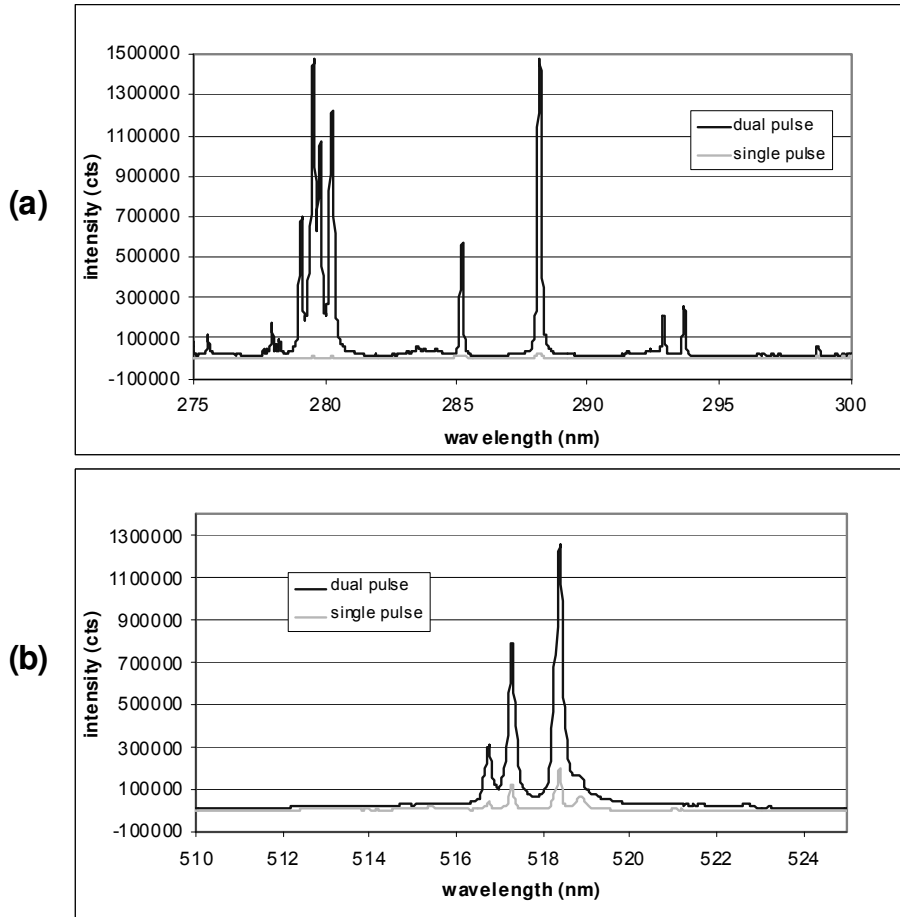
Figure 12. LIBS sample spectra demonstrating (a) the addition of more spectral lines and (b) signal enhancement of dual pulse LIBS.

Another variable studied and compared for these initial LIBS experiments was the variation between sample replicates or precision (across the 41 glass set). The dual pulse LIBS provided superior precision for the Sr line at 407.7nm over single pulse LIBS, which can be seen in Figure 13, and this same pattern was observed for the other emission lines used in this study. Many of the precision values are less than 10% RSD, which is good for LIBS analyses. Nevertheless, despite the observed improvement in precision for dual LIBS, the said values are still higher in magnitude to the precision of

strontium (concentrations) obtained via LA-ICP-MS analyses. Considering the two techniques and the principles behind them, it would be remarkable if LIBS was able to achieve the low %RSDs typically acquired with LA-ICP-MS.
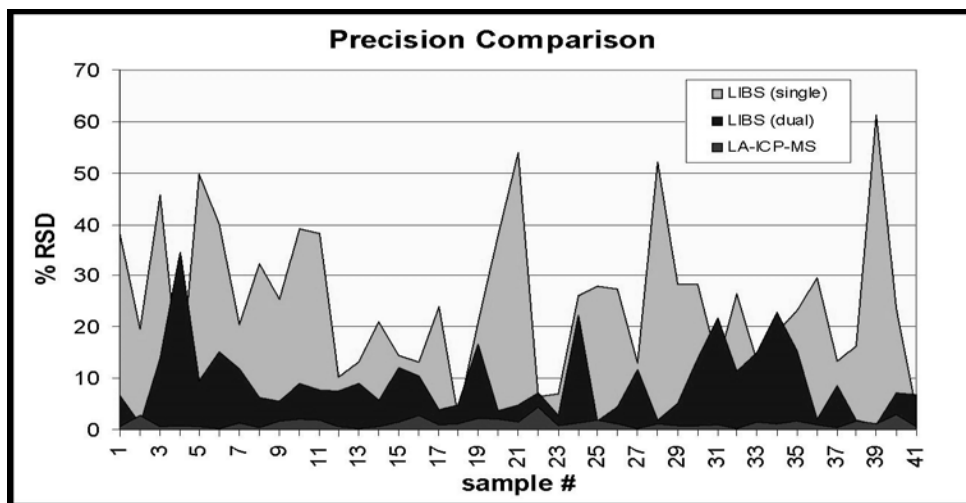
Figure 13. Precision comparison of single pulse LIBS, dual pulse LIBS and LA-ICP-MS for the glass sample set, strontium intensities (LIBS) and strontium concentrations (LA-ICP-MS).

The gains made in precision by dual pulse LIBS were overshadowed by the lack of discrimination power. Using all of the possible combinations of ratios, the number of indistinguishable pairs found was 385 out of a possible 820, which accounts for 53% discrimination power. Table 12 shows the discrimination results per element ratio utilized for pairwise comparison analysis. The large number of indistinguishable pairs encountered with this early discrimination study was discouraging at first glance, especially given the fact that the LA-ICP-MS results had already been tabulated (where just 9 indistinguishable pairs resulted from ANOVA).

Furthermore, the lack of discrimination power shown in this early experiment simply meant that the lines chosen were not discriminating, and more importantly that a more advanced data analysis protocol was necessary to achieve competitive discrimination results, when compared to other elemental analysis techniques.

Table 12. Discrimination results per element ratio, dual pulse LIBS, early Crossfire studies.

element ratio	# indist.pairs	% discrimin.
Ca/Sr	459	44.0
Fe/Sr	466	43.2
Ca/Mg	627	23.5
Ti/Sr	637	22.3
Mg/Sr	657	19.9
Ti/Mg	665	18.9
Mg/Fe	672	18.0
Ti/Ca	753	8.2
Ca/Fe	757	7.7
Ti/Fe	763	7.0
combined	385	53.0

3.4.2   Discrimination

3.4.2.1   LIBS

All of the possible combinations of the 10 optimized ratios (using 6 different ratios in each combination) were assessed and further ranked in terms of discrimination power. In total, 210 different combinations {[n!/[(n-m)!m!] where n is the total number of ratios and m is the number of ratios used per discrimination} were evaluated (i.e. 1,2,3,4,5,6… 1,2,3,4,5,7… etc). Recall that at this point in the data evaluation process, the best discriminating ratios have been selected and the possibility of committing a Type II error (false exclusion) had been eliminated.

Of the 210 combinations, 60 of them provided inaccurate discrimination results; more specifically, these particular ratio combinations gave one or more false inclusions (Type I errors) whereby two samples were found to be indistinguishable that should have been discriminated. The reason why the samples should be discriminated is because they originated from different vehicle makes and models which were consequently manufactured in different years. In the worst case scenario (combination #127), 9 indistinguishable pairs were found, 6 of which were false inclusions leaving 3 pairs that had valid explanations (or were valid associations). Therefore, combination #127 would not be used to discriminate glass samples; actually, none of the 60 combinations that produced false inclusions would be considered adequate for the discrimination of glass by LIBS.

Nevertheless, 150 combinations (of the possible 210) did provide accurate discrimination results, with no Type I or Type II errors. The indistinguishable pairs found by these combinations were all explainable, meaning that they originated from the same vehicle and thus were likely produced in the same manufacturing plant during approximately the same time. The best case scenario in this category resulted in only 1 indistinguishable pair, sample 6 and sample 7, which are side and rear window fragments extracted from a 2004 Chevrolet Cavalier. Thirty-six different combinations concluded the same result, namely 1 indistinguishable pair (6:7). Interestingly, this particular pair was found to be indistinguishable by every combination of ratios (210 times or 100%). In addition, this pair was also found to be indistinguishable by μXRF, as referenced in Table 13, which concludes that these two fragments share very similar elemental profiles. There were 4 other indistinguishable pairs that were found by several of the ratio combinations,

which were also found indistinguishable by LA-ICP-MS and/or µXRF, these pairs and the associated frequency of occurrence (out of a possible 210 combinations) are: 11:12 (28 times or 13.3%), 13:14 (7 times or 3.3%), 23:24 (84 times or 40.0%), and 28:29 (84 times or 40.0%). Actual sample descriptions for these pairs can be found in Table 13 where the indistinguishable pairs determined by LIBS are depicted by the superscript "a".

Table 13. Description of the indistinguishable pairs found by LIBS, µXRF and LA-ICP-MS. [a] = indistinguishable pairs found by LIBS; [b] = indistinguishable pairs by µXRF; [c] = indistinguishable pairs by LA-ICP-MS.

pair #	sample #	vehicle make	vehicle model	year	sample location
1[a,b]	6	Chevrolet	Cavalier	2004	outside windshield
	7	Chevrolet	Cavalier	2004	inside windshield
2[b,c]	8	Chevrolet	Cavalier	2004	side window
	9	Chevrolet	Cavalier	2004	rear window
3[a,b,c]	11	Oldsmobile	Intrigue	1998	outside windshield
	12	Oldsmobile	Intrigue	1998	inside windshield
4[a,b,c]	13	Dodge	Neon	2000	outside windshield
	14	Dodge	Neon	2000	inside windshield
5[b,c]	20	Chevrolet	Cavalier	2003	outside windshield
	21	Chevrolet	Cavalier	2003	inside windshield
6[a,b,c]	23	Dodge	Stratus	1998	outside windshield
	24	Dodge	Stratus	1998	inside windshield
7[a,b]	28	Ford	Expedition	2004	inside windshield
	29	Ford	Expedition	2004	outside windshield
8[b]	37	Jeep	Grand Cherokee	2001	outside windshield
	38	Jeep	Grand Cherokee	2001	inside windshield

3.4.2.2 µXRF

The µXRF discrimination results concluded 14 indistinguishable pairs (98.3 %

discrimination) using the three-sigma criteria discussed earlier. Again, this approach is

routinely used in casework by the Florida Department of Law Enforcement (FDLE) and

has been in place and validated through years of experience and multiple studies. Of

these pairs, only three originated from different vehicles, each of these given pairs were

discriminated by application of the t-test at the 95% confidence interval. Therefore,

application of the t-test at the 95% confidence interval to the remaining 11 pairs yielded 8

indistinguishable pairs out of a possible 820 comparisons (again, the number of possible

pairs is equal to N(N-1)/2, where N is the number of samples). The discrimination

analysis approach demonstrated 99.0% discrimination for µXRF, which is excellent

discrimination power.

Furthermore, all of the provided indistinguishable pairs have explanation as to

why they exhibit similar elemental profiles. Each indistinguishable pair originated from

the same vehicle and thus they have similar elemental profiles, meaning that the

fragments (representing the glass source as a whole) were likely produced in the same

manufacturing plant at about the same time period. Seven of the 8 pairs found

indistinguishable were attributed to samples from the same laminated windshield (inside

and outside fragments originating from the same windshield), while the eighth

indistinguishable pair represents side and rear window fragments that also originated

from the same vehicle. The pairs found indistinguishable overall by this method are listed

and described in Table 13; in the given table the indistinguishable pairs found by µXRF

are labeled by the superscript "b".

73

3.4.2.3 LA-ICP-MS

Pairwise comparison analysis (ANOVA with Tukey's post hoc test) yielded 11 indistinguishable pairs out of a possible 820 comparisons (or 98.7% discrimination). Six of these 11 pairs were discriminated by application of a t-test including three pairs that originated from different vehicles produced in different years. The end result is that these fragments should be discriminated and were by the combined discrimination analysis approach. Nevertheless, the other three pairs discriminated by t-test did originate from the same vehicle; the reason that some pairs were discriminated is likely due to a sampling and/or a precision-related issue. If the precision of the measurement for a given fragment is smaller than the overall precision of the glass pane as a whole, it is possible that fragments obtained from the same source (i.e. inside and outside fragments from the same windshield) can be discriminated. In forensic casework it is important that proper sampling techniques are followed to ensure that correct characterization of a glass source is achieved and that correct associations or discriminations are made.

The net result for LA-ICP-MS, combining ANOVA and t-test, was that five indistinguishable pairs were found out of a possible 820 pairs (equating to 99.4% discrimination). Remarkably, these five pairs were identical to five of the eight pairs found indistinguishable by XRF; therefore, despite LA-ICP-MS having slightly better discrimination power (0.4% greater), the results are well correlated. The correlation between LA-ICP-MS and μXRF data for strontium pertaining to this sample set will be addressed in the next section. The five indistinguishable pairs by LA-ICP-MS are summarized in Table 13 where the pairs marked with a superscript "c" represent the five indistinguishable pairs determined by LA-ICP-MS. The fact that both methods generated

the same output, namely the same indistinguishable pairs, demonstrates the strength and validity of these two methods for forensic glass comparisons. Again, the indistinguishable pairs all had valid explanations as to why they exhibited very similar elemental profiles. The top discriminating elements by LA-ICP-MS and the associated results per element can be found in Table 14. Take note that the top discriminating element is strontium, which overall has been consistently a top discriminator for the trace elemental analysis of float glass. Therefore, given its wide variation across glass sample sets, strontium was the element chosen for the correlation studies in this work.

Table 14. Percent discrimination by element, LA-ICP-MS, 990 possible comparisons.

element	# indist. pairs	% discrimination
Sr	76	90.7
Zr	127	85.5
Ti	142	82.7
Rb	176	78.5
Ba	191	76.7
All (5)	5	99.4

3.4.3 Correlation Study

The three analytical techniques are compared in terms of concentration (LA-ICP-MS) versus intensity (μXRF or LIBS), and the results are summarized here. Figure 14 shows the distribution of strontium (mean concentration or mean intensity), as determined by LIBS, μXRF and LA-ICP-MS. The plot shows the variation (or in some cases the association) of strontium in the glass sample set analyzed for this study; also, it partially demonstrates the correlation of the strontium signal for the three methods. It can be observed that when the strontium concentration or intensity is increased for one method (for instance, when going from one sample to the next), the strontium signal is

also increased in similar magnitude for the other methods. Nevertheless, more descriptive correlations of such results can be found in Figure 15, where concentration (LA-ICP-MS) is plotted against intensity (μXRF or LIBS) and the associated correlation coefficients are found.
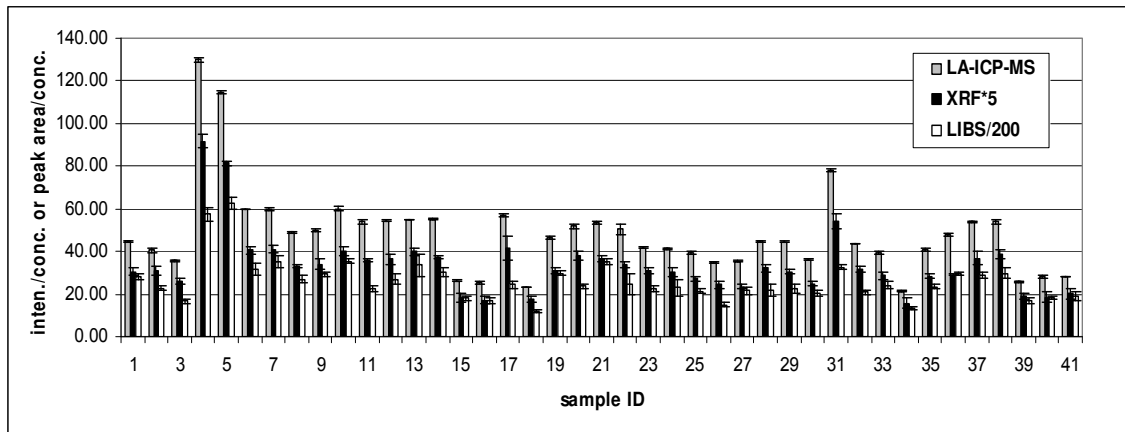
Figure 14. Strontium distribution among the 41 glass set, a comparison of means for μXRF (signal intensity), LA-ICP-MS (concentration), and LIBS (peak area). Note that the LIBS intensities were divided by 200 and the μXRF intensities were multiplied by five to achieve similar scaling factors.

The correlation between LA-ICP-MS and μXRF data using strontium mean concentrations and intensities (with the associated error bars), respectively, for the 41 glass set was plotted and compared. As depicted in Figure 15(a), a strong correlation between the two data sets is demonstrated, represented by a correlation coefficient of 0.9911. The excellent correlation between these two methods further establishes why similar discrimination results were obtained.

76

A correlation between LA-ICP-MS and LIBS data was also plotted using LA-ICP-MS strontium concentrations versus LIBS intensities for strontium (mean values with respective standard deviations) for the 41 glass set. As observed, the correlation for LIBS and LA-ICP-MS (R^2 = 0.8813) [reference Figure 15(b)] is not as strong as the correlation between the LA-ICP-MS and µXRF data sets (R^2 = 0.9911). However, the plot helps to illustrate the small degree of variation between sample replicates for LIBS using the setup outlined earlier (which is excellent for LIBS analyses) and by combining the observed precision with the correct choice of peak ratios, excellent discrimination was achieved for LIBS glass comparison analyses.
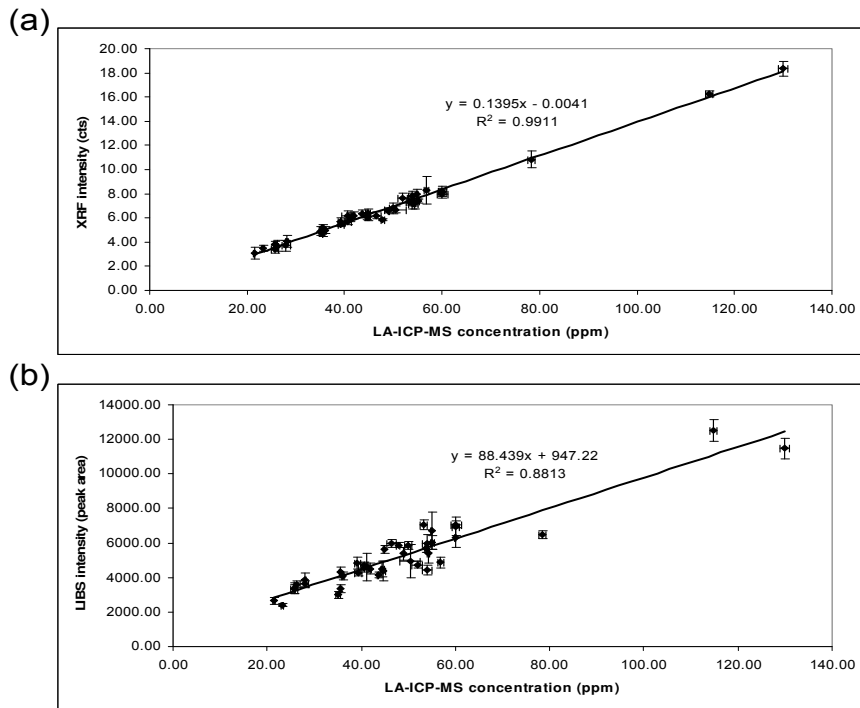
Figure 15. (a) Correlation of LA-ICP-MS and µXRF results across the glass sample set, Sr concentration versus peak intensity and (b) correlation of LA-ICP-MS and LIBS results, Sr concentration versus peak area.

3.5   Conclusions

Discrimination of forensic glass fragments by LIBS came from humble beginnings (see LIBS Crossfire results) where discrimination power looked to be comparable (or actually worse) than what was reported in the literature by Bridge et al. [48] or ~53% discrimination versus ~83% discrimination, respectively. Nevertheless, a relentless pursuit to achieve improvements soon followed; these improvements (and the resulting discrimination) were the product of both the method by which LIBS analyses were generated and the data analysis protocol that was developed to ensure accurate comparisons between sample fragments. The LIBS results obtained were in part due to the tremendous help Dr. Cleon Barnett, who deserves some credit in the evolution of forensic glass examinations by LIBS reported here.

Nevertheless, two of the leading techniques in elemental analysis, LA-ICP-MS and µXRF, were compared to a less mature technique, LIBS, in terms of discrimination power for a set of automotive glass samples. Significantly, all three analytical approaches yielded similar discrimination results (≥99% discrimination). Moreover, the five indistinguishable pairs found by LA-ICP-MS were the same as five of the eight indistinguishable pairs determined by µXRF and many of the ratio combinations used to discriminate the glass samples by LIBS concluded the same pairs found indistinguishable by the other methods.

The indistinguishable pairs obtained for LA-ICP-MS, µXRF and LIBS retained good explanation as to why the associated elemental profiles were similar (or statistically the same, with respect to those elements analyzed) and thus could not be discriminated. These indistinguishable pairs originated from the same vehicle and thus were likely to have been manufactured in the same plant at about the same time.

With respect to analyzing LIBS spectra and making sample comparisons, an extensive study was conducted comparing different data reduction procedures to ensure accurate discrimination. The probability of committing Type I or Type II errors was reduced and/or eliminated using the sample comparison approach outlined in the paper; reducing these types of errors is especially crucial for forensic casework. The net result was a data reduction protocol being adopted and then utilized to successfully discriminate the glass sample set of interest. The best combination of ratios produced only 1 indistinguishable pair (out of the possible 820 pairs) and this pair was explainable.

Furthermore, 10 ratios are suggested are thus considered optimum for the analysis and discrimination of glass by LIBS based the data analysis study outlined. Those proposed ratios include: 394.4nm/330.0nm (Al/Na), 766.5nm/643.9nm (K/Ca), 394.4nm/371.9nm (Al/Fe), 438.4nm/766.5nm (Fe/K), 534nm/766.5nm (Ca/K), 371.9nm/396.2nm (Fe/Al), 766.5nm/645.0nm (K/Ca), 394.4nm/460.7nm (Al/Sr), 460.7nm/766.5nm (Sr/K), and 818.3nm/766.5nm (Na/K).

In summation, given its low cost, high sample throughput, good sensitivity, and ease of use, the application of LIBS for forensic glass examinations looks promising and can present a viable alternative to LA-ICP-MS and µXRF in the forensic laboratory.

4 ELEMENTAL ANALYSIS OF GEL INKS BY LA-ICP-MS

4.1 Introduction

Ink manufacturers are continually introducing newer formulations in the attempt to make improvements to their respective products and/or to meet current market demands. There are a multitude of inks which may be encountered in forensic casework, some of which include, but not limited to: roller ball ink, ballpoint ink, fiber-tip pen ink, fountain pen ink, stamp ink, copier toner, ink jet printer ink, marker ink, and gel pen ink (which is the matrix of interest in this study). By far the most common type of ink found in forensic analyses is ballpoint pen ink. Nevertheless, gel ink pens (which can also use a ball mechanism for ink distribution) are the fastest growing group of pens in the market today and are chemically different than all the other pen types, which puts them in a class of their own [11].

Gel ink pens were first produced in Japan in the 1980s, came to the United States in the early 1990s and have become a staple in the US pen market ever since [11]. Gel ink pens have gained rapid popularity among consumers primarily because of their bold and vivid, yet well defined, appearance upon application. The characteristic appearance of the applied gel ink compliments its smooth writing capabilities and its remarkable stability or robustness over long periods of time. And, markedly, gel ink pens are fairly inexpensive to produce, which is attractive to manufacturers as well [11].

Gel ink pens are expected to hold increasing percentages of use the US and abroad in the years to come, which makes them of interest to the forensic community, especially to document examiners who will likely encounter gel inks more often when analyzing questioned documents.

4.2   Gel Ink Matrix

Ink writing devices in general contain various chemical components that ultimately serve very different functions, but collectively work together as a specific formulation to achieve the desired product or application. The bulk of these chemical components found in ink sources are organic compounds, which in some cases can be distinguishing in themselves [11]. However, when the major (chemical) components are used for discrimination, there is likely to be less variation between two sources that originate from different manufacturers. In other words, the greater the concentration (or amount), the more difficult it will be to detect variations of those constituents from one sample to the next.

Some of the main constituents found in these writing devices include: dyes and pigments (which provide color), solvents (often called the vehicle of the pen, which are water-based and/or organic solvents that carry the colorant to the substrate), resins (used for adjusting ink viscosity), biocides (which help prevent microbial growth), lubricants (added to the ball of ink devices which allows rotation and assistance with ink delivery), surfactants (which are used to adjust surface tension between the metal tip or ball and the flowing ink), corrosion inhibitors (that help preserve the metal tip or ball), sequestrants (which hold certain substances in solution, i.e. metallic ions), shear-thinning agents

(which allow the ink to flow freely through the ball or pen tip) emulsifying agents and other additives (which are used to alter pH, viscosity, etc.). Gel inks also contain pseudo-plasticizers which are unique additives added to provide the unique consistency sustained by gel-based writing devices [11].

4.2.1 Trace Elements in Gel Ink

Several different examples of ink formulations can be found in the book by Brunelle and Crawford [11] or via the internet. However, although such formulations provide some insight as to the composition (or components) of a particular ink, the information provides very broad descriptions at best, which is likely the intention of manufacturer for proprietary related reasons.

Nonetheless, the inorganic (elemental) constituents within gel inks can come from a wide range of sources. The process of sourcing these constituents of course starts with the raw materials from which the main ingredients are produced. One of the main contributors to the elemental content of gel inks is from the colorant(s) which may include the addition of any number of inorganic pigments (i.e. titanium dioxide, carbon black, "metal powder", iron oxide, etc.) or organic pigments may be added (which are not as rich in elemental content) or a combination of [11]. The vehicle of the pen (especially for water based solvents) is another key source from which elemental composition may arise.

Otherwise, the elemental composition of gel inks can come from the various additives, such as antiseptics (i.e. potassium sorbate, sodium benzoate), pH adjusting agents (i.e. sodium hydroxide, sodium carbonate), surfactants (i.e. sodium lauryl sulfate,

etc.) [11]. In other words, the trace element constituents found in gel inks can virtually come from any of the stated raw materials and from the manufacturing process itself.

4.2.2 Elemental Analysis of Ink

Although gel inks have not been characterized to date in the literature in terms of elemental analysis via one of the many analytical techniques described earlier. Other types of inks have been analyzed and characterized based on their elemental composition [51-55] and thus initially provided some insight as to the types of elements that may be found gel ink samples, with the assumption that the same raw materials are used in their respective formulations. In addition, it is unfair to only present elemental compositions of inks because in the case of a forensic document, the paper itself may provide additional discrimination potential (though that is not the work that will be presented in this chapter). Given that it is physically impossible to separate an ink from its substrate (paper) without removing some of the constituents of the paper, the elements found in paper (and the compositions thereof) are important as well.

In a focal point article by Anglos, the origin (and date of first use) of inorganic pigments is presented as used in archeological inks, paints, and prints; the list of pigments also provides the elemental composition associated to a given pigment name (i.e. Egyptian blue = $CaCuSi_4O_{10}$ and Naples yellow = $Pb_2Sb_8O_7$, etc) [51]. From this a derived list of possible elements included: Al, As, Ba, Ca, Cd, Co, Cr, Cu, Fe, Hg, K, Mn, Na, Pb, Sb, Se, Si, Sn, Sr, Ti, and Zn. Anglos also presented some LIBS spectra for a group of the pigments [51], although such spectra are of the pigment and not the pigment as part of an ink matrix (where it will be certainly diluted plus the other ink components

would potentially cause more erratic LIBS spectra as versus the "clean" spectra presented in the mentioned work. Maind et al. analyzed 22 different blue ball-point ink samples by neutron activation analysis and dissolution ICP-MS in order to quantify the components and help identify the rare earth elements that have historically been added to ballpoint inks [52]. The elements list from this publication included: La, Pr, Nd, Sm, Eu, Gd, Tb, Dy, Ho, Er, Tm, Yb, and Lu [52] these elements were subsequently added to the growing list of possible element contributors in gel inks. Zieba-Palus et al. used a combination of Raman, FTIR, and μXRF in the attempt to discriminate a large number of blue and black ballpoint inks, and a small set of gel inks; the elements present in these samples included: Cu, Si, Zn, Ca, Cr, Pb, Mn, Fe, and Ni [53]. XRF, an elemental analysis technique, was solely used to identify the colorant (pigment) used in the associated pen set and with respect to the analysis of gel inks, good discrimination was reported using a combination of Raman and FTIR [53]. In a recent article by Fittschen et al., picoliter droplets (HNO_3 spiked with As, Co, Fe, and Ti) were delivered from an ink-jet printer onto acrylic glass, allowed to dry, and then analyzed by LA-ICP-MS [54]. Fairly linear calibration curves were generated from the dried picoliter drops [54], the work offers a potential quantification approach for ink analysis, provided that a matrix-matched standard can be produced. Spence et al. used dissolution ICP-MS to study document paper wherein Na, Mg, Al, Mn, Sr, Y, Ba, La, and Ce (from a starting list of 23 elements) were used to discriminate 17 different paper sources (Australian document paper) by t-test at the 95% confidence interval [55].

4.3   Methodology

4.3.1   Introduction

Although many types of experiments were designed and performed in order to evaluate gel inks and eventually arrive at the best analysis protocol (by LA-ICP-MS) for that matrix, including a qualitative study on paper, only some of those early experiments will be discussed here because they were either irrelevant or were simply failed attempts. At any rate, some of the early data will be presented, and in some cases the failures will be discussed solely for the interest and understanding of those who will pick up where this project has left off. For the most part, the first round of experiments were mostly trial and error en route to ultimately determining which laser ablation parameters best suited this type of analysis. The initial goal of LA-ICP-MS as applied to ink analysis was to achieve the maximum analyte signal (ink) while sampling the least background signal (paper). Finding this "happy medium" between the two competing variables (elemental compositions attributed to ink and those attributed to paper) was difficult at times and, early on it was determined that only removing ink (with no attributing signal to the paper substrate itself) was impossible.

Below the respective paragraphs outlining the final analytical method for LA-ICP-MS of gel inks, the set of experiments alluded to earlier in addition to other ink and paper studies will be presented. In brief, included in this part of the dissertation is one of the initial studies regarding laser energy and some discussion regarding the laser interactions with ink and paper, respectively. A paper study will be highlighted and discussed in which different papers were analyzed to determine which provided the

lowest attributing background signal. Then, two discrimination studies will be presented, one where the gel ink sources were unknown (a blind study) and another where the source of origin for the gel ink sources was known. A within single pen variance study and a within pack (four pens) variance study will also be discussed. Finally, a glimpse into future directions, namely the quantitative analysis of ink using a custom prepared matrix-matched standard, and some preliminary data for that approach will be presented.

4.3.2   Instrumentation

4.3.2.1   LA-ICP-MS Considerations and Experimental Conditions

The general instrumental parameters utilized for the LA-ICP-MS analysis of the majority of the ink analyses described above are outlined in Table 15. The laser ablation system used for the ink and paper studies was a New Wave Research UP213 system (Fremont, CA) which was connected in tandem to a Perkin Elmer Elan 6100 DRC II (Waltham, MA). The ICP-MS was operated in standard (non-DRC) mode.

Table 15. A summary of the instrumentation and optimized parameters for the LA-ICP-MS analyses of ink and paper.

laser ablation (LA)	New Wave Research UP213
wavelength	213nm
energy	0.25mJ (42.5%)
spot size	100µm
fluence	$3.1J/cm^2$
repetition rate	10Hz
ablation mode	line scan
scan rate	10µm/sec
ablation time (amount)	60sec (600µm)
ICP-MS	**Perkin Elmer Elan 6100 DRC II**
detection	simultaneous mode
RF power	1500W
plasma gas flow (Ar)	16 L/min
auxiliary gas flow (Ar)	1.0 L/min
carrier gas flow (He)	0.9 L/min
make-up gas flow (Ar)	0.9 L/min
dwell time	8.3 ms
data acquisition	time-resolved spectra

The laser ablation parameters shown in the attributing table are the product of many attempts towards developing and optimizing a protocol to be used for gel ink analyses. It is important to point out that the laser ablation system used in all the presented studies offered an excellent solid sampling approach, as shown by previous research within our group, and the optics used for sample viewing and laser direction was an important feature necessary for proper ink analysis and success of this work. Without the viewing capabilities and laser direction, achieving an optimized sampling method would have been more difficult. A line scan ablation mode was utilized instead of single spot analysis (performed for glass analyses) to reduce the amount of paper ablated and more importantly achieve a more representative sampling area of the ink. Although different spot sizes were tested, a spot size of 100µm (the maximum spot size for this laser ablation system) was almost immediately settled on for a few reasons. With a 100µm spot size, in comparison to smaller spot sizes, more mass (attributed to the ink)

entered the ICP-MS. In combination with the ablation mode used (line scan), the large

spot size provided a more stable time-resolved spectra which translated into more

reproducibility (or greater precision). A laser scanning rate of 10μm/sec provided the

optimal energy density over the sample for ink removal from the paper without directing

too much energy on a particular location which would produce greater amounts of

ablated paper or even burning. Arguably, the most important factor was the adjustment of

laser energy and the associated experiments to determine the optimum laser parameters

were. Decidedly, 42.5% (or 0.25mJ) laser energy was adopted for the analysis of ink on

paper. It is important to note that it may be necessary to increase or decrease the laser

energy based on the type of ink and/or the type of substrate (paper) on which the ink was

applied. One combination of ink and paper may require a slight modification in the

ablation parameters to achieve optimum laser sampling and elemental detection.

4.3.2.2 LA-ICP-MS Optimization

Prior to use (and thus reduction of laser energy and increase in spot size for ink

analysis), the laser ablation system and ICP-MS were optimized using the optimization

protocol used for glass analysis in our laboratory, which was outlined in section 2.3.1.6.

In short, using the glass optimization protocol, NIST 612 was ablated using 100% laser

energy in combination with a spot size of 55μm and element intensities were optimized

by adjustment of instrument parameters (i.e. sample and carrier gas flows). The final

intensities were then recorded in the proper instrument log book for comparison and to

help troubleshoot maintenance related issues.

4.3.2.3 Element Menu

The initial element list was gathered by first looking through the scientific literature which detailed the elemental analysis of ink by various techniques [51-55]. Essentially, a list of the elements arising from those papers were compared and summarized into an extensive element menu that included all of the possible elements (that could be observed or not in the associated gel ink samples). The original element menu contained 31 different elements (Al, As, Ba, Ca, Cd, Co, Cr, Cu, Fe, Ga, Hf, Hg, K, La, Li, Mg, Mn, Mo, Na, Nd, Ni, Pb, Ru, Sb, Si, Sn, Sr, Ti, Y, Zn and Zr); isotopes were selected based on relative abundance (since it was suspected that the concentrations of such elements in the ink would be fairly low in ink) and avoidance of potential polyatomic interferences encountered in quadrupole ICP-MS. Using this extended element menu, a sample set provided by the United States Secret Service (USSS) were run individually (one replicate each) to qualitatively observe which elements should be included in the final element menu. The USSS sample set will be described in more detail later. The reason why only one sample replicate analysis was performed as a result of analysis time - including 31 elements (and the different isotopes per element) produced a lengthy ICP-MS run. Besides that, additional sample replicates would not provide any additional information with respect to inclusion or exclusion of certain elements in the final menu. As a result of the lengthy ICP-MS analysis time, the ablation time (or distance) had to be increased accordingly in order to achieve a suitable time resolved spectra. Some elements/isotopes were then omitted because they were not detectable in any of the gel ink sources analyzed or because of their poor analytical performance or a combination of both. The final element menu consisted of 14 different elements

represented by the following isotopes: ^{25}Mg, ^{27}Al, ^{39}K, ^{49}Ti, ^{52}Cr, ^{55}Mn, ^{57}Fe, ^{58}Ni, ^{59}Co, ^{65}Cu, ^{88}Sr, ^{120}Sn, ^{137}Ba, ^{206}Pb, ^{207}Pb, and ^{208}Pb. The isotopic intensities corresponding to lead (Pb) were added together for the given sample replicate analyzed (Pb sum = ^{206}Pb + ^{207}Pb + ^{208}Pb intensities, respectively). Rhodium (^{103}Rh) was also included as an internal standard for some analyses.

4.3.3 Sample Descriptions and Preparation

4.3.3.1 Laser Energy Study

In this particular study, MontBlanc (Bethlehem, MA) fountain pen ink (spiked with La) was applied to Whatman 2 filter paper (spiked with Rh). As alluded to earlier, after some general trial and error, an experiment was designed to assist with determining what laser energy provided the most optimum conditions for ink removal from paper. In this study, lanthanum (La) was spiked into a water soluble fountain pen ink manufactured by MontBlanc (Bethlehem, MA) to achieve a final concentration of 10ppm. The prepared ink standard was then applied to a 10ppm rhodium (Rh) was spiked sample of Whatman 2 filter paper. Standard solutions of lanthanum and rhodium were prepared via dilution from a certified stock standard at 1000ppm (CPI International, Santa Rosa, CA). The solvent used for the dilution was 5% HNO_3 (source: Optima Grade, 67%, Fisher Scientific, Pittsburgh, PA diluted in 18Ωm High Purity deionized H_2O). The filter paper was fully immersed in the rhodium standard solution for 5 minutes, at which point the paper was removed using plastic forceps. The filter paper segments were then placed on clean paper to air dry overnight inside a clean fume hood. Once dry, the spiked ink was then applied to the spiked filter paper and the ink was allowed to dry for 24 hours at

which point a section of the prepared sample (~10mm x 10mm) was cut and taped to a glass cover slide. Subsequent analysis by LA-ICP-MS soon followed. In addition, paper samples were also prepared by immersion in the 5% HNO_3 solution used for preparation of the paper and ink standards; these samples were only prepared in the case where quality control measures were questioned.

The two elements used in this study were chosen because Rh was not detected in the ink and La was not detected in the paper source during previous analyses, which made them good candidates for the laser energy study. In other words, there were no attributing concentrations of these elements in the respective matrices which translated into a more controlled experiment.

4.3.3.2 Paper Study

In the paper study, different types of paper were analyzed to see which substrate would provide the lowest background signal, where the paper that demonstrated the least detectable elemental compositions (qualitatively) being used later for the discrimination studies of the collected pen set. As with the ink preparation samples, a 10mm x 10mm sample was cut from each paper source in Table 16 and affixed to a glass cover slide with double sided tape. Although the paper source selection was important to the analysis of the gel ink sources as stated previously, the details for each paper source were not crucial to this study therefore only a general description for each source is included.

The same laser and ICP-MS parameters were followed as depicted in Table 15 with the exception of the laser energy, which was 37.5% (~0.17mJ). The reason that lower laser energy was necessary was because at higher laser energies (>0.17mJ) the

laser was burning through the paper and non-uniformity in ablation (mass removal) signal was observed (equating to a greater chance of elemental fractionation). Three replicates of each paper sample were analyzed, the time resolved spectra were integrated and the integrated intensities were entered into an Excel spreadsheet where a mean, standard deviation, and percent relative standard deviation were tabulated.

Table 16. Source descriptions for the paper study.

source/ID	brand	type/description
A	Hammermill	Copy Plus Paper, 20lb
B	Office Max	Copy Paper, 20lb
C	Staples	Multi-Use Paper, 20lb
D	Hewlett Packard	Office Paper, 20lb
E	Hewlett Packard	Color Laser Presentation Paper, Glossy, 20lb
F	Staples	Exceptional Resume Paper, 25% Cotton, 24lb
G	Whatman	Qualitative, Standard, Grade 2, Filter Paper
H	Whatman	Quantitative, Ashless, Grade 42, Filter Paper
I	Whatman	Quantitative, Hardened Ashless, Grade 542, Filter Paper

4.3.3.3   Discrimination Study: United States Secret Service Sample Set

The United States Secret Service (USSS) has one of the largest (if not the largest) document examination laboratories in the world and have collaborated with our group for part of the ink project. Their role was to provide the ink samples to be analyzed, and since they have an extensive database of ink sources, including gel ink pen sources, their impact was important. Considering that no method currently exists to analyze these types of ink sources (gel inks), officials at the USSS were happy to contribute samples and promote the development of a technique that could analyze gel inks. The USSS sent 45 gel pen samples from that database (not the actual marking devices but markings made from those respective pens); the samples were sent as a blind study. The gel pen markings were made on full sheets of Whatman 42 filter paper, which were shipped inside plastic

sheet protectors (5 sheets in total). As one can see (in Figure 16), the application was

non-uniform and thus was not performed in a controlled/scientific way, at least from the

standpoint of method development and preliminary ink discrimination studies. The

markings (or sources) of ink were essentially "scribbled" on the paper substrate, meaning

that there were no clear-cut lines or even handwriting samples (which would be more

realistic in a forensic case). Regardless, ink was marked on top of ink, which was marked

on top of ink, with little evidence of the paper itself. Again, these issues discussed above

can readily be seen in the photo below (see Figure 16) which represents one of the sheets

of gel ink samples sent by the USSS.
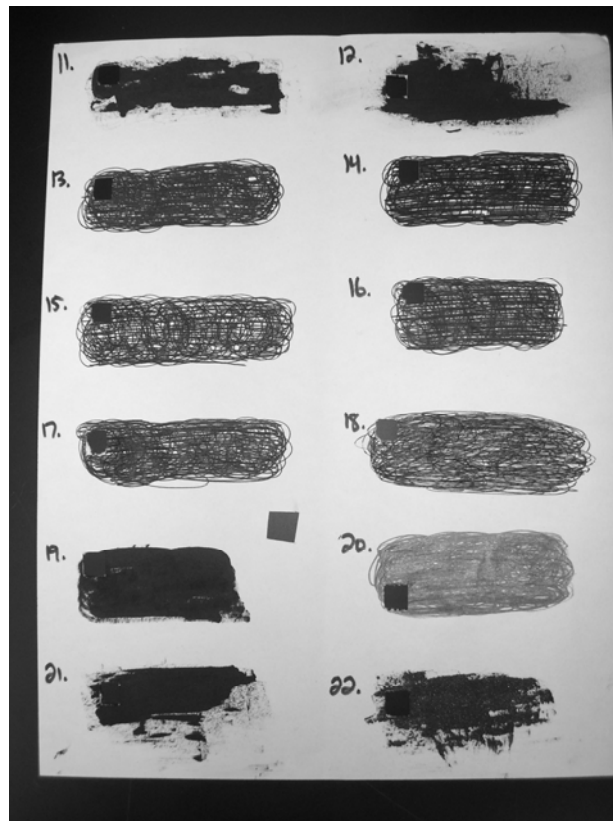
Figure 16: A photo showing one of the five pages of the gel ink samples (source IDs 11-22) sent by USSS.

The approach of the applied ink was not controlled and thus provided additional variables that could have been reduced or eliminated with a more controlled application. For instance, comparing sample #15 to sample #21, there is an obvious visible difference that in itself is distinguishing; however, this research was to attempt discrimination by chemical analysis and therefore these factors were not considered. In addition, some of the samples had a glitter-like appearance or had a lighter black appearance (almost gray) and thus were also discriminating by visible observation. The origin of the United States Secret Service gel ink samples acquired was unknown at the time of sample analysis and during the writing of this dissertation. Therefore it is possible that some of the ink samples (despite possessing a unique identification number) are from the same source of origin.

Prior to analysis by LA-ICP-MS, sections (~ 10mm x 10mm) of the ink (on paper) were cut from the sheet using a generic razor blade. The apportioned segments were then affixed to 24mm x 20mm glass slide covers (Fisher Scientific, Boston, MA) using double-sided tape. The reason why the glass cover slides were used is because they provided a completely flat surface at a relatively inexpensive cost. The utility of the double-sided tape kept the paper affixed to the flat surface (of the cover slides) and more importantly it also kept the complete ink line (or ink lines) at the same relative height (or focal distance from the laser ablation system's objective). This was important to sample the ink efficiently and thus in turn improve signal stability during ablation.

4.3.3.4 Discrimination Study: Collected Gel Pen Set

The black gel ink pens collected for this study and the associated source descriptions, such as the pen make (or brand), the model (or type), the date collected, etc. can be found in Table 17. The pens were collected with the intention of representing the general population of black gel ink pens in public circulation today (circa late 2008 to early 2009). Of the 24 sources, 23 are gel ink pens while one source (B-008) is from a different class of black ink pens (hence, non-gel). This one non-gel ink source is a new product that just became available for consumer purchase in mid-late 2008 and was included for that reason. Considering that this particular ink originates from a marker manufacturer (Sharpie), hypothetically the formulation was expected to be very different from the gel ink pen sources and mimicked by the deposition characteristics. It is the author's opinion that this particular ink should reside in a class of its own and thus be separate from the major classes of ink pens (ballpoint, fountain, roller-ball, and gel). Granted, markers have been available for many decades, however this is the first time a marker is actually being marketed as a pen. Whether or not such marketing is successful and becomes a mainstay in society is difficult to predict; nonetheless, this type of pen could possibly be used for recent documentation purposes and thus is of forensic interest. And, given that this study is related to "newer" types of pens, it makes sense to include the marker-based pen in this study.

Table 17. Collected black gel ink pen inventory and descriptions. * Exact purchase date is unknown (these pens were acquired prior to the onset of the ink project).

inventory number	make (brand)	model (type)	size (mm)	quantity	purchase date	new/used	purchase location	manufacture location
B-001	Gel Writer	R$_x$	0.7	5	1/23/2008	new (refills)	CostCo (Pompano Beach, FL)	China
B-002	Bic	Velocity Gel	0.7	4	8/7/2008	new	Office Depot (Miami, FL)	France
B-003	Foray	Retractable Gel	0.7	6	8/7/2008	new	Office Depot (Miami, FL)	China
B-004	Zebra	GR8 Gel	0.7	5	8/7/2008	new	Office Depot (Miami, FL)	China
B-005	Pilot	BEGREEN G-Knock	0.7	3	8/7/2008	new	Office Depot (Miami, FL)	Japan
B-006	Uni-Ball	Signo 207	0.7	2	8/7/2008	new	Walgreens (Miami, FL)	Japan
B-007	Pilot	FRIXION Erasable	0.7	2	8/7/2008	new	Walgreens (Miami, FL)	Japan
B-008	Sharpie	Pen *fine*	~0.7	2	8/7/2008	new	Walgreens (Miami, FL)	Japan
B-009	Staples	Gel Stick	0.7	12	8/13/2008	new	Staples (Margate, FL)	China
B-010	Pilot	Precise V7 RT	0.7	3	8/13/2008	new	Staples (Margate, FL)	Japan
B-011	Uni-Ball	Signo 207	0.7	4	8/13/2008	new	Staples (Margate, FL)	Japan
B-012	Zebra	Z-Grip	0.7	4	8/13/2008	new	Staples (Margate, FL)	China
B-013	Papermate	Gel Click	0.7	4	8/13/2008	new	Staples (Margate, FL)	China
B-014	Pilot	G2	0.7	4	8/13/2008	new	Staples (Margate, FL)	Japan
B-015	Staples	Sonix Gel	0.7	4	8/13/2008	new	Staples (Margate, FL)	China
B-016	Pilot	G2	0.7	4	9/2/2008	new	Office Depot (Margate, FL)	Japan
B-017	Uni-Ball	Signo Gel RT	0.7	4	9/2/2008	new	Office Depot (Margate, FL)	Japan
B-018	Bic	Velocity Gel	0.7	4	8/21/2008	new	Walmart (St. Louis, MO)	France
B-019	Papermate	Gel Click	0.7	4	8/21/2008	new	Walmart (St. Louis, MO)	China
B-020	Uni-Ball	Signo Gel RT	0.7	4	8/21/2008	new	Walmart (St. Louis, MO)	Japan
B-021	Pilot	G2	0.5	3	2005*	used	Staples (Miami, FL)	Japan
B-022	Staples	Gel Mini	0.7	3	2008*	used	Staples (Margate, FL)	China
B-023	Staples	OptiFlow	~1.0	1	2008*	used	Staples (Miami, FL)	China
B-024	Staples	Gel	0.7	2	2008*	used	Staples (Miami, FL)	China

Nineteen of the 24 gel ink pen sources were purchased new and collected approximately around the same time (within 1 month of each other). Five sources therefore were already possessed (5 sources), most of which were purchased sometime in 2008. It is important to notice that the pens collected within the stated time frame (08/07/2008 to 09/02/2008) were collected from various locations, including Miami, Florida, Margate, Florida and St. Louis, Missouri and in some instances pens were collected from different stores within those respective cities or towns.

In addition, in a few cases the same brand and type of pen was collected for comparison reasons, although it is unknown whether or not those particular pen packs are from the same lot. Also, with the manufacturing process for each brand and type

unknown, drawing associations between the same pens that appear to come from the same source could be inaccurate.

One source, B-021, stands out from the others because the tip size is 0.5mm; tip size translates into narrower or wider ink deposition. So logically the amount of ink deposited on a given paper source by a 0.5mm pen will be less when compared to a 0.7mm tip marking. It must be added that in some cases, since neither the pen nor the packaging stated, the tip size is unknown and had to be estimated. For these sources (B-008 and B-023) the tip size was estimated to be ~0.7mm for B-008 and ~1.0mm for B-023. These estimations were determined by comparing measured ink deposition lines of known tip size markings to the unknown tip sized pen markings.

The paper source utilized for the application and analysis of the respective ink samples was Whatman 542 filter paper (Florham Park, NJ) which is source I in Table 16, and despite providing the lowest background signal, there were a few drawbacks with using filter paper that should be mentioned. The first, and most obvious issue, is that in forensic casework/document analysis, filter paper is probably rarely found and is of minimal forensic interest, unless the suspect is a chemist or someone who would have access to this type of paper (again this would be extremely rare). Another drawback is related to physical characteristics of the ink markings on the filter paper, in which the degree of ink absorption into the filter paper is significantly greater than ink absorption into paper sources typically found in forensic casework, such as copy paper or multi-use paper. Thirdly, given its porous matrix (and, to a certain degree, the softness or brittleness of the paper), the ablation behavior is different with respect to general paper sources so the analysis of ink on paper (or paper itself) may require the analyst to alter the laser

ablation protocol. Simulation to actual casework was not important to these initial studies, instead the goal was to eliminate as many variables as possible and thus gain more control/understanding prior to tackling more complicated scenarios that may be encountered in forensic ink analysis by LA-ICP-MS.

Besides the low background observed with Whatman 542, another advantage of using a filter paper source is that standards can be readily added to the paper (if desired) by soaking segments of the paper in a specified concentration of whatever standards are sought. The assumption that must be made when performing this task is that the degree of absorption into the filter paper is uniformly distributed.

The Whatman 542 filter paper circles were cut into approximately 40mm x 40mm segments using acid washed (~5% HNO_3) all-plastic scissors (Armada Art Materials, Boston, MA). For the ink pen discrimination study, each ink pen source was applied in the same fashion to ensure that accurate comparisons between sources could be made.

The first step in this process was to continuously write with a given new pen for 2 minutes on scratch paper in order to remove any possible source of contamination suspected to arise from the pen tip, the sealant placed on the pen tip, the manufacturing process, etc. Many of the respective pens had a small ball-like glue bulb or other sealant) affixed to the tip of the ink as an attempt to prevent leakage. The sealant was removed prior to this initial step in ink application (or pre-application).

Immediately following the pre-application step, straight lines were hand-drawn on the paper for ~30mm at a rate of approximately 15mm/sec. On a given piece of paper, 4-5 lines were drawn parallel to one another (similar to a musician's sheet music) with about 1mm of separation between. A total of 16-20 total lines were drawn for each ink source, as demonstrated in Figures 17(a) and 17(b).

Figures 17(a) and 17(b). Photos of prepared black gel ink samples on Whatman 542 filter paper, collected pen set.

The ink on paper sample was then labeled with a unique identifier, as represented in Table 17, therefore each ink (plus paper) sample was a direct reference back to the ink pen (or source). The process was repeated for each ink source listed in Table 17, to reach the total of 24 ink source samples collected for analysis via LA-ICP-MS. Once all the respective lines were drawn, the ink was allowed to dry for 5 days on top of clean paper in the same clean fume hood described previously. Each ink sample then was placed in its own individual plastic bag with plastic forceps and remained isolated from the environment until analyzed.

On the 5th day, a section (~ 10mm x 10mm) of the applied ink sample was cut from the second grouping of lines approximately 5mm from the start of application (in the photo, Figure 18, the left most side). Each sample was extracted from the same area to ensure accurate comparisons between samples. The cut segments were then affixed to 24mm x 20mm glass slide covers (Fisher Scientific, Boston, MA) using double-sided tape. Sample analysis was performed subsequently. Again, the reason why the glass cover slides and double-sided tape were used was because the combination of the two provided a completely flat surface, which was necessary for optimum sample removal (ablation) and optimal signal stability. A photo showing the ink samples affixed to the glass slide covers can be seen below (Figure 18).
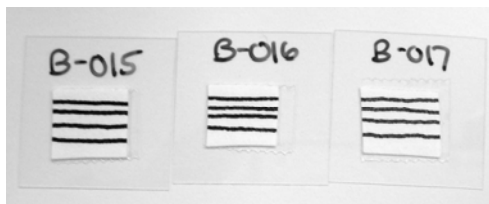
Figure 18. Photos of ink samples cut and affixed to glass cover slides (final preparation step prior to sample analysis by LA-ICP-MS).

4.3.3.4.1 Within Pen Variation Study

For the within pen variance study, the chosen ink source was B-001 (Gel Writer R_x) because of the design of the cartridge, which housed the ink. For this particular pen source, the ink cartridge provided graduations with respect to ink usage (or rather ink remaining). As seen in Figure 19, 100, 80, 60, 40, 20, and 0% graduations were provided by the manufacturer. This in turn allowed the analyst to take respective ink samples from the same pen at different usage intervals, simply by monitoring the amount of ink

remaining in the cartridge. The ink levels chosen for this study, which were strictly estimations, included 100, 75, 50, 25, 10, and 0% (percentage of ink remaining). One line was drawn for each interval in a similar fashion as the ink application procedure for the pen discrimination and the within pack studies, with the exception that the pre-application step was omitted or else there would not be a true 100% (ink remaining) analysis interval. Between the respective sampling intervals, continuous markings were made with the ink pen (in a similar fashion to when the pre-application step was performed for the other studies) until the desired mark or interval was reached.
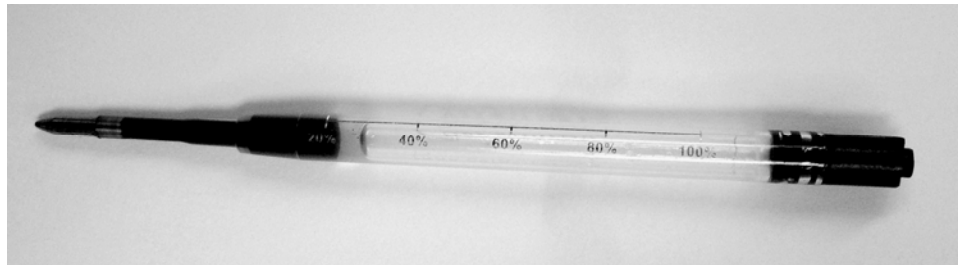
Figure 19. Photo showing the ink level graduations of the gel ink cartridge used for the within pen variation study, gel ink source B-001.

4.3.3.4.2 Within Pack Variation Study

For the within pen pack variance study, the same application format detailed above was followed and was completed in the same time frame as the samples prepared for the discrimination study and the within pen study, respectively. The ink source utilized in the within pack study was B-015 (Staples Sonix Gel), and as seen in Table 17, there were four pens in the associated pack. Thus, for this study, the three remaining pens in the associated pack were subjected to the pre-application, application, and affixation to the glass cover slides steps, as detailed previously. The only difference here is that all the

pens in the pack were sampled as versus one pen from a given pack for the discrimination study; at any rate, the four pens in this pack were all treated in the same manner to ensure accurate comparisons between pens in a single pack.

4.3.3.5   Matrix-Matched Standard Preparation

Matrix-matched standards are a crucial aspect to any quantification approach involving the analysis by LA-ICP-MS. And, given that a standard with detectable concentrations of the elements of interest is non-existent for this type of matrix (ink), it was sought after to produce one. The first approach involved finding a water-soluble ink which would provide the solubility (and matrix-acceptance) necessary for the addition of existing certified aqueous metal/inorganic standards (typically dissolved in 2-5% HNO_3). The one selected because of this requirement, and its commercial availability, was Montblanc fountain ink (Bethlehem, MA), which is typically used for pen refills, calligraphy, etc. General solubility tests were performed to ensure that side reactions and/or precipitation did not occur upon the addition of dilute HNO_3 solutions; there was no evidence of this. The second step in production of this matrix-matched standard was to determine what elements and the concentrations already existing in the matrix. Two methods were used to determine the elemental content (1) standard addition followed by dissolution ICP-MS and (2) standard addition followed by LA-ICP-MS. The first part was performed by two of my fellow group members, Yaribey Rodriguez and Tatiana Trejos, who have taken over the ink project where my work has left off. I performed the analysis for part two of this study (standard addition analysis and determination by LA-ICP-MS).

102

4.3.3.5.1 Digestion Methodology

Several attempts were made to obtain an optimum digestion methodology, including different combinations and varying concentrations of different acids (HNO_3, HCl, H_2SO_4) and hydrogen peroxide (H_2O_2). Open vessel digestion was preferred and therefore utilized because of the numerous complications associated with the microwave digestion assembly at FIU, including faulty equipment/problems with digestions vessels (thus incomplete digestion), sample carryover, and the low amount of sample that can be digested per analysis/interval (13, which includes blanks and other QC samples versus 54 samples/digestion for open vessel). The best overall approach was determined by a couple of factors: (1) complete digestion of the ink with no observable precipitation upon re-constitution, (2) analyte recoveries, based on spiked amounts into the ink/solvent, and, of course (3) safety and health-related conditions.

Approximately 0.1g (or 100mg) was weighed into a 68mL plastic (polypropylene) digestion vessel (Environmental Express, Mt. Pleasant, SC) using an analytical balance. For the samples designed to determine analyte recoveries, 10, 25, 50, 75, and 100ppb (final concentration after reconstitution) of the standards were added to the measured ink samples. Whether or not the sample was spiked, two milliliters of a 1:1 Optima Grade HNO_3(Fisher Scientific, Boston, MA): high purity water solution was added, followed by covering the vessel with a polypropylene reflux cap (Environmental Express) and heating on a hot block (Environmental Express) at 100°C for 20 minutes. The vessels were then removed from the heating device and allowed to cool down, once at room temperature 2mL concentrated HNO_3 was added followed by a 30 minute refluxing time period at 100°C on the hot block. The samples were checked and heating continued for up to an

additional 30 minutes avoiding complete sample dryness. Again, the samples were removed from the heating element and allowed to equilibrate to room temperature, at which point 1mL of 30% Optima Grade H_2O_2 (Fisher Scientific, Boston, MA) was slowly added to the sample vessel. The exothermic reaction of the acid and peroxide was allowed to culminate at room temperature (~5 minutes), after which an additional 1mL of H_2O_2 was added, followed by heating to dryness overnight. The digests were then re-constituted by the addition of 10mL 0.8M (or 5%) HNO_3, sonication for 15 minutes, and finally filtered with a membrane syringe-like filter (Environmental Express), up to a volume of 10.00mL in a volumetric flask. Three replicates of each of the respective standards were digested (0, 10, 25, 50 and 100ppb) as well as three replicates of the reagent blank (utilized for blank subtraction).

4.3.3.5.2 Standard Addition Study by Dissolution ICP-MS

For the standard addition experiments, Al, Mn, Fe, Ni, Cu, Sr, Ba and Pb standards were spiked into 0.1g ink to achieve final concentrations of 0, 25, 50, 75, and 100ppb after the reconstitution step outlined in the previous section (digestion methodology). An internal standard (Sc) at a final concentration of 50ppb was added as well. Both the spiked ink samples, the reagent blanks, and the standard addition samples were then analyzed via dissolution ICP-MS. The digested ink samples were analyzed using an external calibration curve (points on the calibration curve included: 0, 10, 25, 50, and 100ppb). Calibration curves were performed in Microsoft Excel by plotting concentration versus intensity. The unknown elemental concentration of the ink was then tabulated via linear regression statistics and the ICP-MS intensities obtained for the

digested ink samples. The standard addition samples were analyzed (in Excel) by graphically correlating the added element concentrations to the respective signal (or intensity) for each standard addition sample. By using the linear regression statistics obtained by the correlation plots and simply extrapolating back to zero intensity (setting y equal to 0), the respective elemental concentrations in the ink were calculated (by solving for x).

4.3.3.5.3 Standard Addition Study by LA-ICP-MS

For comparison purposes, a standard addition experiment was also prepared and analyzed for LA-ICP-MS. Being a solid sampling technique, many alterations had to be made including the amount of ink and concentration of standards added in addition to a method for application of the ink (spiked and non-spiked) to the substrate. The substrate in this experiment (paper source) was Whatman Grade 42 filter paper. Table 18 outlines the procedure followed for the creation of the ink standard addition experiment to be analyzed by LA-ICP-MS; the ink standards (S0 through S5) below were prepared in polypropylene 2mL sample vials.

Table 18. Sample preparation quantities used for the standard addition experiment, LA-ICP-MS.

	S0	S1	S2	S3	S4	S5
ink amount (µL)	400	400	400	400	400	400
standard conc.(ppm)	0	10	25	50	75	100
amount standard (µL)	0	50	50	50	50	50
amount IS (10ppm Sc)	50	50	50	50	50	50
amount HNO_3 (µL)	50	0	0	0	0	0
final conc.(ppm)	0	1.0	2.5	5.0	7.5	10.0

Following the standard preparation step, 50µL the above standards (containing the stated concentrations of Mn, Fe, Ni, Cu, Sr, Ba and Pb) were applied to Whatman 42 filter paper using a 100µL Eppendorf pipet (Westbury, NY) with each standard comprising its own sample; ink drops were also added onto Office Max Copy paper for comparison purposes only. As with the other applied ink samples, the ink was allowed to dry for five days prior to analysis and three replicates (ablated lines) per standard were analyzed by LA-ICP-MS.

4.3.4   Data Analysis

The data analysis approach used for the ink experiments included an initial data reduction step/analysis by Geopro Software (Cetac Technologies, Omaha, NE) which allows the analyst to integrate specified areas of the time resolved spectra generated by the ICP-MS and then provides a numerical signal for each isotope (in units of counts per second, cps). An example of this data analysis reduction graphical output can be found in Figure 20, which denotes the when the ablation began (at ~18 sec) and ended (~78 sec), the selected integrated signal (ablated area), and the selected signal attributed to the gas blank. The integrated intensities are then copied into Microsoft Excel for further data analysis, including calculation of means, standard deviations, and percent relative standard deviations (% RSDs) as well as generation of graphs (linear regression, bar plots, etc.) and in some cases some statistical analysis approaches (i.e. performance of student t-tests). For the discrimination studies, Systat 11 (Chicago, IL) was utilized to perform pairwise comparisons via the analysis of variance (ANOVA) with Tukey's post hoc test. The combination of ANOVA and Tukey's test allowed for multivariate analysis

(multiple sample and multi element comparisons) without increasing the error probability (the 95% confidence interval was used in all discrimination studies). Without Tukey's post hoc test, the error probabilities become additive when combining all elements for discrimination purposes. Tukey's test allows this 5% error probability to remain in tact regardless of the amount of elements used to discriminate the associated samples.
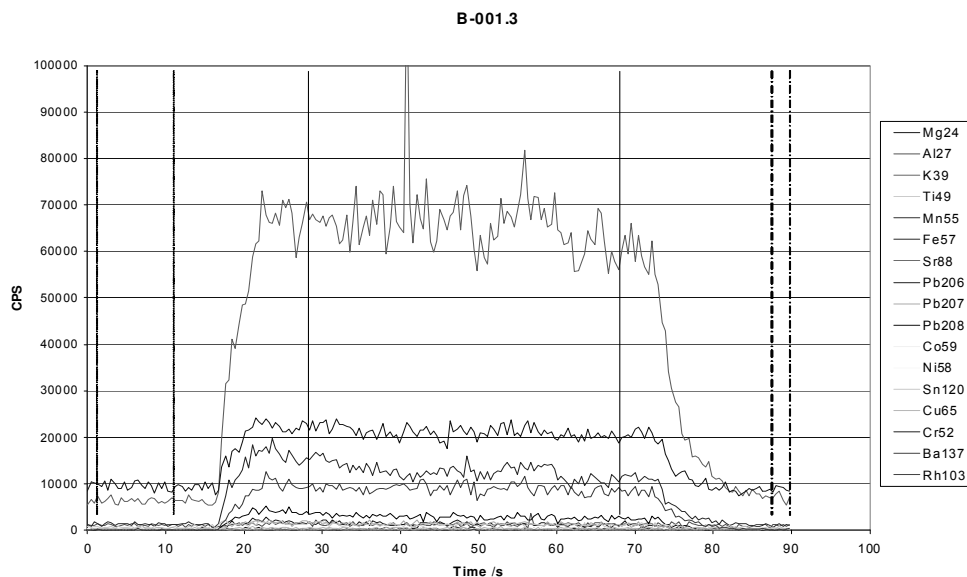
Figure 20. Time resolved spectra for gel ink sample B-001, LA-ICP-MS.

4.4 Results and Discussion

4.4.1 Laser Energy Study

The objective of this experiment was to determine at which laser energy the most analyte signal (ink) and least background signal (paper) was generated. Figure 21 and Figure 22 best summarize the data collected and help show the results discussed in this section. In the given plots intensity is the integrated intensity (in cps), which is correlated to the percentage of laser energy used to generate the time resolved spectra.

107
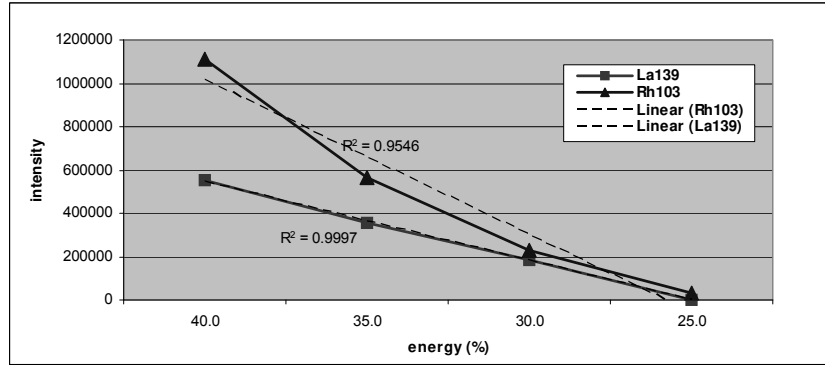
Figure 21. Element intensities as a product of laser energy, 10ppm Rh (spiked paper) and 10ppm La (spiked ink).
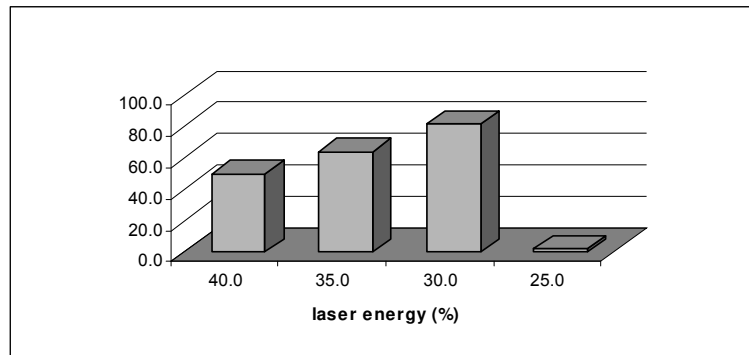
Figure 22. Element ratios based on intensity of the respective signals, La/Rh, at different laser energies.

It can be seen in the given plots that the best approach for this particular combination of ink (MontBlanc fountain ink) and paper (Whatman 2 filter paper) was 30% laser energy (~0.1mJ). More specifically, the first plot shows that when the laser energy is increased (and thus almost reaches a threshold with respect to burning through the paper substrate, > 40% energy) the amount of ink ablated (and thus signal) increases when compared to ablation at lower laser energies. However the amount of paper ablated (and attributing signal) has also increased, assuming that the amount of paper and ink

108

ablated is proportional to the concentration of those respective elements in the paper and ink, respectively. At any rate, in the ideal case, the sought after parameters centralized around reducing the amount of paper ablated while still obtaining an adequate ink signal. Therefore the point at which the two intensities (ink and paper) are close (or closest) together would provide the best analytical approach with respect to laser energy for this particular combination of ink and paper. As an illustration see Figure 22, which is a ratio plot of La (ink ablated) to Rh (paper ablated), which shows that at 30% laser energy the ink to paper ratio is at a maximum (a ratio of La/ink to Rh/paper). Despite the given results, the laser approach of using 30% energy was inadequate for removing gel inks from its paper counterpart, partially due to the difference in the matrix itself (gel versus fountain). The main issue with the given approach was that the estimated or assumed concentrations found in the gel inks was oftentimes lower than 10ppm, thus the amount of ink entering the ICP-MS needed to be increased to achieve detectable levels, meaning that higher laser energies were necessary.

4.4.2 Paper Study

The paper intensities per isotope were ranked by comparing the mean + the standard deviation (or the largest possible attributing signal) for each element. Thus the paper source that had the lowest signal would receive a "1" while the paper source that produced the highest background signal for that particular element/isotope received a "10". These ranked values (for all the elements combined) were then added together to give each paper source an overall sum wherein the lowest sum was awarded the highest ranking (or lowest overall background signal). Table 19 shows the overall rankings by

paper source. Whatman 542 filter paper had the lowest overall background signal with Whatman 42 being a close second. These two paper sources were used in the collected gel ink pen studies (Whatman 542) and the discrimination of the samples provided by the United States Secret Service (Whatman 42).

Table 19. Paper source rankings used to determine the lowest background signal attributed to the substrate (qualitative analysis of paper).

paper source	sum^{rank}	RANK
I	29	1
H	32	2
G	37	3
F	56	4
A	91	5
E	99	6
C	105	7
B	111	8
D	115	9

The following plots (Figure 23 and Figure 24) help to demonstrate the superior performance or low background levels attributed to the Whatman filter paper sources, especially for grades 42 and 542. In several cases, when the gas blank was subtracted from the integrated signal there was zero reported intensity which means these elements are not present in the associated paper sources or, more likely, that for this instrument the amount of certain elements in the paper are below detection limits. The plots demonstrate the large elemental content (in terms of intensity) for paper sources that would be likely encountered in forensic document examinations. The elemental composition stemming from the paper is crucial (and must be taken into account) when interpreting the elemental content for an ink applied to the paper. Namely, it is necessary to establish that a given elemental concentration came from the ink or the ink plus the paper, with the latter scenario being most probable. Additionally, if the background (paper substrate)

110

signal was extremely high (or high in general) for a particular element, then small concentrations of that element in the ink may not be distinguished from the paper source itself. For example, in Figure 23 the Mg signal coming from the paper ($\sim 3 \times 10^6$ to 13×10^6 counts) could mask any Mg signal attributed to an ink if it was applied to that particular paper source. Other elements that may fall within this category (at least for the paper sources included in this study) are Al, Ba and Sr. The potential lack of discrimination (ink from paper) may pose a problem when drawing associations or discriminating ink samples (or documents), especially when two different paper sources are utilized. The problem is less likely to occur for elements such as Cu, Ni, Co and Pb where relatively low background signals in the paper were observed.
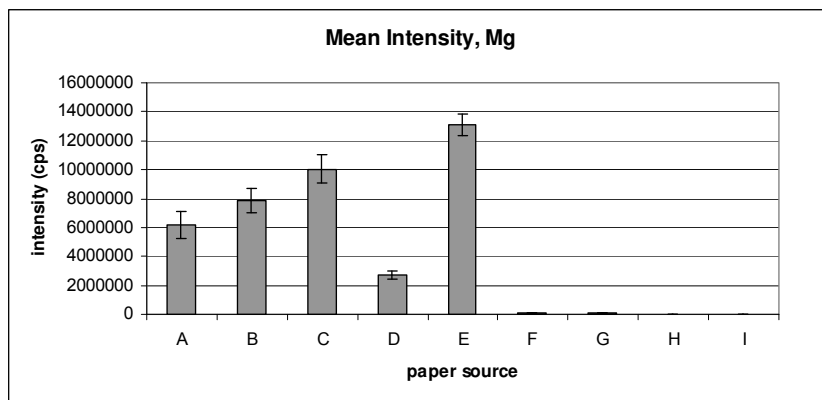

Figure 23. Average Mg integrated signal for different paper sources. Source descriptions for A-I can be found in Table 16.
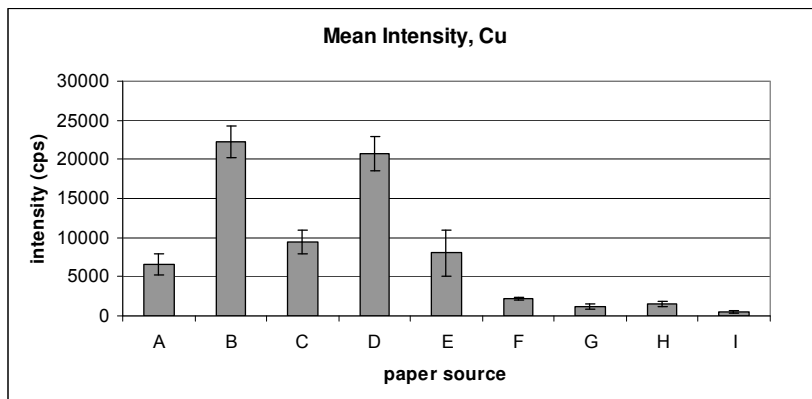
Figure 24. Average Cu integrated signal for different paper sources. Source descriptions for A-I can be found in Table 16.

One paper source (Office Max Copy paper or source B in Table 16) was analyzed for sample homogeneity/heterogeneity where 10 sample replicates were analyzed under the same conditions at different points across the 10mm x 10mm segment cut from a single page. The graph in Figure 25 shows that even in this small section of paper (which only represents approximately 0.2% of the entire sheet) there is a considerable difference from one region to another. Therefore a general everyday paper source (multi-use, copy, etc.) can be assumed to exhibit a high degree of sample heterogeneity (~30% RSD or more) and this should be considered when performing document examinations (including ink analyses) by LA-ICP-MS. Nonetheless, the analysis was only performed for one paper source, further studies should be conducted to establish sample heterogeneity for whole sheets of paper and different pieces within a ream of paper, both of which would be expected to display an even greater amount of heterogeneity. The types of filter paper used in the studies outlined did not exhibit the heterogeneity issues encountered and observed with general or everyday type sources.
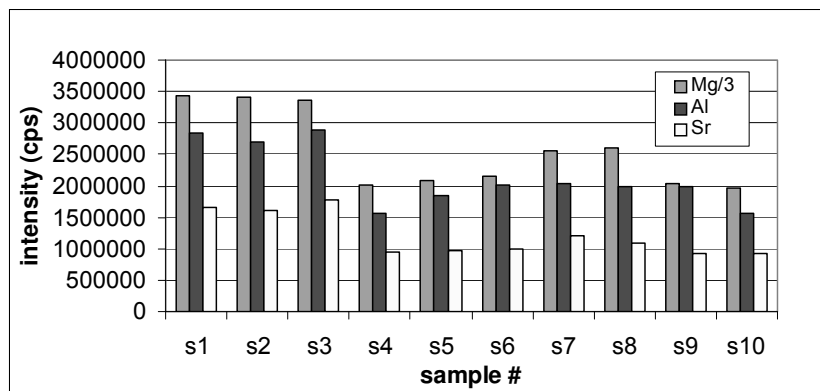
Figure 25. Signal distribution of Mg, Al and Sr for 10 sample replicates ablated from a 10mm x 10mm area of Office Max Copy paper.

4.4.3   Discrimination Study: USSS Sample Set

As previously stated, the number of samples sent to FIU for analysis by the United States Secret Service included 45 samples and at the time of writing this dissertation the source of origin of those samples was unknown. Three replicates of each sample were analyzed qualitatively by LA-ICP-MS where the integrated intensities (via integration of each time resolved spectra) were utilized to make sample pairwise comparisons. Using the equation, the number of possible pairs equals N(N-1)/2, where N represents the number of samples. In this case N=45, therefore the total number of possible comparisons is 990.

Using the statistical analysis approach outlined earlier (ANOVA with Tukey's post hoc test at the 95% confidence interval), the number of indistinguishable pairs found for this sample set was 225 (or 77.3% discrimination) using a combination of 14 elements. The discrimination results per element can be found Table 20, which lists the elements in order of percent discrimination (greatest to lowest discrimination power).

Table 20. Percent discrimination by element for the USSS sample set.

element	# indist.pairs	% discrimination
K	538	45.7
Sr	691	30.2
Cu	718	27.5
Mg	736	25.7
Fe	776	21.6
Co	838	15.4
Ni	860	13.1
Ba	861	13.0
Ti	864	12.7
Sn	867	12.4
Al	903	8.8
Pb	904	8.7
Mn	946	4.4
Cr	947	4.3
combined	225	77.3

A t-test (at the 95% confidence interval) was applied to those 225 pairs found indistinguishable by ANOVA which reduced the number of indistinguishable pairs down to 44 (or 95.6% discrimination). The 44 indistinguishable pairs after the combination of ANOVA and t-test can be found in Table 21. As stated previously, this was a blind study and the sample origins were unknown until the writing of this dissertation. At any rate, according to the United States Secret Service there were five sources which shared common origin and theoretically should share similar elemental profiles, these five pairs include: 13:41, 17:42, 21:43, 29:44, and 37:45. Of these five pairs, only one of the pairs was determined to be indistinguishable by LA-ICP-MS, sample 17 and 42, which leaves four pairs that came from the same pen that were differentiated by LA-ICP-MS. This equates to a 0.4% false exclusion (or Type I error) rate. The 39 remaining pairs that were determined to be indistinguishable by LA-ICP-MS then equate to a maximum false inclusion (or Type II error) rate of 3.9%. Although it must be stated that according to the United States Secret Service, the formulation for these particular ink samples was not available (or unknown) at the time of application, meaning that some of the associated

pairs could have originated from pens from the same pack or pens from the same manufacturer or production plant.

Table 21. USSS samples found indistinguishable by LA-ICP-MS.

sample ID	indistinguishable with…
6	9, 10, 16, 18, 29, 32
7	32
8	17
9	16, 17, 18, 27
10	16, 18, 29
16	18, 29
17	18, 27, 29, 33, 42, 44, 45
18	29
24	36, 39
27	36
29	36, 42
33	36, 42
34	39
35	36
36	37, 38, 42, 44, 45
39	44, 45
42	44, 45
44	45

However in the case that the false inclusion rate is indeed accurate (though given the samples and the fact that qualitative analysis was performed without an internal standard, this error rate is very low), it is important to point out two possible reasons for the potential lack of discrimination power associated with this study. For the most part, the precision was not stellar but it was considered acceptable (many %RSDs were between 25-15% or even less in some cases) depending on the sample, the element or both. Acceptable precision for this matrix and application (in this author's opinion) is anything lower than 15% RSD considering the heterogeneity issues expected and encountered for these samples. For example, some of the heterogeneity issues could have been avoided if a more controlled approach by which these ink samples were applied was followed, avoidance of ink lines being drawn on top of ink lines would have helped as would reducing the possibility of cross-over contamination upon application and during

sample storage. Additionally, some of the provided samples had a greater degree of heterogeneity, such as the inks with glitter; although that fact itself probably increased the discrimination. Another factor that may have influenced the higher % RSDs was that for some elements (in some samples) the limits of detection were being approached. Overall, precision and sample variation (from one sample to the next) are correlated with respect to discrimination, so even if the precision was less than 5% RSD and a great degree of sample variance was not present, then it would be difficult (or in some cases impossible) to discriminate those samples. In other words, the more similar in elemental composition two samples are, the greater the precision needs to be in order to differentiate the samples. At any rate, a few illustrations of the precision across the USSS sample set are presented here (see Figure 26 and Figure 27).
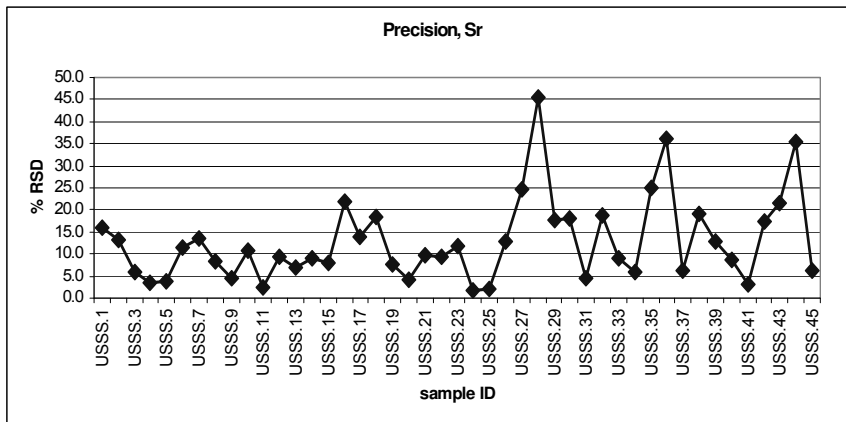

Figure 26. Precision values for Sr across the USSS gel ink sample set.
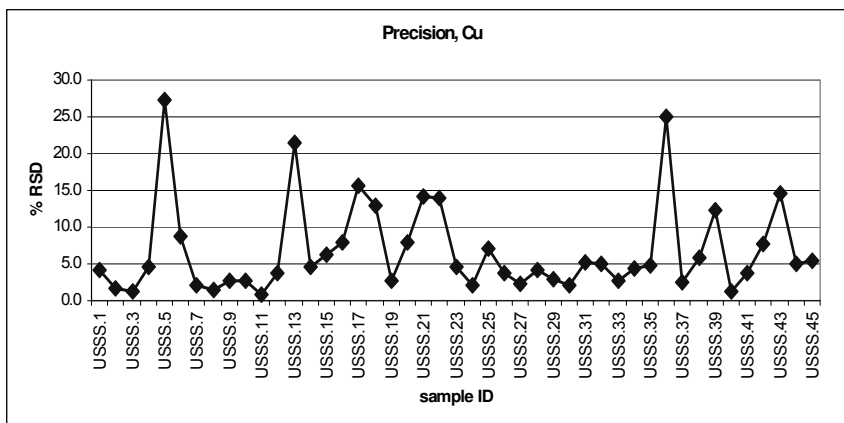
Figure 27. Precision values for Cu across the USSS gel ink sample set.

The following graph (see Figure 28) shows the compositional variations in elemental composition across the USSS sample set using just 5 of the elements used for discrimination (the others were excluded for appearance purposes only). The plot shows that for the elements selected, many samples have similar element profiles, especially when considering the deviation from the elemental means where there is even more overlapping regions. The correlation of precision and compositional variation is even more pronounced by looking at one element, for example the distribution of Cu (see Figure 29), despite having excellent precision (sample IDs USSS.27-33) the lack of variation in the composition of Cu (~50000cps) in those samples prevents discrimination. Nonetheless, there are some samples that have a very different profile than the others in this set with respect to Cu (i.e. USSS.21, 22, and 43), which allows some differentiation and this was observed for other elements as well. Therefore, discrimination between the samples in this set was difficult for many reasons, as described previously. , however again the source of origin is yet unknown and the associated (or match) samples may indeed be from the same source.

117
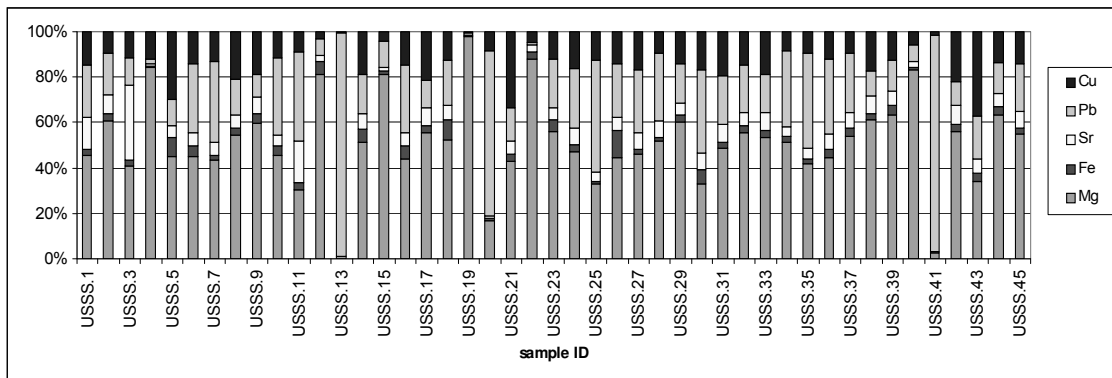
Figure 28. Elemental profiles/distributions (five elements) for the USSS sample set.
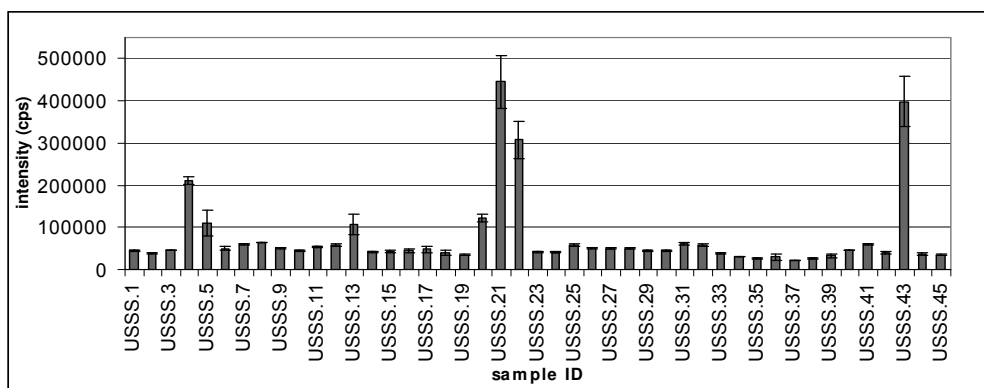
Figure 29. Mean element intensities of Cu (± standard deviations), USSS sample set.

4.4.4   Discrimination Study: Collected Gel Pen Set

Twenty-four samples comprised the set of black gel ink samples collected and analyzed under a more controlled environment, as detailed in the sample preparation section. Following the N(N-1)/2 rule, the total number of possible pairwise comparisons is 276. Three replicates of each sample were analyzed. The precision for most samples (and elements) was typically between 5-20% RSD, in some cases less than 5% RSD was obtained. A few examples of the precision obtained for this sample set can be found in Figure 30 and Figure 31.
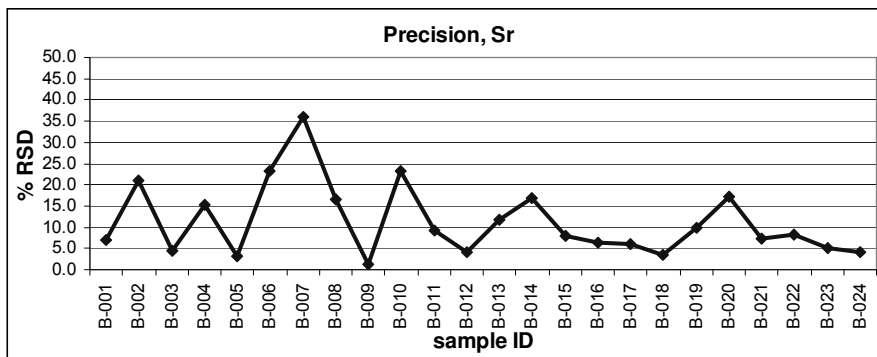
Figure 30. Precision values for Sr intensities across the collected gel pen set.
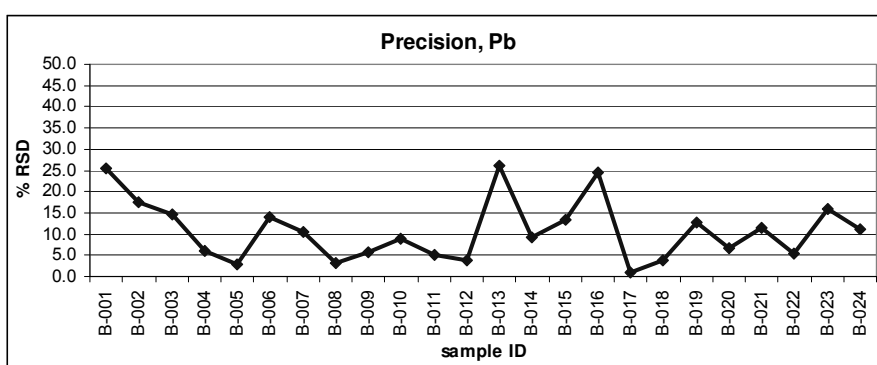
Figure 31. Precision values for Pb intensities across the collected gel pen set.

As with the other discrimination study, the data analysis format followed was the same (the utility of ANOVA with Tukey's post hoc test). Pairwise comparison analysis yielded only eight indistinguishable pairs (or 97.1% discrimination) using a combination of 14 different elements and their respective integrated intensities. A summary of the number of indistinguishable pairs (and the associated percent discrimination) per element can be found in Table 22. Following ANOVA, the eight indistinguishable pairs were subjected to a t-test, which reduced the number of indistinguishable pairs from eight to only two. Therefore, a combination of ANOVA and t-test yielded 99.7% discrimination power for this study.

119

Table 22. Percent discrimination by element for the collected gel ink pen set.

element	# indist.pairs	% discrimin.
Sr	92	66.7
Mg	112	59.4
Pb	115	58.3
Mn	189	31.5
Cu	190	31.2
Co	207	25.0
Fe	212	23.2
K	223	19.2
Al	232	15.9
Ni	232	15.9
Ba	252	8.7
Sn	253	8.3
Ti	254	8.0
Cr	276	0.0
combined	8	97.1

The origins of the 2 indistinguishable pairs found in this discrimination study are listed in the table Table 23. As one can see, these two indistinguishable pairs exhibit a valid explanation as to why similar elemental profiles were found. In each case, the paired ink pens originated from the same source (manufacturer: Uni-Ball). Interestingly, the associated sources were the from the same model, B-006 and B-011 were Uni-Ball Signo 207 pens while B-017 and B-020 were Uni-Ball Signo Gel RT pens. These pens were expected to be indistinguishable considering that the same origin was shared, and furthermore since B-017 was collected from Florida and B-020 was collected from Missouri, it is suspected that the pen packs were manufactured in the same plant (or area of the plant) at about the same time.

Table 23. Description of the indistinguishable pairs found by LA-ICP-MS, collected gel ink pen set.

pair #	sample ID	brand	model
1	B-006	Uni-Ball	Signo 207
	B-011	Uni-Ball	Signo 207
2	B-017	Uni-Ball	Signo Gel RT
	B-020	Uni-Ball	Signo Gel RT

The similarity in the elemental profiles for the indistinguishable pairs can be visualized in the graph below (Figure 32) which is a plot of sample ID versus collective mean intensities (plotted as a percentage in comparison to the amount of elements used). Only five of the elements (five of the more discriminating elements) were chosen for this type of plot so that differences by element between samples can be seen.
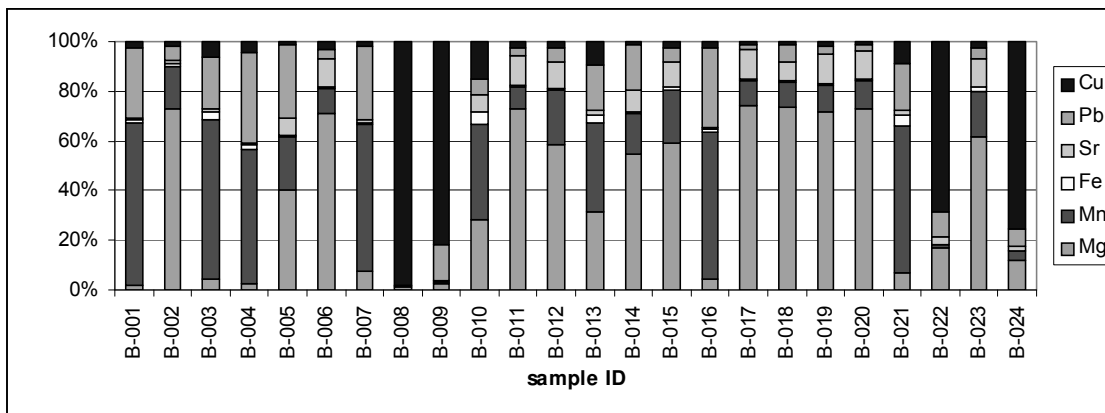
Figure 32. Elemental profiles/distributions (six elements) for the colected gel pen set.

4.4.5 Within Pen Variation Study

As stated in the sample description section, one pen (B-001, Gel Writer Rx) was analyzed by LA-ICP-MS at different ink levels (100, 75, 50, 25, 10, and 0% by approximation) to determine if a given pen has the same elemental composition throughout the cartridge. The results show with the exception of when the pen was first utilized (100% ink level), the usage intervals were found indistinguishable by ANOVA, meaning that the elemental composition is homogeneous throughout the different stages of use. There are many reasons why that particular interval (100% ink level or 0% use) was found different (or discriminating) from the rest of the usage intervals. The first being that for this pen there was a small sealant (glue) affixed to the tip (presumed to

121

prevent leakage prior to use), which could have caused some contamination at initial use of the pen. Also, given that it was the first use of the pen tip (which is metal in content), the elemental composition coming from the tip itself may be the culprit for the increased signal. Once the pen had been used the observed spike in elemental content was removed or neutralized. The figures [Figure 33(a) and 33(b)] below illustrate these results graphically, it is important to note that the observed trend was consistent across all elements (in this case only two examples are shown).
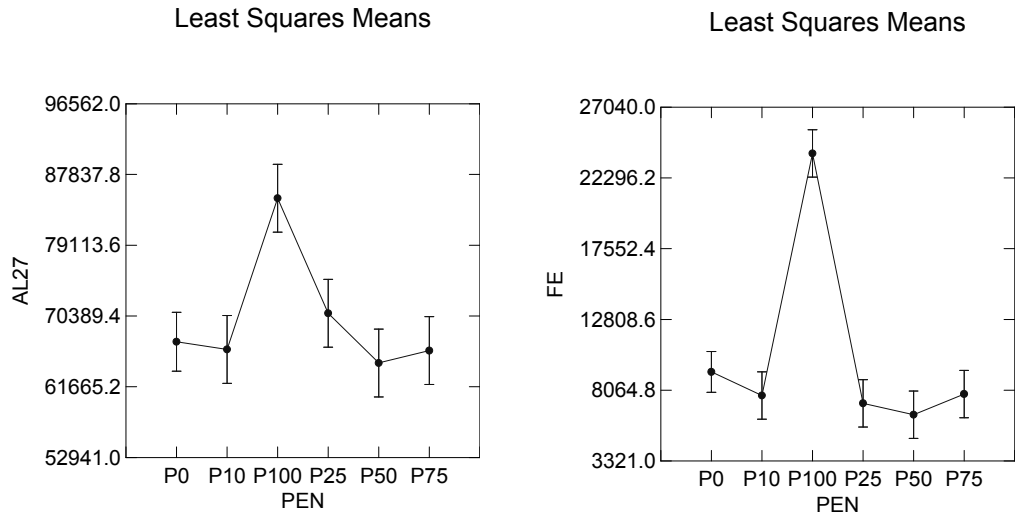
Figures 33(a) and 33(b). ANOVA results for Al and Fe, respectively, for the within pen variation study. X-axis represents the amount of ink remaining in the ink cartridge (0, 10, 25, 50, 75 and 100%). Y-axis represents the mean element intensities (with the associated standard deviations).

4.4.6   Within Pack Variation Study

The homogeneity (or heterogeneity) across a pack of pens (pen source B-015, Staples Sonix Gel) was studied, in this case there were four pens analyzed by LA-ICP-MS at the same point of usage (see the sample description/preparation section). The results (ANOVA) show that each of the pens was indistinguishable from the others in the same pack, meaning that the elemental composition across a pack of pens is the same (at the 95% confidence interval). Along with the within sample variance study, this study is significant from a forensic standpoint because it shows that for at least this pack (4 pens) there is no difference in elemental content. It can then be assumed that pens from the same manufacturer and lot number are indeed similar in elemental composition, which helps to describe why two pens (one unknown source and one known ink source) are a possible match and more importantly the significance of that match. Figure 34 helps to illustrate the mentioned results; the plot shows the overlapping intensities for the four pens originating from the same pack.
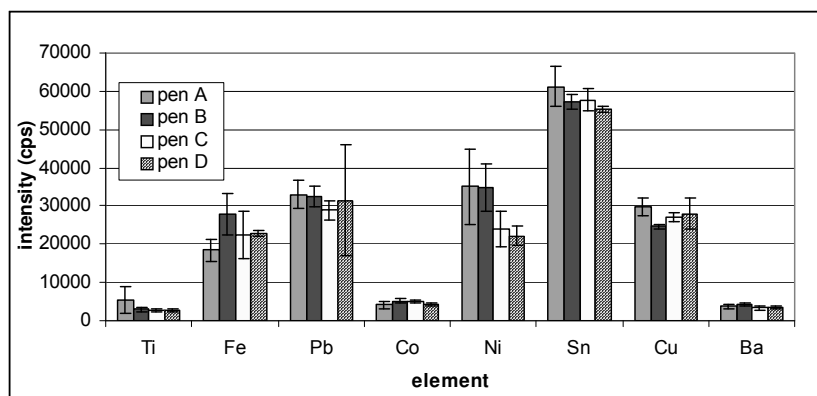
Figure 34. Sample statistics, plot of mean intensities (± standard deviations) for pens in the same pack.

4.4.7   Ink Matrix Matched Standard Preparation

4.4.7.1   Element Distribution

As seen in Figures 35(a) and 35(b) when a single 50µL drop was applied to each of the substrates (filter paper and copy paper) the appearance of the ink was drastically different. The photos and the actual ink applications in this experiment were performed by Tatiana Trejos. A more uniform ink drop (in terms of appearance) was observed for the 50µL drop on filter paper in comparison to the ink drop application to copy paper.
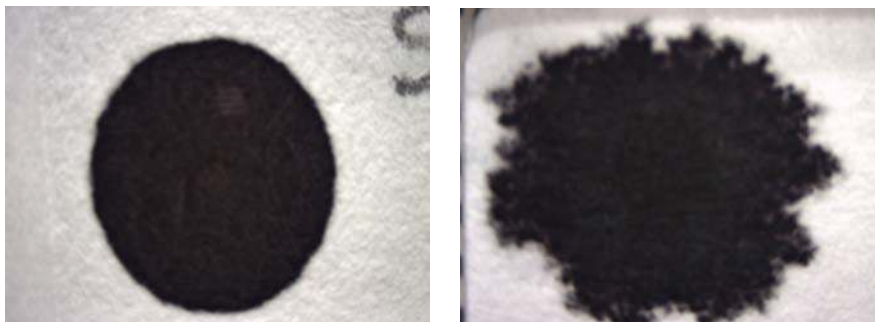
Figures 35(a) and 35(b). A 50µL drop of Montblanc fountain pen ink on Whatman 42 filter paper (a) and Office Max Copy paper (b).

For the filter paper sample, the elemental distribution contained within the ink drop was non-uniform across the entire drop, with higher element intensities generated towards the edges (or where the ink stopped distributing). Figure 36 shows a time resolve spectra created by LA-ICP-MS which demonstrates the elemental distribution across the entire drop (a cross section of the ink drop was sampled/analyzed). The experiment shown in this figure was part of the original laser energy studies mentioned earlier in this work where La at a concentration of 5ppm in the ink was added to filter paper spiked with 20ppm Rh. The intensities of the internal standard in the paper (Rh) are greater at

the edges of the ink drop. One explanation for this is that when the ink was added to the filter paper spiked with Rh, the ink acted as a solvent and then extracted/carried some of the Rh concentration at point of impact to the edge where the ink ceased. In other words, as the ink distributed across the filter paper (via capillary action) greater concentrations of Rh subsided when the ink subsided. There was also an observable difference between the two paper sources with regard to the amount of ink absorbed, though the actual amount absorbed was not determined. The filter paper absorbed more ink (exhibiting surface and subsurface characteristics) whereas when was applied to the copy paper, the fountain ink remained mostly on the surface (with minimal absorption into the paper substrate).
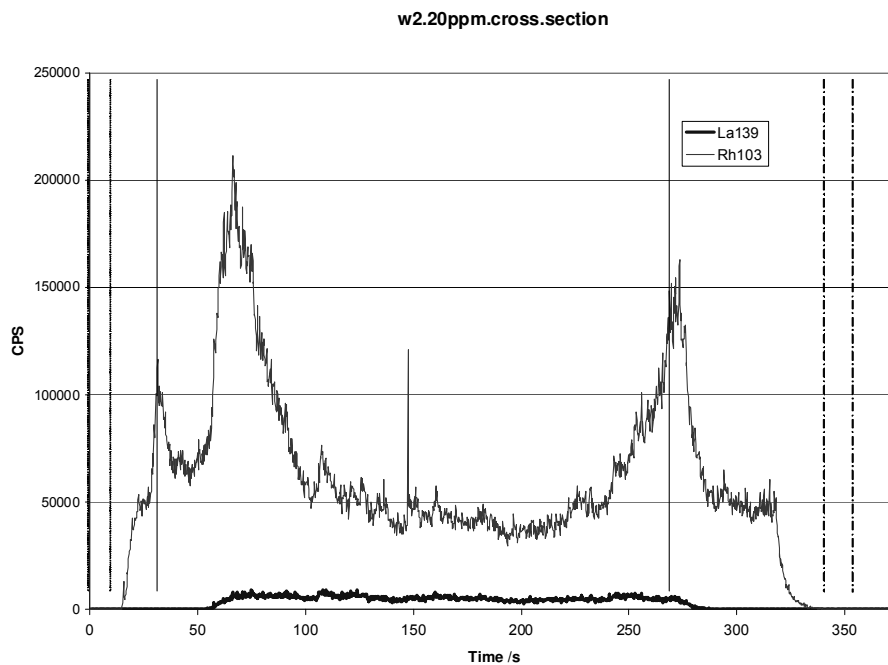
Figure 36. Elemental signal cross section of an ink drop (spiked with 10ppm La) applied to Whatman 42 filter paper (spiked with 20ppm Rh).

125

Ink distribution or potential solubility of components of the paper into the applied ink, which is acting as a solvent, should be considered in future experiments where standards are applied for quantification purposes. It is important to point out that the attributed elemental content stemming from the paper (in this particular case) was even less distinguishable from the elemental content of the ink, which is a verification of this joined marriage between an ink source and the paper it has been applied to. In other words, paper is very important to ink analysis by LA-ICP-MS and must be given proper attention when characterizing ink samples.

4.4.7.2 Standard Addition Studies

The mean analyte recoveries (N = 15) following digestion were as follows: Mn (113%), Fe (110%), Ni (107%), Al (72%), Cu (97%), Sr (107%), Ba (111%), and Pb (97%). For dissolution and laser ablation ICP-MS, the linear regression statistics (R^2 value) for the plots were within the 0.98 – 1.00 range for all the elements used in the study. An example of two standard addition plots for copper generated by the dissolution and laser ablation data sets, respectively, can be found in Figure 37 and Figure 38.

Standard Addition, dissolution, Cu

y = 0.0357x + 0.5212
R^2 = 0.9996
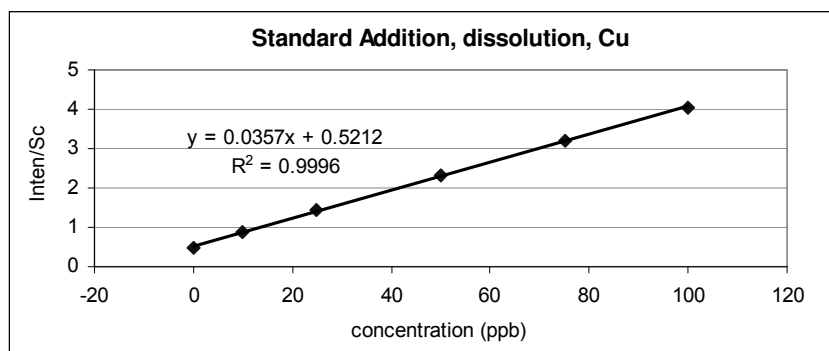
Figure 37. Standard addition plot, Cu, dissolution ICP-MS.
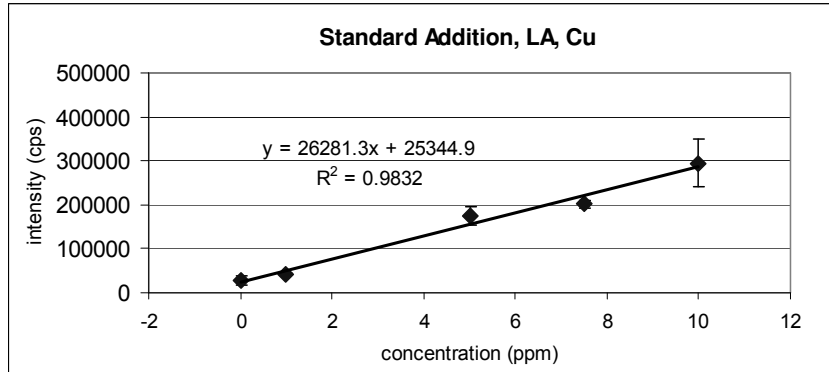
Figure 38. Standard addition plot, Cu, LA-ICP-MS.

The equation for the generated line (and the regression statistics provided by Excel) were then utilized to determine the concentration (x) [and the statistical standard deviation] of each element in the fountain ink by setting y (intensity in the case of LA-ICP-MS and intensity/Sc intensity for dissolution ICP-MS) equal to zero. The resulting concentrations (c_x) and standard deviations (s_c) were tabulated via the equations shown below:

$$c_x = b/m \quad \text{equation (3)} \qquad s_c = c_x \sqrt{\left(\frac{s_m}{m}\right) + \left(\frac{s_b}{b}\right)} \quad \text{equation (4)}$$

The results of these experiments are summarized in Table 24 following this paragraph, which demonstrates that the dissolution method and the LA-ICP-MS methods for determining the concentrations of these elements in the fountain pen ink were in agreement. Less precision for LA-ICP-MS was obtained as versus dissolution ICP-MS, which is a product of the low amount of ink sampled per laser sampling interval, estimated to be 0.8 to 8.0 picograms for the range of concentrations in the standard addition experiment. The estimated mass removal is based on the assumption that the entire mass of a given element was removed from the sampled (ablated) spiked ink line

127

and that the elemental composition was uniform across the drop. Recall that for the dissolution experiment the amount of ink originally digested was in the milligram range; this amount of mass is several orders of magnitude higher than the mass of ink sampled by laser ablation. Given that less mass is entering the ICP-MS with the laser ablation experiment, higher concentrations are often necessary (or higher detection limits are observed) for laser ablation ICP-MS in comparison to dissolution ICP-MS for some applications. The reported results (in terms of the elemental composition of the ink) are in agreement for both analytical approaches (dissolution and LA-ICP-MS) meaning the ink has been characterized by one method and verified by the other. Therefore, the development, preparation, and utilization of a matrix-matched ink standard of known elemental composition (using this fountain pen ink as the model matrix) looks promising for ink analyses by LA-ICP-MS.

Table 24. Comparison of standard addition results per element for Montblanc fountain pen ink, LA-ICP-MS versus dissolution ICP-MS.

Element	Conc. of ink (ppb) Laser Ablation	Conc. of ink (ppb) Dissolution
Al	1892 ± 492	2330 ± 300
Mn	1176 ± 353	1388 ± 56
Fe	3582 ± 931	3677 ± 125
Ni	279 ± 40	250 ± 14
Cu	964 ± 386	1230 ± 64
Sr	286 ± 63	329 ± 16
Ba	322 ± 84	379 ± 6
Pb	174 ± 61	198 ± 26

4.5   Conclusions and Future Considerations

The results demonstrate that a method for the elemental analysis of gel inks on paper has been developed, optimized, and tested. Homogeneity studies show insignificant variation in elemental compositions within a single pen, with the exception of the first ink markings made with a pen (~100% ink remaining). In addition, it has been demonstrated that there are also insignificant differences in the elemental composition across a pack of gel ink pens (in the analyzed set, four pens were found indistinguishable). Two discrimination studies were performed, which demonstrated that there are significant differences in the elemental compositions between samples originating from different sources. In one study, 45 indistinguishable pairs were found out of 990 possible comparisons, which accounts for approximately 95% discrimination. In the second discrimination study, only 2 pairs were found indistinguishable out of a possible 276 comparisons (or ~99% discrimination); these two indistinguishable pairs originated from the same source and thus had an explanation as to why similar elemental profiles were observed. In addition, a water soluble fountain ink matrix (to be later used as a matrix-matched standard for quantitative analysis) was characterized by both dissolution ICP-MS and laser ablation ICP-MS and the results were in agreement. Therefore, preliminary data shows that the development of a matrix-matched standard for quantitative ink analysis by LA-ICP-MS looks promising.

Future direction of this work includes the movement towards quantitative analysis by LA-ICP-MS, which includes further characterization of the ink substrate and then potential addition of detectable quantities to mimic concentrations found in typical gel ink samples. Use of an internal standard (added to an existing ink marking) should also

be explored to help increase accurate determinations and precision values between sample replicates. In addition, once the matrix-matched standard has been developed, method detection limits should be determined. Further studies related to the elemental effects of typical paper sources, such as copy or multi-use paper, and accurate ink determinations are also needed, as is a more in depth paper study (possibly even discrimination studies of multiple paper sources, within paper source studies, etc.). Additional ink population studies are also necessary to validate the developed LA-ICP-MS method found in this dissertation, which should include within plant studies (or within ink lot studies) and a study designed to determine the degree of variation of ink formulations over time. The applied techniques can also be extended and used to analyze other classes of ink, including markers, ink jet ink, copier toner, among others in order to help differentiate or associate a questioned document back to its source.

5   CONCLUSION

The work presented in this dissertation has outlined results that will certainly help the forensic community with respect to both glass and ink analyses. In the first part of the research, nanosecond LA-ICP-MS was proven to offer similar figures of merit for the forensic analysis of glass (in terms of accuracy, precision and discrimination power) when compared to femtosecond LA-ICP-MS, which was hypothetically expected to outperform nanosecond LA-ICP-MS. It was also shown that an internal standard was necessary in order to obtain accurate and precise results for both methods, meaning that internal and matrix matched standardization are important to ensure optimum quantitative analyses by LA-ICP-MS, whether the laser be a nanosecond source or a femtosecond

source. The observed comparable results by nanosecond and femtosecond LA-ICP-MS is attributed to the utilization of quantification from a glass matrix-matched standard, which is readily available to the scientific community. In cases where a matrix-matched standard is not available (and in some cases a good internal standard is not available), femtosecond LA-ICP-MS could provide improved results (in terms of precision and discrimination potential) over nanosecond LA-ICP-MS analyses for the same matrix.

Laser induced breakdown spectroscopy (LIBS) was introduced for the analysis of glass, which was shown to provide similar discrimination potential (>99% discrimination) for an automotive glass sample set of forensic interest when compared to two of the leading techniques in elemental analysis, XRF and LA-ICP-MS. A strict protocol for data evaluation of LIBS spectra was evaluated and then followed to minimize Type I (false exclusion) errors and eliminate Type II (false inclusion) errors, which ultimately addresses the concerns outlined by the National Research Council's report on forensic analyses, as mentioned and detailed in the introduction to this dissertation. Overall, a method using LIBS has been developed, optimized, and validated for the forensic analysis of float glass, which due to its low cost, reduced complexity (user friendliness), faster analysis time, and capability of being a portable technique, makes LIBS a viable alternative to XRF and LA-ICP-MS for the elemental analysis of glass.

Finally, a LA-ICP-MS method has been developed for the trace elemental analysis of gel inks, a matrix that currently could not be analyzed (and samples differentiated) by chromatographic techniques routinely used in forensic document examination laboratories. Qualitative analysis was used to obtain 95.6% discrimination

for a blind black gel ink sample set (consisting of 45 black gel ink samples) provided by the United States Secret Service. It was found that for this sample set, a 0.4% false exclusion (Type I) error rate and a 3.9% false inclusion (Type II) error rate was obtained, which considering that qualitative analysis generated such results and also given the issues regarding the application of these inks, these results are remarkable. A second gel ink sample set was collected representing several manufacturers and different models within those manufacturers, for this set total of 24 black gel ink pens were analyzed qualitatively by LA-ICP-MS and 99% discrimination potential was achieved. The two pairs found indistinguishable by LA-ICP-MS originated from the same source and thus retained explanation as to why similar elemental profiles were observed. In addition, it was found that ink from the same pen at different ink levels (75, 50, 25, 10, and 0%) was indistinguishable with the only exception (and hence discrimination from the other analyses) being the analysis at the very first application of the pen (100% ink level or 0% usage). A same pen pack variation study was also conducted on a pack of four pens, and it was determined that four pens originating from the same pack were indistinguishable.

The original hypothesis that femtosecond LA-ICP-MS was not (or less) matrix-matched dependent was not supported, instead it was found that improved results were obtained when a matrix-matched standard in combination with an internal standard was used. With respect to the LIBS studies on glass discrimination, LIBS was shown to provide comparable or better discrimination power for glass samples when compared to µXRF and LA-ICP-MS, therefore the original hypothesis was supported. Finally, the use of LA-ICP-MS was successfully applied for the analysis and comparison of gel ink sources and therefore the original hypothesis was fully supported.

REFERENCES

[1]   National Research Council Report, Prepublication (2009) Strengthening Forensic Science in the United States: A Path Forward, The National Academies Press, Washington DC

[2]   Hickman D (1986) Forensic Sci Int 33:23-46

[3]   Ryland S (1986) J Forensic Sci 31:1314-1329

[4]   Koons R, Fiedler C, Rawalt R (1988) J Forensic Sci 33:49-67

[5]   Becker S, Gunaratnam L, Hicks T, Stoecklein W, Warman G (2001) Prob of Forens Sci XLVII:80-92

[6]   Trejos T, Montero S, Almirall JR (2003) Anal Bioanal Chem 76:1255-1264

[7]   Almirall JR, Trejos T (2007) Forensic Sci Rev 18:73-96

[8]   Almirall JR (2001) Elemental Analysis of Glass Fragments. In: Caddy B (Ed) Trace Evidence Analysis and Interpretation: Glass and Paint, Taylor and Francis, London, UK

[9]   Buscaglia J (1994) Anal Chim Acta 288:17-24

[10]   Almirall JR (2001) Glass as Evidence of Association In: Houck M (Ed) Mute Witness When Trace Evidence Makes the Case. Academic Press, San Diego, CA

[11]   Brunelle RL, Crawford KR (2002) Advances in the Forensic Analysis and Dating of Writing Ink, Charles C Thomas Publisher, Springfield, IL

[12]   Maloney FT (1968) Glass in the Modern World, Doubleday, New York, NY

[13]   ASTM Annual Book of ASTM Standards (2004) American Society for Testing and Materials 14.02, 1

[14]   Trejos T, Almirall JR (2004) Anal Chem 76:1236-1242

[15]   Trejos T, Almirall JR (2005) Talanta 67:388-395

[16]   Trejos T, Almirall JR (2005) Talanta 67:396-401

[17]   Latkoczy C, Ducking M, Becker S, Gunther D, Hoogewerff J, Almirall JR, Buscaglia J, Dobney A, Koons R, Montero S, van der Peijl GJQ, Stoechlein W, Trejos T, Watling RJ, Zdanowicz V (2005) J Forensic Sci 50:1327-1341

[18] Russo RE, Mao X, Mao SS (2002) Anal Chem 74:70A-77A

[19] Rode AV, Luther-Davies BE, Gamaly EG (1999) J Appl Phys 85:4222-4230

[20] Gamaly EG, Rode AV, Luther-Davies BE (1999) J Appl Phys 85:4213-4221

[21] Mao XL, Russo RE (1997) Appl Phys A 64:1-6

[22] Liu HC, Mao XL, Yoo JH, Russ RE (1999) Spectrochim Acta Part B 54:1607-1624

[23] Vertes A, Gijbels R, Adams F (1993) Laser Ionization Mass Analysis, Wiley-Interscience, New York, NY

[24] Mao S, Mao XL, Greif R, Russo RE (2000) Appl Phys Lett 77:2464-2466

[25] Mao SS, Mao XL, Greif R, Russo RE (2000) Appl Phys Lett 76:3370-3372

[26] Russo RE, Mao X, Liu H, Gonzalez J, Mao SS (2002) Talanta 57:425-451

[27] Gunther D, Hattendorf B, Latkoczy C (2003) Anal Chem 341A-347A

[28] Gonzalez J, Liu C, Wen S, Mao X, Russo RE (2007) Talanta 73:567-576

[29] Gonzalez J, Liu C, Wen S, Mao X, Russo RE (2007) Talanta 73:577-582

[30] Koch J, von Bohlen A, Hergenroder R, Niemax K (2004) J Anal At Spectrom 19:267-272

[31] Russo RE, Mao X, Gonzalez JJ, Mao SS (2002) J Anal At Spectrom 17:1072-1075

[32] Gonzalez J, Lui CY, Mao XL, Russo RE (2004) J Anal At Spectrom 19:1165-1168

[33] Poitrasson F, Mao X, Mao S, Freydier R, Russo RE (2003) Anal Chem 75:6184-6190

[34] Gonzalez J, Dundas SV, Lui CY, Mao X, Russo RE (2006) J Anal At Spectrom 21:778-784

[35] Montaser A (1998) Inductively Coupled Plasma Mass Spectrometry, Wiley-VCH, New York, NY

[36] Skoog DA, Holler FJ, Nieman TA (1998) Principles of Instrumental Analysis, 5th Edition, Harcourt Brace, Philadelphia, PA

[37] Denoyer ER, Tanner SD, Voelkopf U (1999) Spectroscopy 14:43-54

[38] Tanner SD, Baranov VI (1999) J Anal At Spectrom 10:1083-1094

[39] Hattendorf B, Gunther D (2000) J Anal At Spectrom 15:1125-1131

[40] Rowan JT, Houk RS (1989) Appl Spectrosc 43:976-980

[41] Beauchemin D (2002) Anal Chem 74:2873-2893

[42] Trahey N (1998) NIST Standard Reference Material Catalog 1998-1999, National Institute of Standards and Technology

[43] Longerich HP, Jackson SE, Gunther D (1996) J Anal At Spectrom 11:899-904

[44] Guillong M, Gunther D (2002) J Anal At Spectrom 17:831-837

[45] Lui C, Mao XL, Mao SS, Greif R, Russo RE (2004) Anal Chem 76:379-383

[46] Naes BE, Umpierrez S, Ryland S, Barnett C, Almirall JR (2008) Spectrochim Acta B 63:1145-1150

[47] Rodriquez-Celis EM, Gornushkin IB, Heitmann UM, Almirall JR, Smith BW, Winefordner JD, Omenetto N (2008) Anal Bioanal Chem 391:1961-1968

[48] Bridge CM, Powell J, Steele KL, Williams M, MacInnis JM, Sigman ME (2006) Appl Spectrosc 60:1181-1187

[49] Scaffidi J, Angel SM, Cremers DA (2006) Anal Chem 78:25-32

[50] Vadillo JM, Laserna JJ (2004) Spectrochim Acta B 59:147-161

[51] Anglos D (2001) Appl Spectrosc 55:186-205A

[52] Maind SD, Kumar SA, Chattopadhyay N, Gandhi C, Sudersan M (2005) Forensic Sci Int 159:32-42

[53] Zieba-Palus J, Kunicki M (2005) Forensic Sci Int 158:164-172

[54] Fittschen UE, Bings NH, Hauschild S, Forster S, Kiera AF, Karavani E, Fromsdorf A, Thiele J (2008) Anal Chem 80:1967-1977

[55] Spence LD, Baker AT, Byrne JP (2000) J Anal At Spectrom 15:813-819

APPENDICES

The following paper, of which I was the first author on, was accepted and published in

2008. The reference for that publication is as follows, which is also reference as [46] in

the reference section:

A comparison of laser ablation inductively coupled plasma mass spectrometry (LA-ICP-

MS), micro X-ray fluorescence spectroscopy (μXRF), and laser induced breakdown

spectroscopy (LIBS) for the discrimination of automotive glass

Benjamin E Naes [a], Sayuri Umpierrez [a], Scott Ryland [b],
Cleon Barnett [a], Jose R Almirall [a,*]

[a] *Florida International University, Department of Chemistry and Biochemistry,
International Forensic Research Institute, 11200 SW 8th Street,
Miami, FL 33199, United States*
benjamin.naes@fiu.edu, umpierre@fiu.edu, barnettc@fiu.edu, almirall@fiu.edu

[b] *Florida Department of Law Enforcement, Orlando Regional Crime Laboratory, 500
West Robinson Street, Orlando, FL 32801, United States*
ScottRyland@fdle.state.fl.us

* Corresponding Author.

Email address: almirall@fiu.edu

Keywords: LA-ICP-MS, LIBS, XRF, glass, forensic

Abstract

Laser ablation inductively coupled plasma mass spectrometry (LA-ICP-MS), micro X-ray fluorescence spectroscopy (μXRF), and laser induced breakdown spectroscopy (LIBS) are compared in terms of discrimination power for a glass sample set consisting of 41 fragments. Excellent discrimination results (> 99 % discrimination) were obtained for each of the methods. In addition, all three analytical methods produced very similar discrimination results in terms of the number of pairs found to be indistinguishable. The small number of indistinguishable pairs that were identified all originated from the same vehicle. The results also show a strong correlation between the data generated from the use of μXRF and LA-ICP-MS, when comparing μXRF strontium intensities to LA-ICP-MS strontium concentrations. A 266nm laser was utilized for all LIBS analyses, which provided excellent precision (< 10 % RSD for all elements and < 10 % RSD for all ratios, N=5). The paper also presents a thorough data analysis review for forensic glass examinations by LIBS and suggests several element ratios that provide accurate discrimination results related to the LIBS system used for this study. Different combinations of 10 ratios were used for discrimination, all of which assisted with eliminating Type I errors (false exclusions) and reducing Type II errors (false inclusions). The results demonstrate that the LIBS experimental setup described, when combined with a comprehensive data analysis protocol, provides comparable discrimination when compared to LA-ICP-MS and μXRF for the application of forensic glass examinations. Given the many advantages that LIBS offers, most notably reduced complexity and reduced cost of the instrumentation, LIBS is a viable alternative to LA-ICP-MS and μXRF for use in the forensic laboratory.

1. Introduction

The evidential value of forensic glass analysis has increased over the past decade with the utilization of elemental analysis techniques, such as SEM-EDS, µXRF, ICP-MS, LA-ICP-MS, and more recently LIBS. The rise of elemental profiling for glass fragments collected at a crime scene is primarily due to the lack of discrimination power associated with refractive index measurements, which is the method typically employed by forensic laboratories for glass examinations [1]. Since glass manufacturers target a given refractive index to ensure optimum physical and optical properties, there exists only a very small degree of variation in glasses produced by the same manufacturer over time and glasses produced by different manufacturers, this is especially the case with float glass (i.e. automotive and architectural glass) [1]. Therefore, the forensic examiner must often utilize a complimentary technique in order to draw a valid association (or discrimination) between a glass fragment collected at a crime scene and its suspected source or origin.

This paper compares two of the leading techniques in forensic trace elemental analysis, µXRF and LA-ICP-MS, to a less mature method, LIBS, for the analysis of automotive glass fragments collected from fourteen different vehicles in and around Miami, Florida, US. Each of these techniques requires little to no sample preparation and sample consumption is minimal; these attributes favor forensic analyses, where sample size is often an issue. The authors of this paper wish to primarily highlight the main advantages and disadvantages of the mentioned techniques in relation to forensic glass analysis, therefore bypassing the theory and background information behind such techniques. Nevertheless, an extensive review of the theory and application of these

techniques as applied to the analysis of glass can be found in a paper by Almirall and Trejos [2].

Many laboratories employ µXRF for the analysis of different materials of forensic interest, including glass; this method offers lower detection capability versus some methods, such as SEM-EDS, which equates into higher discrimination power. In addition, as mentioned previously µXRF is a non-destructive technique, which is an attractive feature for forensic analyses. Nevertheless, the technique has several drawbacks compared to the other competing techniques, such as increased sample analysis time (lower throughput), as well as sample orientation and size requirements. More specifically, the sample must contain a reasonably flat surface with a sampling area of at least 1mm^2 and a thickness of at least 0.5mm for optimal analysis; unfortunately, these requirements cannot always be met with glass evidence.

The figures of merit for LA-ICP-MS include excellent sensitivity, precision, and accuracy; in addition, the technique is almost non-destructive (µg of sample is removed), requires little if any sample preparation, and sample analysis is relatively fast. Due to its isotopic and multi-element capabilities, combined with the other figures of merit, LA-ICP-MS offers excellent discrimination power. Plus, given that matrix-matched standard reference materials are readily available (i.e. NIST 600 series glasses), quantitative analysis can be performed on respective unknown glass fragments, which is arguably the most advantageous factor LA-ICP-MS offers over the competing elemental techniques. The only disadvantages of this technique are instrumental cost and complexity of operation.

Laser induced breakdown spectroscopy (LIBS) is a relatively new application for the forensic analysis of glass. This technique offers a very sensitive and rapid approach to elemental analysis and, like LA-ICP-MS, small sample sizes can be analyzed with good precision. The main disadvantage of this technique is related to the "infancy" of the method, wherein the overall analytical approach (including data analysis and instrumental optimization) must be studied in order to achieve comparable discrimination power. Despite this drawback, the instrumentation is fairly inexpensive (compared to the more mature μXRF and LA-ICP-MS techniques), is less complex to operate, has the capability for portability, and can generate large quantities of data over a short period of time (high sample throughput). An overall comparison of these three techniques can be found in Table 1.

In recent publications by Bridge et al [3,4] the techniques of LA-ICP-MS and LIBS have been compared for the analysis of glass; however, the authors of this paper would like to point out several distinct differences in the approach reported by that group, as compared to the analytical approaches reported in this paper. With regard to the LIBS data, it was stated that the detector gate delay was varied depending on the sample matrix, between 2.0μs to 6.5μs [4]; this large variation in the delay ultimately affects the spectra generated such that different emission lines are present or absent (a dependence on plasma evolution characteristics). As a result, if samples are being compared for discrimination purposes, as they were in the referenced paper [4], it is absolutely necessary that all parameters remain constant in order to achieve the most accurate comparisons possible.

In relation to the LA-ICP-MS sections, the authors of this paper wish to reference several articles published by our group which depict a well established method for the analysis of glass, where excellent figures of merit were validated, such as accuracy, precision, and discrimination power [5-10]. With this in mind, the rastering technique (ablation mode/type) reported by Bridge et al has been proven by our group and others to provide less accuracy and precision for the analysis of glass when compared to single spot ablation [10,11]. Less accuracy and precision translates into an increased potential of committing Type I and II errors and hence incorrect discriminations or associations. More importantly, however, is that the LA-ICP-MS method developed and utilized by our group is based on quantitative analysis with use of an internal standard. Each sample is characterized based on the actual elemental composition and not intensities or ratios of intensities. The quantification approach with use of an internal standard has several advantages over using isotopic intensities. One advantage is that signal fluctuations are minimized and systematic errors are corrected for. In addition, there is less potential for inter-day and intra-day variation which translates into more accurate sample comparisons (discrimination). Additionally, a secondary source standard can be run daily to check instrumental and method performance. It is also important that one sample is selected and run twice to check the validity of the discrimination results; more specifically, the same sample (analyzed twice throughout a sequence) should be found indistinguishable from itself. These types of quality control measures are necessary, especially in the forensic community.

The results outlined in this paper compare the discrimination results obtained utilizing µXRF, LA-ICP-MS, and LIBS, respectively, for an automotive glass sample set.

141

The research presented in this paper is a collaborative effort between Florida International University (Miami, FL) and the Florida Department of Law Enforcement (Orlando, FL). All LA-ICP-MS and LIBS analyses were performed at Florida International University while the μXRF data was accumulated by the Florida Department of Law Enforcement. To the authors knowledge this is the first publication comparing these three techniques for the forensic analysis of glass.

2. Experimental

2.1 Sample and standard descriptions

The sample set of interest in this study is comprised of 41 different automotive glass fragments obtained from 14 different vehicles located in junkyards in and around Miami, FL. More specifically, the glass samples included 7 side window fragments, 6 rear window fragments, and 28 windshield fragments (14 inside windshield and 14 outside windshield samples) extracted from automotive vehicles spanning the years of 1995 to 2005. The non-float surfaces of the respective glass samples were examined via each of the three respective analytical techniques. Standard reference materials NIST 612 and NIST 1831 were utilized for optimization of each of the instrumental setups. In addition, NIST 612 was used as an external calibration source for quantification by LA-ICP-MS. NIST 1831 was used as a calibration verification sample (second source check standard) for LA-ICP-MS analyses to ensure accurate and precise results.

2.2 Micro X-ray fluorescence (μXRF)

An EDAX Eagle Micro X-Ray Fluorescence Spectrometer (Mahwah, NJ) equipped with a rhodium X-ray tube was utilized for this part of the study. The instrument was operated with a 40 kV excitation potential, a 17 μs time constant, and 40-45 % dead time. Other instrumental parameters included a 300 μm diameter focusing capillary and 1200 s of live count time; the chamber was operated under low vacuum conditions. Five replicate analyses were performed on each fragment with a sampling target area defined by the 300 μm diameter X-ray spot. The element menu consisted of six elements (K, Ca, Ti, Fe, Sr, and Zr), which were subdivided into six element ratios (Ca/Fe, Sr/Zr, Ca/K, Fe/Zr, Fe/Sr, and Fe/Ti) to be used for sample comparisons. The intensities of the K alpha peaks corresponding to each of the respective elements were determined following background subtraction utilizing peak deconvolution and generation software.

2.3 Laser ablation inductively coupled plasma mass spectrometry (LA-ICP-MS)

A New Wave Research UP213 Laser Ablation system (Fremont, CA) coupled to a Perkin Elmer ELAN 6100 DRC II ICP-MS (Waltham, MA) was used for all LA-ICP-MS analyses. The laser is a Nd:YAG (4 ns) Q-switched laser operating at 213 nm and 100 % energy (27.2 J/cm^2 fluence). The repetition rate utilized for this part of the study was 10 Hz and single spot ablation mode was used with a spot size of 55 μm. Helium with a flow rate of 0.9 L/min was the carrier gas into and from the ablation chamber, which then coupled to argon (1 L/min) prior to entering the ICP. The ICP-MS parameters included an RF power of 1500 W, a plasma gas (argon) flow rate of 16 L/min, an auxiliary (argon)

flow rate of 1 L/min, and a dwell time of 8.3 ms. Three replicates (pertaining to different sampling spots) for each sample were analyzed. The element menu included five isotopes: ^{49}Ti, ^{85}Rb, ^{88}Sr, ^{90}Zr, and ^{137}Ba, with ^{29}Si used as the internal standard. The quantification of each elemental concentration was calculated using Glitter software (Macquarie Ltd, Australia), where a single point calibration source (NIST 612) and the internal standard (^{29}Si) were used to convert intensity (counts per second) via integration of time-resolved spectra into concentration (in ppm). The resulting elemental concentrations were then used to characterize the given samples and ultimately to associate and/or discriminate one fragment from another. This quantification approach has been described in more detail elsewhere [5-7].

2.4 Laser induced breakdown spectroscopy (LIBS)

Experiments were conducted using a LIBS system constructed at FIU that was equipped with a New Wave Research Q-switched Nd:YAG Tempest laser (Fremont, CA) operating at 266 nm and a pulse width of 3-5 ns (full width half maximum). A 266 nm laser was chosen for this analysis due to an observed improved laser-to-sample coupling with glass (as compared to the more generally used 1064 nm irradiation for LIBS), which resulted in an increase in precision. A 3X beam expander was utilized to enlarge the beam diameter to approximately 11 mm; the laser beam was then focused perpendicularly to the sample using a plan-convex lens with a focal length (f) of 150 mm. An energy of 25 mJ per laser pulse and a spot size of approximately 190 μm remained constant throughout the analytical sequence and all LIBS analyses were conducted under atmospheric pressure in air. Light from the laser induced plasma was imaged from the

side (90^0) by a pair of plano-convex lenses (f = 75 mm) into an optical fiber with a diameter of 50 μm. This fiber was coupled to the entrance slit of an Andor Mechelle 5000 spectrometer (South Windsor, CT) equipped with an Andor iStar intensified CCD, which converted the image into a spectrograph. The spectral range collected for each sample ranged from 200-950 nm with a resolution of ~5000. The repetition rate for the spectrometer was set at 0.67 Hz such that the spectrometer would capture a complete set of data for each laser shot. Both the laser flashlamp and the Q-switch were externally controlled using a Berkeley Nucleonics' Model 565 Delay Generator (San Rafael, CA). The emission lines were accumulated at a 1.2 μs delay upon plasma ignition, with an integration time of 3.5 μs. A schematic of the LIBS setup utilized for this part of the study can be found in Figure 1.

Each sample replicate spectra was collected as a result of the accumulation of 50 laser shots. After each spectrum was acquired, the sample was rotated to a new spot for a total of 5 spots/replicate analyses per sample.

3. Results and discussion

3.1 Discrimination study

3.1.1 Micro X-ray fluorescence (μXRF)

The μXRF discrimination results found 14 indistinguishable pairs (98.3 % discrimination) using a three-sigma criteria (three times the standard deviation), which is routinely used in casework by the Florida Department of Law Enforcement (FDLE). Of these pairs, only three originated from different vehicles; each of given pairs and these

were all discriminated by application of the t-test at the 95 % confidence interval. Therefore, application of the t-test at the 95 % confidence interval to the remaining 11 pairs yielded 8 indistinguishable pairs out of a possible 820 comparisons (the number of possible pairs is equal to N(N-1)/2, where N is the number of samples). This combined approach demonstrated 99.0 % discrimination for µXRF, which is excellent discrimination power. All of the indistinguishable pairs have explanation as to why they exhibit similar elemental profiles, namely that each indistinguishable pair originated from the same vehicle and were likely produced by the same manufacturing plant at approximately the same. Seven of the 8 pairs found indistinguishable were attributed to samples from the same laminated windshield (inside and outside fragments originating from the same windshield), while the eighth indistinguishable pair represents side and rear window fragments that also originated from the same vehicle. The pairs found indistinguishable by this method are listed and described in Table 2 with the indistinguishable pairs found by µXRF are labeled by the superscript "a".

3.1.2 Laser ablation inductively coupled plasma mass spectrometry (LA-ICP-MS)

The data analysis utilized for the LA-ICP-MS results included a combination of pairwise comparison analysis using ANOVA and the General Linear Model (GLM) in Systat 11 (San Jose, CA) with Tukey's honestly significant different test (HSD). To the pairs found indistinguishable by pairwise comparison analysis a t-test at the 95 % confidence interval was applied (via Microsoft Excel, Redmond, WA). A given pair found indistinguishable using the combination of the two data analysis strategies was ultimately determined indistinguishable, meaning the fragments have very similar

elemental profiles. A more thorough review of this data analysis approach can be found elsewhere [5,7]. Pairwise comparison analysis alone yielded 11 indistinguishable pairs (98.7 % discrimination); 6 of these pairs were discriminated by application of a t-test of which 3 pairs originated from different vehicles that were produced in different years. The other 3 pairs discriminated by t-test originated from the same vehicle. The reason why some glass fragments that originate from the same source can be discriminated is a result of sampling and/or precision across the entire pane of glass. If the precision of the measurement for a given fragment is smaller than the overall precision of the glass pane as a whole, it is possible that fragments obtained from the same source (i.e. inside and outside fragments from the same windshield) can be discriminated. Therefore, in forensic casework it is important that proper sampling techniques are followed to ensure that correct characterization of a glass source is achieved and that correct associations or discriminations are made. For LA-ICP-MS, combining pairwise comparison analysis and t-test, 5 indistinguishable pairs were found out of a possible 820 pairs (99.4 % discrimination). Remarkably, these 5 pairs were identical to 5 (of the 8) pairs found indistinguishable by μXRF. Despite LA-ICP-MS showing slightly better discrimination power than μXRF (0.4 % greater), the results are well correlated. The correlation between LA-ICP-MS and μXRF data for this sample set will be addressed later in this paper. The 5 indistinguishable pairs by LA-ICP-MS are summarized in Table 2 where the pairs marked with a superscript "b" represent the 5 indistinguishable pairs determined by LA-ICP-MS. The fact that both methods generated the same output, namely the same indistinguishable pairs, demonstrates the strength and validity of these two methods for forensic glass comparisons. Again, the indistinguishable pairs all had explanations as to

147

why they exhibited very similar elemental profiles. The top discriminating elements by LA-ICP-MS and the associated results per element can be found in Table 3. Take note that the top discriminating element is strontium, which overall has been consistently a top discriminator for the trace elemental analysis of float glass. As a result, strontium was chosen for the correlation studies, comparing LA-ICP-MS concentrations to μXRF and LIBS signal intensities.

3.1.3 Laser induced breakdown spectroscopy (LIBS)

3.1.3.1 Data analysis approach

Twenty-two (22) peaks/emission lines were initially chosen for data analysis based on their presence across all 41 glass samples. The selected peaks represent 9 different elements; Al, Ca, Fe, K, Mg, Na, Si, Sr, and Ti. Both intensities by peak heights and peak areas (via integration) were evaluated statistically (between sample replicates) and it was observed that peak areas provided greater precision when compared to using peak heights or intensities. Since precision is one of the important factors in discriminating samples, peak areas were utilized for further data reduction purposes. From the 22 peak areas detailed above, every possible peak ratio (element/element) was evaluated to determine which ratio resulted in the best discrimination out of the 231 possible ratios [N(N-1)/2, where N is the number of peaks].

Discrimination for each individual ratio was conducted on the 41 different glass fragments, in the sample set, using a t-test at the 95 % confidence interval to coincide with the 95 % confidence interval utilized for both LA-ICP-MS and μXRF. In addition, a 42nd sample fragment was added as a quality control measure. This sample was the same

sample analyzed twice during the analytical sequence, once towards the middle of the run and again at the end. Thus, the sample duplicate was treated as an unknown throughout the entire analytical scheme. The results related to this same sample analysis were then used to eliminate ratios that provided a false exclusion (or Type I error), meaning that the same sample was discriminated. A total number of 85 ratios produced no false exclusions following this format.

Of the 85 ratios, 10 were selected based on their respective degrees of discrimination for the glass sample set, with none of the ratios being repeated, such as 394.4 nm/460.7 nm (Al/Sr) and 460.7 nm/394.4 nm (Sr/Al). These 10 ratios and their individual discrimination results are reported in Table 3. The final step in this approach was to limit the number of ratios used in combination to only 6 ratios (of the 10), in order to remain consistent with the number of ratios used to discriminate the glass sample set by μXRF.

3.1.3.2 Discrimination results

All of the possible combinations of the 10 optimized ratios (using 6 different ratios in each combination) were assessed and further ranked in terms of discrimination power. In total, 210 different ratio combinations were evaluated [n!/(n-m)!m! where n is the total number of ratios (10) and m is the number of ratios used per discrimination (6)], confirming that no Type I errors were detected.

Of the 210 combinations, 60 combinations provided one to six false inclusions (Type II errors), whereby these combinations resulted in the discrimination of pairs originating from different vehicle makes/models manufactured in different years. In the

149

worst case scenario, 9 indistinguishable pairs were found, 6 of which were false inclusions and 3 pairs with an explanation (same glass or same car origin). The authors wish to stress that this worst-case combination would not be used to discriminate glass samples and that none of the 60 combinations that produced false inclusions would be considered suitable for the discrimination of glass by LIBS.

It was determined that 150 combinations (of the possible 210) produced no Type I or Type II errors, with all associations resulting from plausible explanations (same glass or same car origin), which was the same result as with the µXRF and the LA-ICP-MS. Samples 6 and 7, which are fragments originating from the side and rear windows of a 2004 Chevrolet Cavalier, were indistinguishable by all 210 possible combinations with 36 combinations resulting with samples 6 and 7 as the only indistinguishable pair. In addition, this pair was also found to be indistinguishable by µXRF, as referenced in Table 2, which concludes that these two fragments share very similar elemental profiles. There were 4 other indistinguishable pairs that were found by several of the ratio combinations, which were also found indistinguishable by LA-ICP-MS and/or µXRF, these pairs and the associated frequency of occurrence (out of a possible 210 combinations) are: 11:12 (28 occurrences or 13.3%), 13:14 (7 occurrences or 3.3%), 23:24 (84 occurrences or 40.0%), and 28:29 (84 occurrences, or 40.0%). Actual sample descriptions for these pairs can be found in Table 2 with the pairs found indistinguishable by LIBS depicted by the superscript "c".

It should be noted that although the group at FIU (LA-ICP-MS and LIBS analyses) did know the origin of each fragment prior to instrumental analysis, the potential bias of comparison was avoided given that the data generation format (pairwise

comparison analysis and/or t-test) treats each sample as if the identity is unknown and the user must decipher the results generated to determine which pairs are indistinguishable. Furthermore, with respect to the LIBS and LA-ICP-MS discrimination results, the analyst did not know which samples were associated (samples from the same vehicle) until after the discmination results were generated. In the case of the µXRF analyses, the samples were analyzed as a blind study where the analyst did not know the origin of the samples until the final results were submitted. Overall, the discrimination results were well correlated, even though the methods for elemental analysis are different and each data analysis approach was performed by a different analyst.

3.2 Correlation study

The three analytical techniques are compared in terms of concentration (LA-ICP-MS) versus intensity (µXRF or LIBS), the results are summarized here. Figure 2 shows the distribution of strontium (mean concentration or mean intensity), as determined by µXRF, LA-ICP-MS, and LIBS. The plot shows the variation (or in some cases the association) of strontium in the glass sample set analyzed for this study; also, it partially demonstrates the correlation of the strontium signal for the three methods. It can be observed in most cases that as a strontium concentration or intensity is increased for one method moving from one sample to the next, the strontium signal also increased in similar magnitude for the other methods. Nevertheless, a more descriptive (or visual) correlation of such results can be found in Figure 3.

The correlation between LA-ICP-MS and μXRF data using strontium mean concentrations and intensities (with the associated error bars), respectively, for the 41 glass set was plotted and compared. As depicted in Figure 3(a), a strong correlation between the two data sets is demonstrated, represented by a correlation coefficient of 0.9911. The excellent correlation between these two methods further establishes why similar discrimination results were obtained. A correlation between LA-ICP-MS and LIBS data was also plotted using LA-ICP-MS determined strontium concentrations versus LIBS intensities (mean values with respective standard deviations) for the 41 glass set. As observed in Figure 3(b), the correlation for LIBS and LA-ICP-MS was determined to have a correlation coefficient of 0.8813. The correlation plot also illustrates the small degree of variation between sample replicates for LIBS using the setup described in this study.

Conclusions

Two of the leading techniques in elemental analysis, LA-ICP-MS and μXRF, were compared to the less mature technique, LIBS, in terms of discrimination power for a set of automotive glass samples. Significantly, all three analytical approaches yielded similar discrimination results with a percent discrimination of 99 % or greater. The 5 indistinguishable pairs found by LA-ICP-MS were the same as 5 (of the 8) indistinguishable pairs determined by μXRF, and many of the ratio combinations used to discriminate the glass samples by LIBS resulted in the same pairs found to be indistinguishable by the other methods. In addition, the indistinguishable pairs obtained for LA-ICP-MS, μXRF, and LIBS had a good explanation as to why the elemental

profiles were similar and thus could not be discriminated. These indistinguishable pairs originated from the same vehicle and thus were likely to have been manufactured in the same plant at approximately the same time. With respect to analyzing LIBS spectra and making sample comparisons, an extensive study was conducted comparing different data reduction procedures. The final approach resulted in good discrimination and was in agreement with the other elemental analysis methods. The probability of committing Type I or Type II errors is reduced and/or eliminated using the sample comparison approach for LIBS outlined in this paper. Avoiding such errors is a requirement for forensic casework. The best combination of ratios produced only 1 indistinguishable pair (out of the possible 820 pairs) and this pair was explainable. Based the data analysis study outlined, the authors suggest 10 ratios that are considered optimum for the analysis and discrimination of glass by LIBS. The proposed ratios include: 394.4nm/330.0nm (Al/Na), 766.5nm/643.9nm (K/Ca), 394.4nm/371.9nm (Al/Fe), 438.4nm/766.5nm (Fe/K), 534nm/766.5nm (Ca/K), 371.9nm/396.2nm (Fe/Al), 766.5nm/645.0nm (K/Ca), 394.4nm/460.7nm (Al/Sr), 460.7nm/766.5nm (Sr/K), and 818.3nm/766.5nm (Na/K). Given its low cost, high sample throughput, good sensitivity, and ease of use, the application of LIBS for forensic glass examinations has been shown to provide the same discrimination as other, more established methods and now presents a viable alternative to LA-ICP-MS and μXRF in the forensic laboratory.

References

[1] J.R. Almirall, Elemental Analysis of Glass Fragments, In: Trace Evidence Analysis and Interpretation: Glass and Paint, B. Caddy, ed., Taylor and Francis, London, 2001.

[2] J.R. Almirall, T. Trejos, Advances in the forensic analysis of glass fragments with a focus on refractive index and elemental analysis, Forensic Science Review 18 (2006) 73-96.

[3] C.M. Bridge, J. Powell, K.L. Steele, M. Williams, J.M. MacInnis, M.E. Sigman, Characterization of automobile float glass with laser-induced breakdown spectroscopy and laser ablation inductively coupled plasma mass spectrometry, Applied Spectroscopy 60 (2006) 1181-1187.

[4] C.M. Bridge, J. Powell, K.L. Steele, M.E. Sigman, Forensic comparative glass analysis by laser-induced breakdown spectroscopy, Spectrochimica Acta, Part B 62 (2007) 1419-1425.

[5] T. Trejos, J.R. Almirall, Sampling strategies for the analysis of glass fragments by LA-ICP-MS, Talanta 67 (2005) 396-401.

[6] T. Trejos, J.R. Almirall, Sampling strategies for the analysis of glass fragments by LA-ICP-MS, Talanta 67 (2005) 388-395.

[7] T. Trejos, S. Montero, J.R. Almirall, Analysis and comparison of glass fragments by laser ablation inductively coupled plasma mass spectrometry (LA-ICP-MS) and ICP-MS, Analytical and Bioanalytical Chemistry 376 (2003) 1255-1264

[8] T. Trejos, J.R. Almirall, Effect of Fractionation on the Forensic Elemental Analysis of Glass Using Laser Ablation Inductively Coupled Plasma Mass Spectrometry, Analytical Chemistry 76 (2004) 1236-1242.

[9] C. Latkoczy, B.Stefan, M. Ducking, D. Gunther, J.A. Hoogewerff, J.R. Almirall, J. Buscaglia, A. Dobney, R.D. Koons, S. Montero, G.J.Q. van der Peijl, W.R.S. Stoecklein, T. Trejos, J.R. Watling, V.S. Zdanowicz, Development and evaluation of a standard method for the quantitative determination of elements in float glass samples by LA-ICP-MS, Journal of Forensic Sciences 50 (2005) 1327-41.

[10] K. Smith, T. Trejos, R.J. Walting, J.R. Almirall, A guide for the quantitative elemental analysis of glass using laser ablation inductively coupled plasma mass spectrometry, Atomic Spectroscopy 27 (2006) 69-75.

[11] J.J. Gonzalez, A. Fernandez, X. Mao, R.E. Russo, Scanning vs. single spot laser ablation (λ =213 nm) inductively coupled plasma mass spectrometry, Spectrochimica Acta, Part B: Atomic Spectroscopy 59B (2004) 369-374.

Tables and figure captions:

Table 1. A comparison of various figures of merit for LA-ICP-MS, µXRF, and LIBS.

Table 2. Description of the indistinguishable pairs found by µXRF, LA-ICP-MS, and LIBS. [a] = indistinguishable pairs found by µXRF; [b] = indistinguishable pairs by LA-ICP-MS; [c] = indistinguishable pairs by LIBS.

Table 3. Percent discrimination by element, LA-ICP-MS.

Table 4. Percent discrimination for the most discriminating ratios by LIBS.

Figure 1. Experimental setup for LIBS measurements. ICCD = intensified charge-coupled device; f = focal length

Figure 2. Strontium distribution among the 41 glass set, a comparison of means for µXRF (signal intensity), LA-ICP-MS (concentration), and LIBS (signal intensity). Note that the µXRF intensities were multiplied by 5 and the LIBS peak areas were divided by 200.

Figure 3. (a) Correlation of LA-ICP-MS and µXRF strontium results, (b) Correlation of LA-ICP-MS and LIBS strontium results; concentration versus peak area.

Parameter	µXRF	LA-ICP-MS	LIBS
Operating Principle	Highly energetic X-rays knock out an inner shell electron. Relaxation of an outer shell electron into the vacant position causes emission of characteristic X-rays	Laser photons remove material from sample. Submicron-sized particles are transported into the ICP which atomizes and ionizes the ablated material; ions are detected by MS	Laser photons induce matrix breakdown at sample surface. Characteristic emission lines are produced in the UV, VIS, and near IR range
Accuracy	Semi-quantitative	Quantitative	Semi-quantitative
Precision	Fair – good (5-10 % RSD)	Excellent (< 5 % RSD)	Fair – good (5-20 % RSD)
Sensitivity	100 ppm	< 1 ppm	10 - 50 ppm
Discrimination	Very good - excellent	Excellent	Very good - excellent
Complexity	Easy to use	Difficult to use	Very easy to use
Sample Consumption	Nondestructive	Almost nondestructive	Almost nondestructive
Throughput	~30 min / analysis	~3 min / analysis	~30 sec / analysis
Cost	~ $120,000	~ $210,000	$50,000 - $150,000

Table 1. A comparison of various figures of merit for LA-ICP-MS, µXRF, and LIBS.

pair #	sample #	vehicle make	vehicle model	year	sample location
1[a,c]	6	Chevrolet	Cavalier	2004	outside windshield
	7	Chevrolet	Cavalier	2004	inside windshield
2[a,b]	8	Chevrolet	Cavalier	2004	side window
	9	Chevrolet	Cavalier	2004	rear window
3[a,b,c]	11	Oldsmobile	Intrigue	1998	outside windshield
	12	Oldsmobile	Intrigue	1998	inside windshield
4[a,b,c]	13	Dodge	Neon	2000	outside windshield
	14	Dodge	Neon	2000	inside windshield
5[a,b]	20	Chevrolet	Cavalier	2003	outside windshield
	21	Chevrolet	Cavalier	2003	inside windshield
6[a,b,c]	23	Dodge	Stratus	1998	outside windshield
	24	Dodge	Stratus	1998	inside windshield
7[a,c]	28	Ford	Expedition	2004	inside windshield
	29	Ford	Expedition	2004	outside windshield
8[a]	37	Jeep	Grand Cherokee	2001	outside windshield
	38	Jeep	Grand Cherokee	2001	inside windshield

Table 2. Description of the indistinguishable pairs found by µXRF, LA-ICP-MS, and LIBS. [a] = indistinguishable pairs found by µXRF; [b] = indistinguishable pairs by LA-ICP-MS; [c] = indistinguishable pairs by LIBS.

element	# indistinguishable pairs	% discrimination
Sr	76	90.7
Zr	127	85.5
Ti	142	82.7
Rb	176	78.5
Ba	191	76.7
All (5)	5	99.4

Table 3. Percent discrimination by element, LA-ICP-MS.

sample #	peak ratio	description	# indist.pairs	% discrimination
1	394.4nm / 330.0nm	Al/Na	70	91.5
2	766.5nm / 643.9nm	K/Ca	84	89.8
3	394.4nm / 371.9nm	Al/Fe	86	89.5
4	438.4nm / 766.5nm	Fe/K	90	89.0
5	534.9nm / 766.5nm	Ca/K	91	88.9
6	371.9nm / 396.2nm	Fe/Al	91	88.9
7	766.5nm / 645.0nm	K/Ca	93	88.7
8	394.4nm / 460.7nm	Al/Sr	104	87.3
9	460.7nm / 766.5nm	Sr/K	104	87.3
10	818.3nm / 766.5nm	Na/K	141	82.8

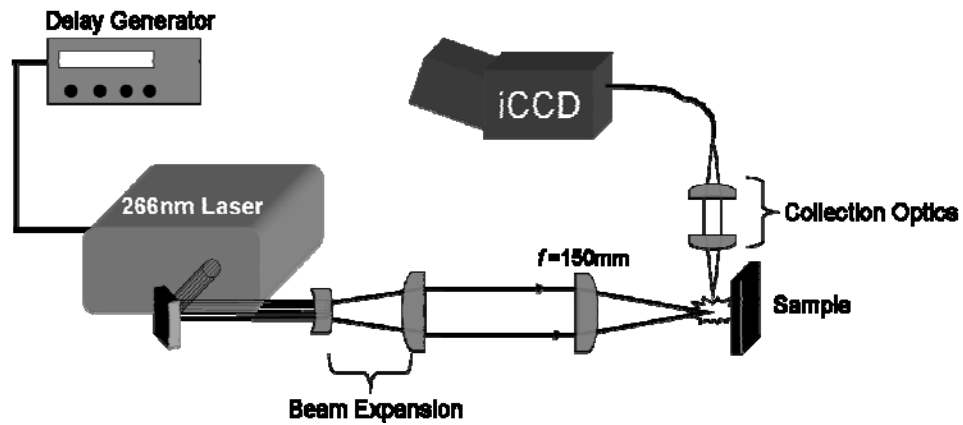Table 4. Percent discrimination for the most discriminating ratios by LIBS.

Figure 1. Experimental setup for LIBS measurements. ICCD = intensified charge-coupled device; f = focal length.
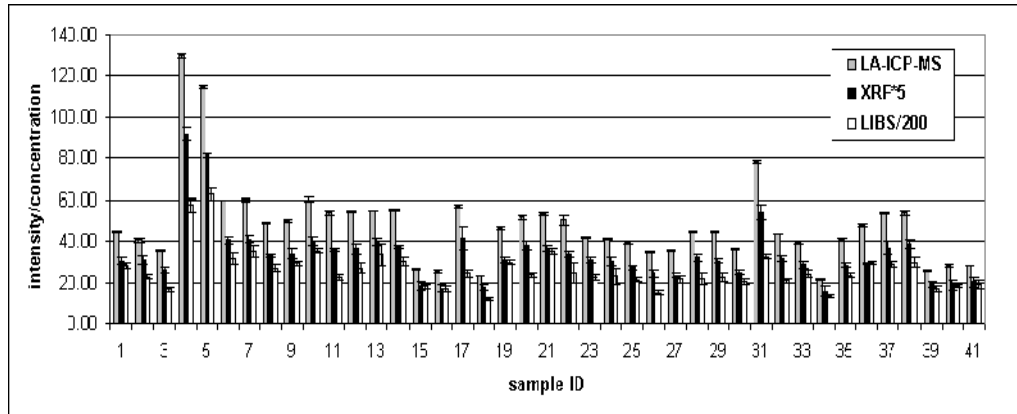
Figure 2. Strontium distribution among the 41 glass set, a comparison of means for μXRF (signal intensity), LA-ICP-MS (concentration), and LIBS (peak area). Note that the LIBS intensities were divided by 200 and the μXRF intensities were multiplied by 5.
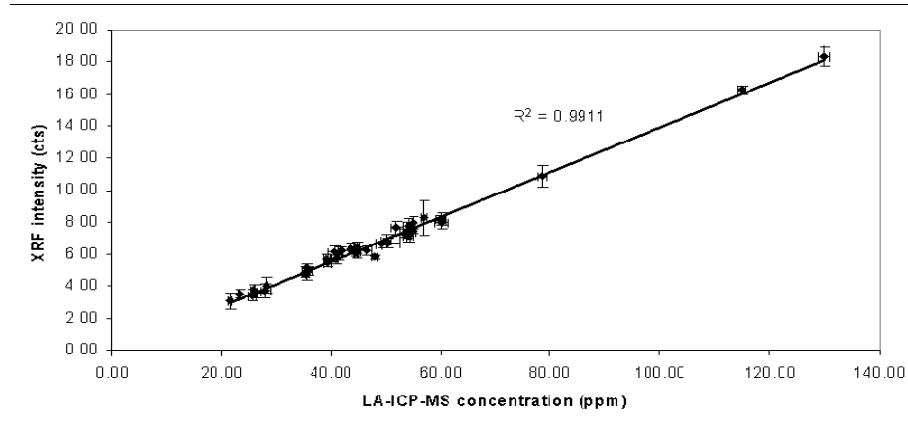

Figure 3(a). Correlation of LA-ICP-MS and μXRF strontium results.
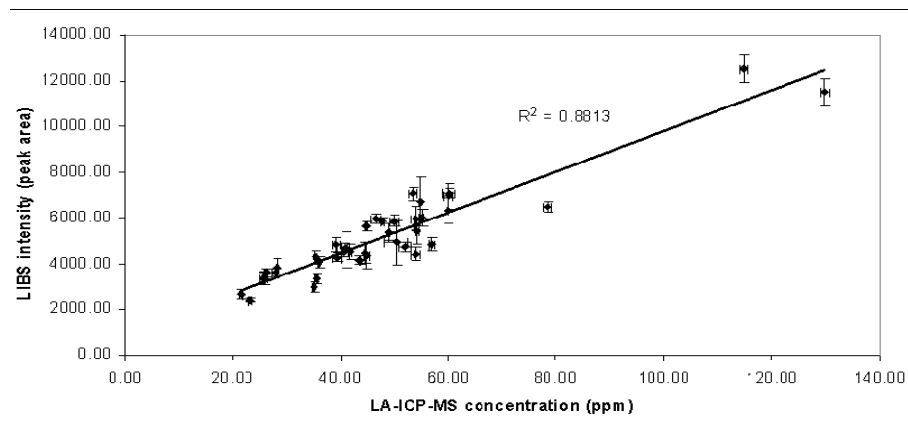

Figure 3(b). Correlation of LA-ICP-MS and LIBS strontium results.

BENJAMIN E NAES

January 1976	Saint Louis, Missouri, USA

May 1999   Bachelor of Science in Chemistry
Southeast Missouri State University
Cape Girardeau, Missouri, USA

PUBLICATIONS:

Naes, B.; Umpeirrez, S., Ryland, S., Barnett, C., and Almirall, J.R. A comparison of laser ablation inductively coupled plasma mass spectrometry (LA-ICP-MS), micro X-ray fluorescence spectroscopy (μXRF), and laser induced breakdown spectroscopy (LIBS) for the discrimination of automotive glass. *Spectrochimica Acta B* 2008, *63*, 1145-1150.

Castro, W.; Trejos, T.; Naes, B.; Almirall, J. Comparison of high-resolution and dynamic reaction cell ICP-MS capabilities for forensic analysis in glass. *Anal Bioanal Chem* 2008, *392*, 663–672.

PRESENTATIONS:

Naes, B., Gonzalez, J., Russo, R., and Almirall, J.R. *A Comparison Of Nanosecond vs Femtosecond LA-ICP-MS for the Analysis of Glass.* Winter Plasma Conference on Spectrochemistry, January 2006.

Naes, B., Gonzalez, J., Russo, R., and Almirall, J.R. *Elemental Analysis of Glass by LA-ICP-MS, a Comparison of Various Laser Methods to Optimize Sensitivity, Precision, and Accuracy.* American Academy of Forensic Sciences, February 2006.

Naes, B., Gonzalez, J., Russo, R., and Almirall, J.R. *The Analysis of Glass by Laser Ablation Inductively Coupled Plasma Mass Spectrometry, a Comparison of Nanosecond Laser Ablation to Femtosecond Laser Ablation.* American Academy of Forensic Sciences, February 2007.

Naes, B., Gonzalez, J., Russo, R., and Almirall, J.R. *Comparison of Femtosecond vs Nanosecond Laser Ablation Sampling Coupled to ICP-MS for the Analysis of Glass and Other Matrices of Interest to Forensic Scientists.* American Academy of Forensic Sciences, February 2007.

Naes, B., Umpeirrez, S., Ryland, S., and Almirall, J.R. *Forensic Analysis of Glass by LIBS, A Comparison to XRF and LA-ICP-MS for Elemental Profiling.* Pittsburgh Conference on Analytical Chemistry, March 2008.